CHARACTERIZATION OF FINE PARTICLE AIR POLLUTION IN THE INDIAN SUBCONTINENT

A Dissertation
Presented to
The Academic Faculty

By

Muhammed Zohir Chowdhury

In Partial Fulfillment
Of the Requirements for the Degree
Doctor of Philosophy in Atmospheric Chemistry

Georgia Institute of Technology

June 2004

CHARACTERIZATION OF FINE PARTICLE AIR POLLUTION IN THE INDIAN
SUBCONTINENT

Approved by

Dr. Michael H. Bergin   Dr. Ellery D. Ingall

Dr. Mei Zheng   Dr. Rodney Weber

Dr. Armistead G. Russell, Advisor

Date Approved: June 4, 2004

A man is but what he knows.

Francis Bacon

To

Late Prof. Glen R. Cass

ACKNOWLEDGEMENT

Not until one embarks into the rigorous and demanding life of a graduate student for the first time, does one realize how much determination and focus are needed to complete the intense requirements for a Ph.D. As a senior in undergraduate school, I came with a fresh and open mind to succeed, but I lacked the realization and expectation of what would be needed to complete this journey towards a Ph.D. It has been my coworkers, professors, friends, and relatives who provided me with the push, encouragement, and emotional support that were needed to complete this big step in my life. I thank everybody who came into my life during these tough graduate years both at Caltech and at Georgia Tech.

My graduate life has been somewhat unconventional. I started off at Caltech under Prof. Glen R. Cass's supervision and later moved with him to Georgia Tech and witnessed Glen's rapid health decline until he passed away on July 30, 2001. The period encompassing a few months prior and post his death was the lowest point in my graduate life. It was Prof. Ted Russell that assisted me in regaining my momentum by taking me into his research group.

First and foremost, Prof. Ted Russell deserves my intense appreciation and gratitude for taking me under his wings and guiding me in the last several years after the death of my primary advisor Glen R. Cass. Ted has given me plenty of liberty to continue my work in understanding the fine particle air pollution in India that I started while Glen was still alive. Writing proposals and communicating with the funding agency to meet their needs have been valuable experiences that I learned while working with Ted. Ted has always pushed me and supported me in tough times. I will always remember his supporting words when my entire first run from the GC/MS instrument

turned out bad. He has also provided me with valuable career advices, and because of his recommendations I now have a Post Doctoral position with Prof. Kirk Smith at the University of California, Berkeley.

Similarly, coming in contact with Glen in my earlier half of graduate school has been a blessing. He showed me how to develop a coherent thesis, and imparted to me a small part of his great enthusiasm for science. It has been him who gave me the opportunity to pursue interesting research in parts of the world that I wanted to work in future, and provided support at every step. If it weren't for Glen, I would have left graduate school right after I completed my Master's at Caltech. I still remember Glen coming to my office late at night and explaining why I should continue pursing a Ph.D. His constant encouragement and support have rekindled my passion for science and I will forever remain indebted to him for being my mentor and for taking an active interest in the progress of my thesis. One week before his death, I was amazed to see him how much he cared for his work and for his students. With a shaky hand, he scribbled what was the outline of my thesis. In that state of health, he fixed my committee and fixed funding for the coming years. I owe to him for believing in me and in my research abilities. May his soul rest in peace.

Sincere appreciation and thanks are due to Dr. Mei Zheng at Georgia Tech, Lynn Salmon at Caltech, Prof. Jamie Schauer at University of Wisconsin--Madison, and Dr. Lara Hughes at Caltech for their time in guiding me understand air pollution sampling, source emission testing, organic analysis, and source apportionment. Without these four people, I would not have been able to learn

the skills required to be an experimental scientist. Working with them have been one of the most enriching and fruitful experiences of my life.

My committee members have also taken an active role in bringing the best out of me. Prof. Michael Bergin, Prof. Ellery Ingall, and Prof. Rodney Weber have pushed me really hard to better understand my work, to think critically about my results, and more importantly to write good quality scientific work. I hope this thesis meets their expectations. The lesson that they provided me will go beyond the work of this thesis as several papers are being prepared directly from this work.

Professor Chandra Venkataraman from the Indian Institute of Technology—Bombay (IIT-Bombay), deserves a special recognition for helping me settle down in India where I needed to setup four sampling sites, find organizations that would be interested in my work, train them to sample for fine particles—all in 15 days time so that we could start with the sampling events that Glen and I had planned. On top of this, Chandra has been very crucial in helping me understand the major emission sources in India.

I would also like to thank Dr. A. P. Mitra, Dr. Sharma, and Dr. A. K. Sarkar from the National Physical Laboratory in Delhi, India, in assisting me in establishing the sampling network in India. Thanks are also due to Mr. Biswas at the NEERI Zonal laboratory at Kolkata and Dr. Rakesh Kumar at the NEERI Zonal laboratory at Mumbai and their entire team for participating in this exciting work. I hope our NEERI colleagues have also found this work

cooperative school in Rome, I understood that if I continue to study and work hard, I could probably reach that top academic spot. Since then, my goal has been to reach the top of this academic chart. I'm glad that I've been able to reach this goal and thanks are due to everybody that has contributed in my life.

TABLE OF CONTENTS

LIST OF TABLES

LIST OF FIGURES

xviii

LIST OF ACRONYMS

AIHL   Air and Industrial Hygiene Laboratory

CNG   Compressed Natural Gas

CMB   Chemical Mass Balance

CPCB   Central Pollution Control Board

CR   Concentration Response

CSE   Center for Science and Environment

D_a Particle Aerodynamic Diameter

DRI   Desert Research Institute

EC   Elemental Carbon

EC/OC   Elemental Carbon/Organic Carbon

EF   Emission Factor

EPA   Environmental Protection Agency

ESP   Electro Static Precipitator

GC/MS   Gas Chromatography Mass Spectrometry

HEPA   High Efficiency Particulate Arrestance

IC   Ion Chromatography

IC Engine   Internal Combustion Engine

INAA   Instrumental Neutron Activation Analysis

INDOEX	Indian Ocean Experiment
INDOEX-IFP	Indian Ocean Experiment Intensive Field Phase
KCO	Kaashidhoo Climate Observatory
LT	Local Time
MPNG	Ministry of Petroleum and Natural Gas
MOUDI	Micro-Orifice Uniform Deposit Impactor
ND	Nylon Denuded
NEERI	National Environmental Engineering Research Institute
NOAA	National Oceanic and Atmospheric Administration
NU	Nylon Undenuded
OC	Organic Carbon
OM	Organic Matter
PAH	Poly Aromatic Hydrocarbon
PM	Particulate Matter
$PM_{2.5}$	Particulate Matter with aerodynamic diameter of 2.5 micron
PM_{10}	Particulate Matter with aerodynamic diameter of 10 micron
ppm wt	Parts per Million by Weight
PTFE	Poly Tetra Fluoro Ethylene
QU	Quartz Undenuded

RH   Relative Humidity

SERDP   Strategic Environmental Research and Development Program

TST   Total Suspended Particulates

TU   Teflon Undenuded

UNEP   United Nations Environmental Program

UCAR   University Corporation for Atmospheric Research

WHO   World Health Organization

XRF   X-Ray Fluorescence

SUMMARY

This thesis characterizes the mass and chemical composition of the fine particle air pollution over several cities in South Asia and quantifies how major sources impact the observed levels by using Chemical Mass Balance modeling with organic compounds as tracers. During February 1999, as part of the INDOEX program, a study was conducted to measure the size distribution and chemical composition of the fine particles in a remote island in Maldives off the coast of India. We found that the fine particle concentrations were comparable to those found in major cities in the United States, and were surprisingly high for a background site. 10-day backwind trajectories pointed the source region towards the Indian subcontinent; other INDOEX studies confirmed the presence of a thick haze layer over the Indian Ocean and the subcontinent during the time of the experiment. Motivated by these findings, a detailed analysis of ambient $PM_{2.5}$ was carried out in Delhi, Mumbai, Kolkata, and Chandigarh—four cities located upwind of the island in Maldives. Seasonality of the fine particle concentrations was observed in each of these cities with the highest concentrations occurring during the wintertime and the lowest concentrations during the summer. Size distribution and chemical composition of the fine particle emissions from five Bangladeshi biomass (rice straw, coconut leaves, dried cow dung, synthetic biomass log, and jackfruit wood) and three Asian coals (Bangladeshi, Indian, and Chinese) were characterized and important source signatures were identified. Finally, recently developed chemical tracer techniques were applied to the ambient samples from North India to differentiate between the contributions from the many different source types. The emission profiles and source signatures from the source tests conducted previously along with the ones conducted using the Indian Subcontinent fuels were used as inputs to the model.

These results serve several purposes. First, they provide a description of the mass and detailed inorganic and organic chemical characteristics of fine particulate matter conducted for the first time ever in this region. Second, the source apportionment study will help to define the relative importance of those sources that should be included within an air quality control program. Chemical tracer techniques are particularly attractive for application in regions that have not been studied previously because they are able to yield rapid insights into the causes of a local air pollution problem before the completion of an accurate emissions inventory. Third, the source tests results will prove useful in constructing and evaluating regional emission inventory and assessing source impacts on air quality. Fourth, this work has been carried out with collaborations from Georgia Tech and several other Indian research institutions where pollution control personnel in India was trained in the operation of air sampling equipments that were left for continued monitoring, thus contributing to technology transfer and knowledge transfer from the US.

CHAPTER-1

Introduction

1.1. Air Quality Problem in South Asia

The speed with which urban air pollution has grown in cities like Delhi, Mumbai, and Kolkata, across the Indian subcontinent in the last decade is alarming [Aggarwal, 1999]. The World Health Organization once ranked Delhi as the fourth-most polluted mega city of the world [WHO-UNEP, 1992]. However, in Indian subcontinent, it is not just Delhi, but even small and medium towns which are finding themselves in the grip of deteriorating air quality [CPCB, 1995]. Dehradun, located in the Himalayan foothills in western Uttar Pradesh, now often tops the list of one of the most polluted places in urban India [CPCB, 1995]. So does Gajroula, a relatively unknown little town of western Uttar Pradesh, India [CPCB, 1995]. Historically, Total Suspended Particulate (TSP) levels in a number of South Asian cities have been high (CPCB, 1989; CPCB, 1991; CPCB, 1992; CPCB, 1993; CPCB, 1995]. In comparison, the ambient concentrations of NO_2, SO_2, CO, and ozone have been relatively low, typically not exceeding the WHO health-based guidelines [Aggarwal, 1999]. CO, NO_2, and SO_2 can be elevated in mega

cities but the exceedances above internationally recognized air quality standards are not of the magnitude observed for particulate matter [Aggarwal, 1999]. Large cities in India and Pakistan appear to have very high concentrations of fine particles [World Bank, 2004]. Outside of these countries, Dhaka in Bangladesh and Kathmandu in Nepal suffer from serious particulate air pollution, the latter in part because of its topography (being located in a valley which traps polluted air) [Begum et al., 2004; Carrico et al., 2003].

In response to the emerging scientific evidence that small particles are especially damaging to health [Dockery et al., 1993; Pope et al., 2002], environmental agencies in American and European countries began requiring monitoring of smaller particles, first with a cut-point of 10 μm aerodynamic diameter (PM_{10}) and more recently with a 2.5 μm aerodynamic diameter ($PM_{2.5}$). Recently, several large cities in South Asia have begun monitoring PM_{10} and in some cases also $PM_{2.5}$. Consistent with high ambient TSP levels, the recorded levels of PM_{10} and $PM_{2.5}$ have been found to be elevated [Begum et al., 2004, Carrico et al., 2003, NEERI, 2000, Khaliquzzaman, 1997].

Because of the growing concerns about the adverse impact of deteriorating air quality, governments from these countries over the years have implemented a number of policy measures and initiatives to curb urban air pollution. One of the most successful policy interventions in this regard is the gasoline lead elimination in South Asia [World Bank, 2004]. However, one crucial question for formulating policy to combat urban air pollution is to identify the sources that are contributing significantly to airborne particulate matter. This information is not available for most cities in South Asia since detailed emission inventory with appropriate emission factors has

not been constructed so far. The popular perception is that vehicle exhaust contributes significantly [Aggarwal, 1999]. As a result, much of the governments' efforts have historically focused on controlling emissions from vehicles. This has ranged from tightening fuel quality and emission standards and promoting Compressed Natural Gas (CNG) to establishing a vehicle inspection system [Aggarwal, 1999]. Five of the seven countries in the Indian subcontinent are either in the process of establishing, or have already established and been operating, an emissions inspection system [World Bank, 2004]. Yet in India, which has the longest history of such an inspection system, it is widely acknowledged to be making little contribution to air quality improvement [World Bank, 2004]. It has thus become very important to have accurate ambient measurements in key cities, identify the major sources causing the air pollution problem, and take stringent action in controlling the sources. However, because of the lack of key air pollution measurements, scientists and policy makers are facing difficulty in improving the air quality [Aggarwal, 1999]. The actual concentrations in the air and the mixture of sources that produce this air pollution problem in a particular area will remain undetermined until detailed measurements can be made. The work presented in this thesis has attempted to fill these gaps by confirming the yearlong variability of the fine particle air pollution, and identifying as well as quantifying the major sources responsible for this type of air pollution in four cities in India.

1.2. Public Exposure

Urban air pollution, primarily in the form of highly elevated ambient concentrations of small particulate matter, poses a serious threat to the health of urban dwellers in many cities in

India [WHO-UNEP, 1987]. The most significant health effects of air pollution in South Asia are associated with exposure to particulate matter and these are: premature death from heart and lung disease, and chronic bronchitis, asthma attacks, and other forms of respiratory illness [Smith, 2000]. The analysis of the health benefits associated with air pollution reduction has made great progress over the past 10–15 years. Estimates of the health impact of air pollution are generally obtained from epidemiological studies that are designed to determine relationships—referred to as concentration-response (CR) functions—between air pollution and health effects in human populations. The most extensive body of evidence for adverse health effects at ambient concentrations that the general public is typically exposed to (as opposed to occupational exposure) exists for particulate matter. Although quantification of health impact is testing, the consistent findings across a wide array of cities, including those in developing countries with diverse population and possibly diverse particle characteristics, strongly indicate that the health gains indeed result from PM pollution reductions [World Bank, 2004]. The impact of PM increases with decreasing particle size, with studies increasingly focusing on particles smaller than 2.5 μm and even 0.1 μm (called ultrafines) [Dockery et al., 1993; Pope et al., 2002]. Particles larger than about 10 μm are deposited almost exclusively in the nose and throat, whereas particles smaller than 1 μm are able to reach the lower regions of the lungs. The intermediate size range gets deposited in between these two extremes of the respiratory tract. A statistically significant association has been found between adverse health effects and ambient PM_{10} concentrations, and recent studies using $PM_{2.5}$ data have shown an even stronger association between health outcomes and particles in this size range [Dockery et al., 1993; Pope et al., 2002]. Populations at risk from inhaled particles are those most susceptible to pulmonary and heart diseases, infants and elderly people. A 1997 joint study of the World Health

4

Organization (WHO), the World Resources Institute (WRI) and the US Environmental Protection Agency (EPA) estimated that nearly 700,000 deaths worldwide are related to air pollution and that this number can escalate to 8 million deaths by 2020 (Working Group, 1997). Occurrences of respiratory diseases in South Asia resulting from air pollution both indoors and outdoors, is estimated to be quite substantial [Smith, 2000]. In each of the 23 cities with a million plus population in India, air pollution levels exceed WHO standards. It has been estimated that in India alone about 500,000 premature deaths are caused by indoor pollution, for mothers and their children who are under 5 years of age [Smith, 2000]. Serious respiratory disease related problems have been identified for both indoor and outdoor pollution in Indian cities like Kolkata, Delhi, Lucknow, Mumbai, Ahmedabad, and in several other countries in East Asia including China, Thailand and Korea. There is still inadequate knowledge of the relative effectiveness of sub micron particles compared with larger particles, or the specific roles of black carbon and organic carbon. Such studies need to be performed in the future.

1.3. Climate Effects

The problem of air pollution is no longer confined only at local scale. The new scenario encompasses complex interlinkages of several issues, including air pollution, haze, smog, ozone and global warming. Aerosol influences climate directly by the scattering and absorption of solar radiation and indirectly through their role as cloud condensation nuclei. The magnitude of the direct forcing of aerosols at a particular time and location depends on the amount of radiation scattered back to space, which itself depends on the size and optical properties of the particles,

their abundance, and the solar zenith angle [Seinfeld and Pandis, 1998]. The so-called indirect effect arises if increases in aerosol number concentrations from anthropogenic sources lead to increased concentrations of cloud condensation nuclei, which, in turn, lead to clouds with larger number concentrations of droplets with smaller radii, which, in turn lead to higher cloud albedos [Seinfeld and Pandis, 1998]. Particles can both scatter and absorb radiation; as particles become increasingly absorbing versus scattering a point is reached, depending on their size and the albedo of the underlying surface, where the overall effect of the particle layer changes from one of cooling to heating. In addition, if the particles consist of a mixture of purely scattering material, such as ammonium sulfate, and partially absorbing material, such as soot, the cooling versus heating effect depends on the manner in which the two substances are mixed throughout the particle population [Kiehl and Briegleb, 1993, Kiehl, 1994]. During INDOEX, a series of experiments have been conducted to understand the indirect effect of the aerosol over the Indian Ocean and a thick aerosol haze layer spreading all over the North Indian Ocean as well as over South and Southeast Asia was discovered and its contribution to the regional climate forcing was measured [Ramanathan et al., 2001a; Ramanathan and Crutzen, 2002].

1.4. Visibility Reduction

Visibility degradation is probably the most readily perceived impact of air pollution. Visibility is reduced by the absorption and scattering of light by both gases and particles. Light scattering by particles is the most important phenomenon responsible for impairment of visibility. Visibility is reduced when there is significant scattering because particles in the

atmosphere between the observer and the object scatter light from the sub and other parts of the sky through the line of sight of the observer [Seinfeld and Pandis, 1998]. This light decreases the contrast between the object and the background sky, thereby reducing visibility. Scattering by particles of sizes comparable to the wavelength of visible light (the Mie scattering range) is mostly responsible for visibility reduction in the atmosphere [Seinfeld and Pandis, 1998]. Particles in the range 0.1 to 1 μm in diameter are the most effective, per unit aerosol mass, in reducing visibility. The brown haze characteristic of smoggy atmosphere is largely a result of aerosol scattering. The Indian Ocean Experiment (INDOEX) has revealed that this haze is transported far beyond the source region, particularly during December to April [Ramanathan et al., 2001a]. The discovery during INDOEX of the so-called South Asian haze is clear evidence of the magnitude of the aerosol pollution problem.

The results presented in this thesis, particularly the particle size distribution work measured by the Micro-Orifice Uniform Deposit Impactor (MOUDI) will be very useful in calculating and in understanding visibility problem in the Indian subcontinent.

1.5. Research Objectives

From the above discussion of the effect of particulate pollution, we realize the importance of understanding and characterizing the mass, size distribution, and the chemical makeup of the ambient fine particles in the Indian subcontinent. The principal objective of this research work is thus to characterize this fine particle air pollution over the Indian subcontinent. A receptor-based

air pollution model which uses emissions data as well as the measured ambient data was further used to identify and quantify the primary contributions of air pollution sources responsible for the fine particle air pollution problem in this region.

Another objective of this work is to understand the emission pattern from burning biomass samples typically used in this region as well as to characterize coal emission profiles. This emission data are collected and analyzed by sampling techniques which are the same as those used for the quantification of the ambient atmosphere [Hildemann et al., 1991a, 1991b]. The source testing work requires the use of a dilution source sampler which can dilute hot exhaust emissions from combustion sources to near ambient temperatures and pressure prior to sampling, such that the compounds in the cooled diluted exhaust are present at near their atmospheric equilibrium distribution between the gas-phases and particle-phases [Hildemann et al., 1989].

The results from this work can be useful at several levels. First, the baseline fine particle air quality characterization study has documented the concentration and chemical composition of the North Indian fine particle problem. Second, the source apportionment study has helped to define the relative importance of those sources that should be included within an air quality control program. Third, this work was carried out with collaborations from Georgia Tech and several other Indian Research Institutions where pollution control personnel in India has becoming trained in the operation of air sampling equipment, thus contributing to technology transfer and knowledge transfer from the US.

1.6. Approach

To accomplish the work presented in this thesis, the following approach was followed:

1. A month-long study was conducted in a remote island off the coast of South India in a small island, Kaashidhoo, located in the Republic of Maldives. The fine particulate matter found in this work was surprisingly high, and trajectory analysis showed the source region to be the Indian subcontinent which is located immediately upwind. To understand the ambient fine particle air pollution in this region, a year long (months of March, June, October, and December) ambient monitoring study in three major Indian cities (Delhi, Mumbai, and Kolkata) and an upwind site (Chandigarh) was conducted. Detailed mass and chemical analysis provided a baseline fine particle air pollution for this region.

2. The size distribution and chemical composition of particles emitted from the smokes of a variety of Indian subcontinent biomass fuels (jackfruit wood, cow dung, synthetic fuel, rice straw, and coconut leaves) and coals (from India, Bangladesh, and China) have been characterized. The results of these source tests provided the particle emission profiles and the source signatures needed for the chemical tracer method.

3. Recently developed chemical tracer techniques have been applied to the ambient samples from North India to differentiate between the contributions from the many different source types. The emission profiles and source signatures from the source tests conducted by Schauer et al. [1996, 2000] along with the ones conducted using the Indian subcontinent fuels have been used as inputs to the model. These Chemical Tracer

techniques are particularly attractive for application in regions that have not been studied previously because they are able to yield rapid insights into the causes of a local air pollution problem before the completion of an accurate emissions inventory.

1.7 Outline of Thesis

This section provides an overview of the research presented in the following chapters. This thesis is divided into seven chapters. The second chapter comprises the work conducted during the INDOEX experiment and discusses the fine particle mass and chemical composition as well as the size distribution of the aerosol found over a small island in the Republic of Maldives off the coast from India [Chowdhury et al., 2001]. The results obtained during this experiment have been used to conduct light scattering calculations [Eldering et al., 2002] as well as to achieve closure between measured CCN spectra and the CCN spectra calculated on the basis of measured aerosol number distributions and measured chemical composition [Cantrell et al., 2001]. The detailed model of aerosol light scattering and absorption from Eldering et al. [2002] was driven by the measurements of the size distribution and chemical composition of airborne particles sampled using cascade impactors reported in chapter two of this thesis. Models for both an internally mixed and externally mixed aerosol were considered, and the relative importance of the different chemical species to the atmospheric light extinction coefficient was presented for the externally mixed aerosol case. Light scattering and absorption by particles were calculated from Mei theory, which requires real and imaginary refractive indices and aerosol size distributions. The method of calculating refractive indices and light scattering has been discussed previously in Larson et al. [1988], Eldering et al. [1994], and Eldering et al. [1993]. In the paper

10

from Eldering et al. [2002], comparison were made to direct measurements of light scattering, light absorption, single scattering albedo, and growth in scattering as a function of relative humidity. Light scattering coefficients were predicted to within a few percent over relative humidities of 20 to 90%. Single scattering albedoes calculated from the measured elemental carbon size distributions and concentrations in conjuction with other aerosol species had a relative error of 4.0% when compared to measured values. The single scattering albedo for the aerosols measured during INDOEX is both predicted and observed to be about 0.86 at an ambient relative humidity of 80%. These results demonstrate that the light scattering, light absorption and hence climate forcing due to aerosols over the Indian Ocean were consistent with the chemical and physical properties of the aerosol at that location.

Backwind trajectory analysis from Maldives during the time of the experiment lead to the conclusion that the high amount of pollution seen over the Indian Ocean came from the Indian subcontinent located immediately upwind, In order to understand the ambient concentration levels of fine particles upwind, it was necessary to conduct further monitoring. The third chapter measures the fine particle concentrations in this source region by selecting four key cities: Delhi, Mumbai, Kolkata—the three Indian megacities and a background site, Chandigarh. Ambient concentration was measured for the entire year of 2001 in each of these cities and chemical analysis was conducted. In order to conduct source apportionment, Indian subcontinent specific source emissions needed to be tested. For this purpose, several tests were conducted to understand the emissions from biomass and coal from this region. The fourth and the fifth chapters report the results obtained from these source tests. Chapter four discusses the emissions from Meghalaya (India), Dinajpur (Bangladesh), and Datong (China) coals. On the other hand,

11

Chapter five discusses the emissions from five Bangladeshi biomass samples: rice straw, coconut leaves, cow dung, jackfruit wood, and synthetic fuel. The sixth chapter reports the results from the detailed organic analysis conducted on the same Indian ambient samples as previously described in Chapter three. Chemical Mass Balance modeling was used to understand and quantify the major sources of air pollution in these cities by using organic compounds as tracers.

1.8. References

Aggarwal, A. L., N. Sunita, and S. Sen (Eds.) (1999), *The citizens' fifth report*, Centre for Science and Environment, New Delhi, India.

Begum, B. A., Eugene, K., Biswas, S. K., Hopke, P. K., 2004, "Investigation of sources of atmospheric aerosol at urban and semi-urban areas in Bangladesh", *Atmos. Env.,* accepted.

Cantrell, Will; Shaw, Glenn; Cass, Glen R.; Chowdhury, Zohir; Hughes, Lara S.; Prather, Kimberly A.; Guazotti, Sergio A.; and Coffee, Keith R. (2001) ``Closure Between Aerosol Particles and Cloud Condensation Nuclei at Kaashidhoo Climate Observatory," *Journal of Geophysical Research*, 106 28,711-28,718.

Carrico, C.M., Bergin, M.H., Shrestha, A.B., Dibb, J.E., Gomes, L., Harris, J.M., The importance of carbon and desert dust to seasonal aerosol properties in the Nepal Himalaya, *Atmos. Environ.*, in press, 2003.

Chowdhury, Zohir; Hughes, Lara S.; Salmon, Lynn G.; and Cass, Glen R. (2001) ``Atmospheric Particle Size and Composition Measurements to Support Light Extinction Calculations over the Indian Ocean,'' *Journal of Geophysical Research*, 106, 28,597-28,605.

CPCB, 1989. National Ambient Air Quality Monitoring Series 1989-90, Central Pollution Control Board, New Delhi.

CPCB, 1991. National Ambient Air Quality Statistics of India 1991, National Ambient Air Quality Monitoring Series 1990-91, Central Pollution Control Board, New Delhi.

CPCB, 1992. National Ambient Air Quality Statistics of India 1992, National Ambient Air Quality Monitoring Series 1994-95, Central Pollution Control Board, New Delhi.

CPCB, 1993. Ambient Air Quality—Status and Statistics (1993 & 1994), National Ambient Air Quality Monitoring Series 1995-96, Central Pollution Control Board, New Delhi.

CPCB, 1995. Ambient Air Quality—Status and Statistics (1995), National Ambient Air Quality Monitoring Series 1996-97, Central Pollution Control Board, New Delhi.

Dockery, D.W., C. A. Pope, X. P. Xu, J. D. Spengler, J. H. Ware, M. E. Fay, B. G. Ferris, and F. E. Speizer (1993), An association between air-pollution and mortality in 6 United-States cities, *New England Journal of Medicine, 329,* 1753-1759.

Eldering, A., Larson, S. M., Hall, J. R., Hussey, K. J., and Cass, G. R. (1993). Development of an improved image processing based visibility model. Environ. Sci. Technol., 27, 626-635, 1993.

Eldering, A.; Cass, G. R.; and Moon, K. C. (1994). An air monitoring network using continuous particle size distribution monitors: connecting pollutant properties to visibility via Mie scattering calculations. Atmospheric Environ., 28, 2733-2749, 1994.

Eldering, Annmarie; Ogren, J. A., Chowdhury, Zohir; Hughes, Lara S.; Cass, Glen R.. (2002) "Aerosol optical properties during INDOEX based on measured aerosol particle size and composition", *Journal of Geophysical Research-Atmospheres*, 107.

Hildemann, L. M., G. R. Cass, and G. R. Markowski, A dilution stack sampler for collection of organic aerosol emissions - design, characterization and field-tests, Aerosol Sci. Technol., 10(1), 193– 204, 1989.

Hildemann LM, Markowski GR, Cass GR. 1991a. Chemical-Composition of Emissions from Urban Sources of Fine Organic Aerosol. *Environmental Science & Technology*. 25: 744-759.

Hildemann LM, Markowski GR, Jones MC, Cass GR. 1991b. Submicrometer aerosol mass distributions of emissions from boilers, fireplaces, automobiles, diesel trucks, and meat cooking operations. *Aerosol Science and Technology*. 14: 138-152.

Khaliquzzaman, M., Biswas, S. K., Tarafdar, S. A., Islam, A., and Khan, A.H. (1997) Trace Element Composition of Size Fractionated Airborne Particulate Matter in Urban and Rural Areas in Bangladesh, Report AECD/AFD-CH/6-4.

Kiehl, J. T., and B. P. Briegleb, The relative roles of sulfate aerosols and greenhouse gases in climate forcing, Science, 260, 311-314, 1993.

Kiehl, J. T., Clouds and their effects on the climate system, Phys. Today, 47, 36-42, 1994.

Larson, S. M.; Cass, G. R.; Hussey, K. J.; and Luce, F. (1988). Verification of an image processing based visibility model, Environ. Sci. Technol., 22, 629-637.

NEERI (2000), Ambient Air Quality Status for Ten Cities of India, *Report*, National Environmental Engineering Research Institute, Nagpur, India, October 2000.

Pope, C. A. III, R. T. Burnett, M. J. Thun, et al., 2002, "Lung cancer, cardiopulmonary mortality, and long-term exposure to fine particulate air pollution," *JAMA, 287*, 1,132-1,141.

Ramanathan, V. , P. J. Crutzen, J. Lelieveld, A. P. Mitra, D. Althausen, J. Anderson, M. O. Andreae, W. Cantrell, G. R. Cass, C. E. Chung, A. D. Clarke, J. A. Coakley, W. D. Collins, W. C. Conant, F. Dulac, J. Heintzenberg, A. J. Heymsfield, B. Holben, S. Howell, J. Hudson, A. Jayaraman, J. T. Kiehl, T. N. Krishnamurti, D. Lubin, G. McFarquhar, T. Novakov, J. A. Ogren, I. A. Podgorny, K. Prather, K. Priestley, J. M. Prospero, P. K. Quinn, K. Rajeev, P. Rasch, S. Rupert, R. Sadourny, S. K. Satheesh, G. E. Shaw, P. Sheridan, and F. P. J. Valero (2001a), Indian Ocean Experiment: An integrated analysis of the climate forcing and effects of the great Indo-Asian haze, *J. Geophys. Res. Vol. 106* (D22) p. 28,371-28,398.

Ramanathan VP, Crutzen J, Kiehl JT, Rosenfeld D (2001b): Aerosols, Climate, and the Hydrological Cycle. Science 294 (5549): 2119–2124, Dec. 7

Ramanathan V. and Crutzen P. J. (2002). Asian Brown Cloud Concept Paper, Environ Sci & Pollut Res 9 (5) 289 – 295.

Seinfeld, J. H. and Pandis, S. N. (1998). "Atmospheric Chemistry and Physics: From Air Pollution to Climate Change." John Wiley & Sons, Inc.

Smith K. R. (2000). National burden of disease in India from indoor air pollution. Proceedings of the US National Academy of Sciences 97(24): 13,286–13,293

WHO-UNEP, 1987. Global pollution and health: results of health-related environmental monitoring, World Health Organization—United Nations Environmental Programme, London.

WHO-UNEP, 1992. Urban air pollution in megacities of the world, Blackwell Publishers, Oxford, p. 69.

Working Group on Public Health and Fossil Fuel Combustion (1997). Lancet 350:1341 (http://www.epa.gov/oppeoee1/globalwarming/greenhouse/greenhouse6/part.html)

World Bank (2004). Toward cleaner urban air in South Asia: tackling transport pollution, understanding sources, Joint UNDP/World Bank ESMAP, March 2004.

CHAPTER-2

Atmospheric particle size and composition measurements to support light extinction calculations over the Indian Ocean

2.1. Abstract

The size distribution and chemical composition of the atmospheric aerosol at the Kaashidhoo Climate Observatory (KCO) in the Republic of Maldives was determined during the winter northeast monsoon season to aid in determining the light scattering and light absorption properties of the aerosol particles in that region. These experiments were conducted over 8 two-day periods during February 11-26, 1999, using filter-based samplers and cascade impactors operated at ambient relative humidity which was in the range of 80-89% RH over 83% of the period sampled. Fine particle concentrations ($D_a < 1.8$ μm) averaged 17.7 ± 0.2 μg m^{-3} and varied

between 8.4±0.3 –24.7±0.2 µg m^{-3} over the period studied. Sulfate ion and carbonaceous aerosols are the largest contributors to the fine particle mass concentration, accounting for 33-37% and 26-27% of the fine mass, respectively. Calcium carbonate contributes 3% of the mass measured on the impactor stages. Ammonium, nitrate, and chloride ion account for 7-9%, 1%, and 0-1% of the fine particle mass respectively. The residual mass of as yet undetermined fine particle material stands at 28-30%. Black elemental carbon particles contribute 6–11% of the fine particle mass concentration and dominate light absorption in the atmosphere at KCO [Eldering et al., 2001]. These fine particle concentrations are comparable to those found in major cities in the United States, and are surprisingly high for a remote location such as the Maldive Islands, which is located downwind of the Indian subcontinent.

2.2. Introduction

Increased airborne particle concentrations due to human activities have the potential to increase both light scattering and light absorption in the atmosphere. Light scattering and light absorption by atmospheric particles over broad regions of the Earth, such as the Indian Ocean, can affect regional climatic conditions by altering the distribution of solar radiation and hence atmospheric and surface temperature. This is particularly true in the vicinity of the Indian subcontinent where 40-hour average fine particle concentrations (aerodynamic diameter D_a < 2.1 µm) in the atmosphere of the city of Mumbai have been measured at levels as high as 113 µg m^{-3} (S. K. Varghese et al., Aerosol and inorganic ion size distributions at Mumbai, India, during the INDOEX-IFP (1999), manuscript in preparation, 2001). Even after substantial dilution, fine

particle concentrations of more than 15.8 μg m^{-3} have been reported in the regional plume advected over the Indian Ocean during the northeast monsoon [Krishnamurti et al., 1998].

The earliest investigations of the potential for climate forcing by airborne particles focused on light scattering by sulfate aerosols. These studies showed that in clear-sky conditions the scattering of light back into space by atmospheric particles cools the planet [Charlson et al., 1990, 1991, 1992; Wigley, 1989; Kiehl and Briegleb, 1993; Taylor and Penner, 1994]. In contrast, if atmospheric particles in the polluted layer near the ocean's or earth's surface absorb a significant amount of light, the conversion of that energy into heat could raise the temperature of the lower atmosphere and at the same time affect the ocean's or earth's surface temperature, thereby altering climate through changes in water vapor and heat fluxes [Kiehl, 1994].

Common aerosol components like sulfate and nitrate scatter light but produce negligible light absorption [Larson et al., 1989; Zhang et al., 1993; Eldering et al., 1994]. In contrast, most of the light absorption in the atmosphere is thought to arise from light absorption by particle-phase black or elemental carbon [Andreae, 1995], with generally smaller contributions from some types of suspended soil dust [Prospero, 1979]. In order to calculate the light absorption by a particular mixture of aerosol particles it is necessary to know the concentration, composition, and size distribution of the airborne particles, especially the black elemental carbon content of the aerosol. Yet, at present, there are no data that describe in detail how the various aerosol chemical components, and especially black carbon, are distributed as a function of size over the Indian Ocean.

The purpose of the present paper is to describe a series of experiments in which the size distributions and concentrations of the component chemical substances in the airborne particles were measured at the Maldive Islands in the Indian Ocean during February 1999. The data were taken as part of the 1999 Indian Ocean Experiment (INDOEX) intensive field study conducted at Kaashidhoo in the Maldive Islands and thus are accompanied by extensive supporting measurements of light scattering, light absorption, and aerosol properties taken by other investigators during INDOEX .

2.3. Experimental Methods

During the period of February 11 to 26, 1999, atmospheric particle samples were collected over consecutive 2-day periods at the Kaashidhoo Climate Observatory (KCO) on Kaashidhoo Island (4.96^{o}N, 73.47^{o}E) in the Republic of Maldives. Two filter samplers and four microorifice uniform deposit impactors (MOUDIs) were operated simultaneously on the roof of the observatory's laboratory building at an elevation of 3 m above ground level. Filter samplers were used because the comparatively large samples collected place most aerosol parameters readily within tight detection limits. The impactors are seen as the most practical way to measure bulk particle chemical composition as a function of particle size. The sampling equipment is shown schematically in Figure 2.1.

Figure 2.1. Schematic diagram of sampling equipment used to measure particle size distributions and chemical compositions.

Samples were collected at ambient temperature (typically 27°–29°C) and relative humidity (typically 80–89% RH) for 46 hours out of every 48 hours, starting at 1800 local time (LT) every second day. Samples collected on the lower three stages of the impactors are very small, with ~1 µg m^{-3} of particulate matter or less in the size ranges sampled by each of the last three impactor stages. Samples of 2-day duration were taken in order to bring sample sizes on the

impactor stages to a level where one standard deviation of the mass determination would be approximately ± 0.2 µg m^{-3}. This permits very accurate mass determination on the third from last impactor stage at all times and significant mass measurements on the second to last stage much of the time. This increased accuracy of the measurements is of course obtained at the expense of the ability to detect short-term fluctuations in aerosol concentration. Vasiliou et al. [1999] have shown that particle bounce within impactors is effectively suppressed by sampling at ~80% RH. Since the ambient RH at Kaashidhoo Island was in this range during these experiments, we both size the particles as they actually exist in the atmosphere and in a way that suppresses particle bounce by sampling at ambient RH.

Total suspended particulate matter (no particle size discrimination) and fine particulate matter (aerodynamic diameter $D_a < 1.8$ µm) samples were collected using a Caltech-built filter sampling system. In this work we emphasize fine particle characterization because previous research shows that fine particles contribute approximately two thirds of the aerosol optical depth over the Indian Ocean [Satheesh et al., 1999]. The flow rates for the total and fine particulate matter filter sampling lines are shown in Figure 2.1 above. Total suspended particulate matter was collected on one open-face quartz fiber filter (Pallflex, 2500 QAO, 47-mm diameter) and on two parallel open-faced Poly Tetra Fluoro Ethylene (PTFE) filters (Gelman Sciences, Teflo, 47-mm diameter, 1.0-µm pore size). Fine particulate matter was collected on one quartz fiber filter (Pallflex, 2500 QAO, 47-mm diameter) and on two PTFE filters (Gelman Sciences, Teflo, 1.0-µm pore size). For collection of the fine particles, ambient air was drawn at a rate of 30 lpm through a glass inlet line to a Teflon-coated AIHL-design cyclone separator [John and Reischl, 1980], which removed large particles according to a collection efficiency

curve having a 50% aerodynamic cutoff diameter at 1.8 μm before the air passed through the fine

particle collection filters. The 15 and 85% particle collection cut points for this cyclone at this

flowrate are at ~1.7- and 2.2-μm aerodynamic diameter, respectively, based on visual

extrapolation of the collection efficiency curves presented by John and Reischl [1980]. The

airflow rate through each filter assembly was measured before and after each 46-hour sampling

period using a rotameter that had been calibrated against a bubble flow meter; uncertainties in

the airflow rate are ±3% and would affect the cyclone 50% cutoff diameter by ±0.05 μm.

Four 10-stage microorifice uniform deposit impactors (MOUDI, MSP Corporation,

Model 100) [Marple et al., 1991] were simultaneously operated to measure 46-hour average

particulate mass concentration and chemical composition as a function of particle size. To

suppress particle bounce from the upper stages of the impactors, ambient air was passed through

a Teflon-coated AIHL-design cyclone separator placed upstream of the inlet of each of the four

impactors to capture coarse particles ($D_a > 1.8$ μm) [John and Reischl, 1980]. Particles over the

size range 0.056–1.8 μm particle diameter were collected on impaction stages 5 through 10 of

the impactors. All 10 stages of the impactors were in place during the experiment, but only the

lower 6 stages collected meaningful samples because of the presence of the cyclone separator

upstream of the impactors. Two of the four impactors were loaded with aluminum foil substrates

(MSP Corporation, 47-mm diameter) and a quartz fiber afterfilter (Pallflex, 2500 QAO, 47-mm

diameter). The remaining two impactors were operated with PTFE impaction substrates and

afterfilters (Gelman Sciences, 47-mm diameter, Teflo material, 1.0-μm pore size). Foil impaction

substrates and quartz fiber filters were baked before use in order to lower their carbon blank

values, since these materials were dedicated to the analysis of carbonaceous aerosol species; foil

substrates were baked for 48 hours at 550°C, and quartz fiber filters were baked for 12 hours at 550°C. To avoid contamination by organic compounds, no grease or oil was applied to the impaction substrates.   Filter samples and samples on impaction substrates were placed in petri dishes, sealed with Teflon tape, then frozen immediately after collection and until subsequent analysis.

All foil and PTFE impaction substrates and PTFE filters were gravimetrically analyzed by repeated weighing before and after the experiment on a Mettler model M-55-A mechanical microbalance maintained in a temperature and humidity-controlled environment (21.0 ± 0.2°C, 39 ± 3% RH). PTFE impactor substrates were cut in half before chemical analysis to allow the use of several different chemical analysis techniques. One half of the each of the PTFE impactor substrates and one of each pair of PTFE filter samples were analyzed by ion chromatography (Dionex Corporation, Model 2020i) for the anions NO_3, SO_4^{2-}, and Cl^- [Mulik et al., 1976] and by an indophenol colorimetric procedure for NH_4^+ [Bolleter et al., 1976] using an Alpkem rapid flow analyzer (Model RFA-300). The second half of each of these sample sets is being analyzed for trace elements using neutron activation analysis [Olmez, 1989], and trace elements concentration values will be posted to the INDOEX Web site when they become available.

Foil and quartz fiber substrates were analyzed for elemental and organic carbon content using the thermal-optical carbon analysis method of Huntzicker et al. [1982] as modified by Birch and Cary [1996]. Correction for pyrolytic formation of elemental carbon during organic carbon determination from the impactor samples was accomplished using the methodology described in the paper by Kleeman et al. [1999a]. Elemental carbon is a form of impure graphite

produced by combustion processes [Cass et al., 1982]. Analytical standards for atmospheric elemental carbon particles do not presently exist, and thus elemental carbon concentrations are defined operationally by the analytical method that is used. In the thermal evolution and combustion method of Birch and Cary [1996], elemental carbon is defined as carbon that resists volatilization up to a temperature of $900^{\circ}C$ in an inert atmosphere in a manner similar to graphite and also is black. For this reason, we use the terms elemental carbon and black carbon interchangeably but with the realization that it is the measurement method of Birch and Cary [1996] that operationally defines the concentration values reported. Variations in elemental carbon values between alternative methods can arise owing to differences in the way that alternative methods correct for charring of the samples during analysis. In the case of the present samples, comparison of the EC values attained by the method of Birch and Cary [1996] versus values obtained without any pyrolysis correction shows an absolute difference in the EC values of 0.47 ± 0.61 μg EC per cm^2 of filter surface analyzed, corresponding to an average 17% change in the EC concentrations and a 6% change in the OC concentrations.

For gravimetric mass determination the average precision of the impactor measurements, calculated from the nominally four replicate impactor samples taken each event, was found to be $\pm5.3\%$ for samples greater than or equal to 2.0 μg m^{-3}, and $\pm22.5\%$ for samples less than 2.0 μg m^{-3} whose values were still significantly greater than zero. For sulfate, ammonium ion, organic matter, and elemental carbon the average precision of the measurements based on repeated analysis of standard solutions was ±2.3, ±5.4, ±11.1, and $\pm5.9\%$, respectively, for samples greater than or equal to 0.2 μg m^{-3}. No nitrate concentrations above 0.2 μg m^{-3} were measured on any single impactor stage. For sulfate, nitrate, ammonium ion, organic matter, and elemental

25

carbon the average precision for samples having significant values smaller than 0.2 μg m^{-3} was ±16.4, ±12.4, ±18.4, ±34.9, and ±12.4%, respectively.

The uncertainty values just described are based on random errors. There are possible sources of systematic errors that have not been quantified. First, losses in inlets to the samplers (measured by sampling directly from outdoor ambient air into the cyclone inlets). Second, cyclone and impactor size segregation errors minimized by use of the cyclones and high RH sampling to suppress particle bounce in the impactors. Third, volatilization of aerosol ammonium nitrate (potentially serious if NH_4NO_3 is present; see Hering and Cass [1999], positive organic aerosol artifacts due to vapor adsorption or negative organic aerosol artifacts due to volatilization of organics (potentially serious, see McDow [1999]). Finally, uncertainties in the assumed ratio of organic compound mass to organic carbon mass (see Turpin and Lim [2000]; while we assume a value of 1.4 as the ratio of organic compound mass to organic carbon mass, the value calculated from ambient concentration data when the actual organic compounds present are known ranges from 1.2 to 3.0).

In addition to the above instruments, a prototype Graseby-Andersen Sampler (Andersen RAAS, PM$_{2.5}$ speciation) was used to collect fine airborne particulate matter in sizes smaller than 2.5-μm aerodynamic diameter. Airflow rates and sampling streams for this sampler are shown in Figure 2.1.

2.4. Results and Discussions

The time series plot in Figure 2.2 shows the mass concentration and chemical composition of the fine particles ($D_a < 1.8$ μm) based on the Caltech filter sampler results over the entire study period. In these and subsequent mass balance plots, organic compound concentrations are estimated as 1.4 times organic carbon concentrations in order to account for the H, O, S, and N in organic matter [Gray et al.,1986].

Figure 2.2. Time series of fine particle ($D_a < 1.8$ μm) mass concentration and chemical composition at Kaashidhoo Island, February 11-26, 1999 based on the Caltech filter sampler.

The most polluted 46-hour event (fine particle mass concentration 24.7±0.21 μg m^{-3}) occurred from February 16 to 18. This episode was characterized by continental pollution transported from the Indian subcontinent, as explained later in this section. The least polluted 46-hour event (fine particle mass concentration 8.4±0.3 μg m^{-3}) occurred from February 20 to 22. Whenever uncertainties are presented throughout this paper, they reflect ±1σ confidence intervals for the individual samples when a single sample is described or ±1σ confidence intervals for the mean if the mean of a group of samples is described; these values are determined through analysis of replicate measurements. Because of rain on February 21 and 22, wet deposition of particles probably removed most of the atmospheric pollution. Moreover, backward trajectories indicate that the air parcels sampled at KCO during February 20–22 originated from the comparatively less polluted environment off the coast of Thailand. As seen in Figure 2.2, the major fine particle chemical components are SO_4^{-2}, NH_4^+, organic compounds, and elemental (black) carbon. The sulfate aerosol cannot be present entirely as ammonium sulfate as there are less than 2 moles of NH_4^+ for every mole of SO_4^{-2} in the aerosol.

A material balance on the average concentration of the fine particle (D_a < 1.8 μm) chemical species measured by filter-based sampling throughout the entire study period is shown in Figure 2.3a. Over this measurement period, fine particle mass concentrations averaged 17.7±0.2 μg m^{-3}; 37% of the mass is sulfate, 7% is ammonium ion, and 27% consists of organic compounds plus elemental carbon. The chemical identity of 5.8±0.4 μg m^{-3} (28%) of the fine particle material remains unknown; this residual material is expected to consist of the oxides of crustal trace elements (e.g., Al, Fe, and Si) plus sea salt and some water that remains in the samples despite the fact that they were weighed at 39% RH.

a)

Chloride
0%

Nitrate
1%

Other
28%

Sulfate
37%

Organic Matter
21%

Ammonium
7%

Elemental Carbon
6%

Total Dry Mass (Filter Samples) = 17.7 μg m^{-3}

b)

Chloride
1%

Nitrate
1%

Other
30%

Sulfate
33%

Calcium Carbonate
3%

Ammonium
9%

Organic Matter
12%

Elemental Carbon
11%

Total Dry Mass (MOUDI) = 17.1 μg m^{-3}

Figure 2.3. Material balance on the average concentration and chemical composition of fine particles ($D_a < 1.8$ μm) at Kaashidhoo Island during the entire study period based on (a) the Caltech filter sampler and (b) the integration over all MOUDI impactor stages with $D_a < 1.8$ μm.

A small amount of the crustal material is found in nearly all of the fine particle samples that we have taken elsewhere [e.g., Christoforou et al., 1999; Gray et al., 1986; Salmon et al., 1999], while sea salt is expected given the coastal location at Kaashidhoo Island. Total suspended particulate matter (TSP) concentrations averaged 10 times higher than fine particle concentrations over the four sampling events where TSP data are available; we do not have enough chemical information on the composition of the coarse particles to warrant further discussion.

The sum of the masses collected on impactor stages 5 to 10 provides an additional measure of overall fine particle mass concentration ($D_a < 1.8$ µm) that can be compared to the sub-1.8 µm and sub-2.5 µm fine particle mass concentrations measured by the Caltech filter sampler and Graseby-Andersen filter sampler, respectively. The sub-1.8 µm particle mass concentrations measured by the impactors and Caltech filter sampler match very closely throughout the entire study period, as shown in the lower 2 curves in Figure 2.4, indicating consistency in measurement and in sample analysis.

Figure 2.4. Comparison of the sum of the fine particle mass concentrations measured from impactor stages collecting particles with $D_a < 1.8$ μm versus fine particle mass concentrations measured from the Caltech filter sampler ($D_a < 1.8$ μm) and Graseby-Andersen sampler ($D_a < 2.5$ μm).

A material balance on the chemical composition of the impactor samples integrated over all particle sizes $D_a < 1.8$ μm is presented in Figure 2.3b for comparison to the sub-1.8 μm diameter particles measured from the filter-based samples. The results of these independent

31

measurements are very close for fine particle mass concentration and for Cl^-, NO_3^-, SO_4^{-2}, NH_4^+, and total carbon. The principal difference seen is in the speciation of the aerosol carbon. The impactor samples suggest that some of the "organic carbon" measured on the quartz fiber filters is actually carbonate carbon that is seen on the largest stage of the impactor samples; a possible source is the coral material from which Kaashidhoo Island is formed. The EC/OC split determined from the impactor samples is more heavily weighted toward elemental carbon. The fine particle mass concentrations as measured by the Graseby-Andersen filter sampler ($D_a < 2.5$ µm) exceed the concentrations obtained from the sub-1.8 µm aerodynamic diameter samplers, as expected (see Figure 2.4).

The size distribution of the chemical components of the atmospheric particle mixture at KCO is shown in Figure 2.5 based on the impactor data. The particle size distribution is largely unimodal in the submicron particle size range. The peak in the particle mass distribution typically occurs in the 0.56–1.0 µm aerodynamic diameter size range, which corresponds approximately to the size range of 0.44–0.79 µm particle physical diameter. The density used was 1.55 g cm^{-3}. This value was calculated by first forming model compounds from the measured aerosol species as described by Larson et al. [1988], then averaging the densities of those materials followed by estimation of the amount of water present at the sampled RH [Larson et al., 1988; Eldering et al., 1994]. The relative humidities at KCO averaged (range given in brackets) 81% (76-83)%, 82% (77-86)%, 83% (77-87)%, 85% (78-87)%, 84.5% (75-92)%, 87% (82-97)%, 86.5% (84-92)%, and 84% (78-87)% over the eight consecutive sampling periods shown in Figure 2.5, respectively.

Figure 2.5. Size distribution and chemical composition of the ambient particles during the eight 46-h sampling periods.

The size distributions of SO_4^{-2} and NH_4^+ ions follow each other closely, indicating that some $(NH_4)_2SO_4$ and/or NH_4HSO_4 probably are present in the fine particles. Cl^- and NO_3^- are found in relatively small amounts, principally in the 1.0–1.8 μm aerodynamic diameter range. The chloride indicates the presence of sea salt and the nitrate in particle sizes >1 μm indicates that a small amount of sea-salt has been in some cases partly transformed by atmospheric chemical reactions to produce sodium nitrate. Since chloride can be displaced from the aerosol

by reaction with sulfuric or nitric acid, chloride concentrations alone do not permit an accurate assessment of the amount of sea salt present. Given the large amounts of sulfate in the largest impactor size bin, there may be a considerable amount of sodium sulfate present. Once the sodium concentrations become available from neutron activation analysis, they will be posted to the INDOEX Web site and will provide a basis for estimation of sea-salt concentrations subject to the uncertainties of the sodium measurements.

Organic carbon and elemental (black) carbon are most abundant in the size range between 0.32- and 1.0-μm aerodynamic diameter; this size range extends to larger particle sizes than the 0.1–0.3 μm diameter peak characteristic of black carbon from diesel engines in the United States [Kleeman et al., 1999]. Black carbon from coal or biomass burning might be responsible for this pattern; at present the size distribution of elemental carbon from small-scale coal combustion and Indian subcontinent biomass burning is unknown. Alternatively, small primary black carbon-containing particles may become larger through accumulation of secondary aerosol species (e.g., sulfates, secondary organics) over time during multi-day transport across India and the Indian Ocean. The other mass values shown in Figures 2.2, 2.3, and 2.5 are believed to consist largely of mineral matter and sea-salt, plus water that is retained in the samples despite the fact that they were weighed at 39% RH. The mineral matter concentrations can be more thoroughly explored once trace element data become available from neutron activation analysis.

During the northeast monsoon the aerosol concentrations measured at KCO were much higher than one would expect at a remote island location. Fine particle mass concentrations in

particles smaller than 1.8-μm aerodynamic diameter reached 24.7 ± 0.2 μg m^{-3} over one 2-day period and averaged 17.7 ± 0.2 μg m^{-3} over the entire 16 days of this study. By comparison, fine particle concentrations in center of the city of Los Angeles averaged 27.4 μg m^{-3} during 1993, while such concentrations at San Nicolas Island, upwind and offshore of Los Angeles, averaged 7.7 μg m^{-3} [Christoforou et al., 2000].

Meteorological data link these high aerosol concentrations at KCO during the February 11–26, 1999, period to transport from the Indian subcontinent. Figures 2.6a and 2.6b show characteristic 10-day backward trajectories arriving at KCO during the study period for high pollution events and low pollution events, respectively (methodology described by Harris and Kahl [1994]). During high pollution events the air masses originated in Bangladesh, West Bengal, and the northern part of India and accumulated pollutants as they passed down the eastern coast and southern tip of India before reaching KCO. Although coarse particles larger than several microns in diameter may settle from the atmosphere via dry deposition, there is a strong possibility that smaller fine aerosols from India and Bangladesh will be transported to the area of the Indian ocean near KCO without experiencing wet or dry removal. During February 20–22 a different wind trajectory was observed, accompanied by lower levels of pollution (see Figure 2.6b). That air mass originated from southern Thailand and crossed the Bay of Bengal before reaching KCO. During passage of this air mass, rain occurred thus removing particles by wet deposition.

a)

b)

Figure 2.6. Typical 10 day backward trajectory for air parcels arriving at Kaashidhoo Island at 0600 hours local time on Feb 16 during a high pollution event (a) and arriving at 0600 hours local time on February 22 during a low pollution event (b).

36

The Indian Ocean aerosol during the winter monsoon contains a mixture of aerosol components at concentrations typical of urban pollution levels in the United States and with a surprisingly large amount of black carbon that can be expected to lead to high levels of light absorption. The size distribution and chemical composition data from our cascade impactors is sufficient to support a theoretical analysis of the causes of light scattering and light absorption over the Indian Ocean based on Mie theory scattering and absorption calculations [Eldering and Cass, 1996]. That analysis could be used to directly link the extent of climate forcing by aerosols over the Indian Ocean to the aerosol size distribution and chemical composition. Ultimately, particle size and chemical composition data will permit tests of models that connect source emissions to climate forcing by aerosols.

2.5. Acknowledgments

2.6. References

Andreae, M. O., Future Climates of the World, edited by A. Henderson-Sellers, Elsevier, New York, 1995.

Birch, M. E., and R. A. Cary, Elemental carbon-based method for monitoring occupational exposures to particulate diesel exhaust, Aerosol Sci. Technol., 25, 221-241, 1996.

Bolleter, W.T., C. T. Bushman, and P. W. Tidwell, Spectrophotometric determinations of ammonium as indophenol, Anal. Chem., 33, 592-594, 1961.

Cass. G. R., P. M. Boone, and E. S. Macias, Emissions and air quality relationships for atmospheric carbon particles in Los Angeles, in Particulate Carbon: Atmospheric Life Cycle, edited by G. T. Wolff and R. L. Klimisch, pp. 207-240, Plenum, New York, 1982.

Charlson, R. J., J. Langner, and H. Rodhe, Sulfate aerosol and climate, Nature, 348, 22-22, 1990.

Charlson, R. J., J. Langner, H. Rodhe, C. B. Levoy, and S. G. Warren, Perturbation of the northern-hemisphere radiative balance by backscattering from anthropogenic sulfate aerosols, Tellus, Ser. A, 43, 152-163, 1991.

Charlson, R. J., S. E. Schwartz, J. M. Hales, R. D. Cess, J. A. Coakley, J. E. Hansen, and D. J. Hofman, Climate forcing by anthropogenic aerosols, Science, 255, 423-430, 1992.

Christoforou, C. S., L. G. Salmon, and G. R. Cass, Passive filtration of airborne particles from buildings ventilated by natural convection: Design procedures and a case study at the Buddhist Cave Temples at Yungang, China, Aerosol Sci. and Technol., 30, 530-544, 1999.

Christoforou, C. S., L. G. Salmon, M. P. Hannigan, P. A. Solomon, and G. R. Cass, Trends in fine particle concentration and chemical composition in Southern California, J. Air Waste Manag. Assoc., 50, 43-53, 2000.

Eldering, A., and G. R. Cass, Source-oriented model for air pollutant effects on visibility, J. Geophys. Res., 101, 19,343-19,369, 1996.

Eldering, A., G. R. Cass, and K. C. Moon, An air monitoring network using continuous particle size distribution monitors connecting pollutant properties to visibility via Mie scattering calculations, Atmos. Environ., 28, 2733-2749, 1994.

Gray, H. A., G. R. Cass, J. J. Huntzicker, E. K. Heyerdahl, and J. A. Rau,   Characteristics of atmospheric organic and elemental carbon particle concentrations in Los Angeles, Environ. Sci. Technol., 20, 580-589, 1986.

Harris, J. M., and J. D. W. Kahl, Analysis of 10-day isentropic flow patterns for Barrow, Alaska-1985-1992, J. Geophys. Res., 99, 25,845-25,855, 1994.

Hering, S., and G. Cass, The magnitude of bias in the measurement of PM2.5 arising from volatilization of particulate nitrate from teflon filters, Air Waste Manag. Assoc., 49, 725-733, 1999.

Huntzicker, J. J., R. L. Johnson, J. J. Shah, and R. A. Cary, Particulate Carbon, Atmospheric Life Cycle, edited by G. T. Wolff and R. L. Klimisch, pp. 79-88, Plenum, New York, 1982.

John, W., and G. Reischl, A cyclone for size-selective sampling of ambient air, J. Air Pollut. Control Assoc., 30, 872-876, 1980.

Kiehl, J. T., Clouds and their effects on the climate system, Phys. Today, 47, 36-42, 1994.

Kiehl, J. T., and B. P. Briegleb, The relative roles of sulfate aerosols and greenhouse gases in climate forcing, Science, 260, 311-314, 1993.

Kleeman, M. J., J. J. Schauer, and G. R. Cass, Size and composition distribution of fine particulate matter emitted from wood burning, meat charbroiling, and cigarettes, Environ. Sci. Technol., 33, 3516-3523, 1999.

Kleeman, M. J., L. S. Hughes, J. O. Allen, and G. R. Cass, Source contributions to the size and composition distribution of atmospheric particles: Southern California in September 1996, Environ. Sci. Technol., 33, 4331-4341, 1999.

Krishnamurti, T. N., B. Jha, J. Prospero, A. Jayaraman, and V. Ramanathan, Aerosol and pollutant transport and their impact on radiative forcing over the tropical Indian Ocean during the January-February 1996 pre-INDOEX cruise, Tellus, Ser. B, 50, 521-542, 1998.

Larson, S. M., G. R. Cass, K. J. Hussey, and F. Luce, Verification of image processing based visibility models, Environ. Sci. Technol., 22, 629-637, 1988.

Larson, S. M., G. R. Cass, and H. A. Gray, Atmospheric carbon particles and the Los Angeles visibility problem, Aerosol Sci. Technol., 10, 118-130, 1989.

Marple, V. A., K. L. Rubow, and S. M. Behm, A microorifice uniform deposit impactor (MOUDI), description, calibration, and use, Aerosol Sci. Technol., 14, 434-446, 1991.

McDow S. R., Sampling artifact errors in gas/particle partitioning measurements, in Gas and Particle Phase Measurements of Atmospheric Organic Compounds, edited by Douglas A. Lane, pp. 105-126, Gordon and Breach Sci., Newark, N.J., 1999.

Mulik, J., R. Puckett, D. Williams, and E. Sawicki, Ion chromatographic analysis of sulfate and nitrate in ambient aerosols, Anal. Lett., 9, 653-663, 1976.

Olmez, I., in Methods of Air Sampling Analysis, 3rd ed., edited by J. P. Lodge, pp. 143-150, Lewis, Chelsea, Mich., 1989.

Prospero, J. M., Mineral and sea salt aerosol concentrations in various ocean regions, J. Geophys. Res., 84, 725-31, 1979.

Satheesh, S. K., V. Ramananathan, X. Li-Jones, J. M. Lobert, I. A. Podgorny, J. M. Prospero, B. N. Holben, and N. G. Loeb, A model for the natural and anthropogenic aerosols over the tropical Indian Ocean derived from Indian Ocean Experiment data, J. Geophys. Re.,, 104, 27, 421-40, 1999.

Taylor, K. E., and J. E. Penner, Response of the climate system to atmospheric aerosols and greenhouse gases, Nature, 369, 734-737, 1994.

Turpin, B. J., and H. J. Lim, Species contributions to PM2.5 mass concentrations: Revisiting common assumptions for estimating organic mass, Aerosol Sci. Technol., in press, 2001.

Vasiliou, J. G., D. Sorensen, and P. H. McMurry, Sampling at controlled relative humidity with a cascade impactor, Atmos. Environ., 33, 1049-1056, 1999.

Wigley, T. M. L., Possible climate change due to SO2-derived cloud condensation nuclei, Nature, 339, 365-367, 1989.

Zhang, X. Q., P. H. McMurry, S. V. Hering, and G. S. Casuccio, Mixing characteristics and water-content of submicron aerosols measured in Los Angeles and at the Grand Canyon, Atmos. Environ., 27A, 1593-1607, 1993.

CHAPTER-3

Mass and chemical characterization of the ambient fine particles in Indian cities

3.1. Abstract

Fine particle air pollution is characterized in the four Indian cities of Delhi, Mumbai, Kolkata and Chandigarh. Maximum average fine particle mass concentrations occurred during the winter and the minimum average concentrations occurred during the summer. Average fine particle mass concentrations during the winter were 230 ± 1.6 μg m^{-3} in Delhi, 89 ± 0.5 μg m^{-3} in Mumbai, and 305 ± 1.1 μg m^{-3} in Kolkata. Average fine particle mass concentrations during the summer were 49 ± 0.6 μg m^{-3} in Delhi, 21 ± 1.4 μg m^{-3} in Mumbai, and 27 ± 0.5 μg m^{-3} in Kolkata, and 29 ± 0.7 μg m^{-3} in Chandigarh. Low rainfall, air stagnation, and atmospheric inversions during the winter months lead to increased fine particle mass, whereas the monsoon rains

scavenge particles during the summer, thus reducing the atmospheric concentrations during that time. Most of the observed $PM_{2.5}$ concentrations in Delhi and the wintertime $PM_{2.5}$ concentrations in both Mumbai and Kolkata exceeded the U.S. EPA 24-hour average $PM_{2.5}$ standard of 65 μg m^{-3} signifying unhealthy air quality. Moreover, the apparent fine particle annual average concentrations for all of the cities sampled are well above the annual US standard of 15 μg m^{-3}. Organic carbon (OC), elemental carbon (EC), NO_3^-, SO_4^{2-}, Cl^-, NH_4^+, and trace metals were analyzed. During winter, OM and EC were respectively 58% and 8% in Delhi, 53% and 9% in Mumbai, and 67% and 9% in Kolkata of the PM. Sulfate contributed much of the rest. Relative contributions of crustal oxides or dust to the fine particle mass reached a peak during the spring and the summer time in all the cities. Crustal elements were probably fugitive dust from local sources and long range transport of desert dust from the Arabian desert or as far as the Saharan desert. These measurements provide important information about the seasonal and spatial distribution of fine particle-phase compounds in India.

3.2. Introduction

Rapid industrialization and urbanization during the last several decades in developing countries, like China and India, have led to an increase in anthropogenic emissions from both fossil fuel and biomass combustion. Ramanathan et al. [2001] and other researchers participating in the INDOEX study observed a large anthropogenic haze spreading over most of the North Indian Ocean, and South and Southeast Asia between December 2001 and April 2001. In fact, ground level fine particle concentrations as high as 25 μg m^{-3} were reported during INDOEX at a

remote island off the coast of India [Chowdhury et al., 2001], and trajectory analysis suggested a continental source. Such high PM levels in the Indian Ocean are comparable to the average fine particle concentrations observed in US cities, like Los Angeles [Christoforou et al., 2000]. In India, the Central Pollution Control Board (CPCB) and the National Environmental Engineering Research Institute (NEERI) have focused their efforts on measurements of PM_{10} and TSP [NEERI, 2000]. Studies have shown that it is $PM_{2.5}$ instead of PM_{10} that contributes to the visibility problem and are likely responsible for respiratory and cardio-pulmonary diseases like asthma, bronchitis, and heart disease [Dockery et al., 1993, Pope et al., 2002]. However, mass of $PM_{2.5}$ in India historically has not been measured and chemical analysis of fine particles is not readily available. Notable exception is the study conducted in Mumbai by Venkataraman et al. [2002] during INDOEX. In the absence of detailed measurements of fine particulate matter, quantitative identification of major anthropogenic sources responsible for the worsening of air pollution in key Indian cities has been difficult to achieve. Motivated by the INDOEX findings, in this study, a detailed analysis of ambient $PM_{2.5}$ has been carried out in Delhi, Mumbai, Kolkata, and Chandigarh. These measurements serve many purposes. First, they provide a description of the mass and chemical characteristics of fine particulate matter conducted for the first time ever in those four cities. This work is the subject of the present paper. Second, the data obtained in this study will later be used to quantify sources in these cities using Chemical Mass Balance modeling following the procedures as developed by Schauer et al. [1996], Schauer and Cass [2000], and Zheng et al. [2002].

3.3. Experimental Setup

3.3.1. Sampling Protocol

Ambient sampling over one year was conducted in Delhi, Mumbai, and Kolkata--three of the megacities located in India. Four months from the entire year were selected to represent the seasonal pattern observed in the region. Five samples every six days were taken for each of the four months sampled. The selected four months were:

1. March to represent spring,

2. June to represent summer,

3. October to represent autumn, and

4. December to represent winter.

A fourth site, Chandigarh, upwind of Delhi was selected to represent more regional background conditions in India. After analyzing five years of backwind trajectories from NOAA, Chandigarh appeared to be suitable as a background site upwind to Delhi. It is a smaller city with a population of 809,000 located in the northern side of India. Suitable power supplies, availability of trained personnel, cost of transportation, and ease of communication were limiting factors in selecting Chandigarh as the background site. In spite of efforts to take samples for four seasons, only five samples during the summer season were obtained; the rest of the sampling protocol could not be completed. Figure 3.1 shows the location of the four cities in the Indian subcontinent where the samples were taken and Table 3.1 describes the sites.

Figure 3.1. Location of the PM$_{2.5}$ sampling sites deployed in this study.

The sites at Delhi, Mumbai, and Kolkata were carefully selected to avoid undue influence of

emissions coming from heavy city traffic or industrial work, yet they were located within the

metropolitan cities, thus enabling the capture of the cities' emissions throughout the day and the night. In each location, the samplers were placed either on rooftops or in the middle of open fields to ensure that the sampler inlet was able to sample wind coming from all directions.

Table 3.1. Description of the sampling sites.

City	Site Address	Location Type	Site Description	Source of Pollution
Mumbai	NEERI Zonal Laboratory 89/B, Dr. Annie Basen Rd. Worli, Mumbai-400018 India	Urban Residential	Sampler placed 3 m above ground on a rooftop. A four-story building and slum areas near-by.	City traffic typically seen in residential and business areas, and cooking by slum dwellers.
Delhi	National Physical Laboratory Dr. K. S. Krishnan Marg New Delhi - 110012 India	Urban Residential	Sampler placed 5 m above ground on an office building rooftop in the NPL campus. Unobstructed space around.	City traffic typically seen in residential and business areas, and cooking by slum dwellers.
Kolkata	NEERI Zonal Laboratory I-8, Sector-C, East Kolkata P.O. Box Haltu, Kolkata 700078 India	Urban Residential	Sampler on a 2 meter platform located in an open field. Ruby General Hospital and a diesel truck garage nearby.	City traffic typically seen in residential and business areas, cooking by slum dwellers, and some emission from combustion by diesel trucks parked in nearby garage.

The Chandigarh site needed to be outside the limit of the main town and thus was located at the Postgraduate Institute of Medical Education and Research on a rooftop on the fourth floor. Figure 3.2 shows the sampling schedule that was followed during the year 2001.

Figure 3.2. Diagram of the 24-hr averaging sampling schedule at four Indian cities.

Sampling started on March 4, 2001 and continued until January 16, 2002. Samples were collected at ambient temperatures and relative humidities for 24 hours starting at midnight local time every sixth day for each of the months sampled. After the completion of the sampling campaign, there were 21 samples for Delhi, 25 samples for Mumbai, 20 samples for Kolkata, and 5 samples for Chandigarh. These samples were chemically analyzed, and the results are

described in this paper. A second paper will be presented with findings from the organic speciation work.

3.3.2. Instrumental Setup

A Caltech-built, PM$_{2.5}$ filter sampler was used at each of the four sites. Sampling equipment is shown schematically in Figure 3.3.

* TU1 and TU2 are teflon filters, NU1 and ND1 are undenuded nylon filter and denuded nylon filter respectively, and QU1 is a quartz fiber filter.

Figure 3.3. Schematic diagram of the sampling unit.

Fine particulate matter was collected on one quartz fiber filter (Pallflex, 2500 QAO, 47 mm diameter), two pre-washed Nylon Filters (Gelman Sciences, Nylasorb, 47 mm diameter), and on two PTFE filters (Gelman Sciences, Teflo, 1.0 μm pore size). Ambient air was drawn at a rate of approximately 22.5 lpm through an acid-washed Pyrex glass inlet line to a Teflon-coated Air and Industrial Hygiene Laboratory (AIHL)-design cyclone separator [John and Reischl, 1980], which removed large particles with a collection efficiency curve having a 50% aerodynamic cutoff diameter at 2.5 μm before the air passed through the filters. The nylon filter located downstream of the MgO-coated diffusion denuder was used in conjunction with the nylon filter downstream of the cyclone alone to measure gas-phase nitric acid, hydrochloric acid, and fine particle nitrate by the denuder difference method. The air flowrate through each filter was measured before and after each 24-hour sampling period with a calibrated rotameter.

3.3.3. Analytical Methods:

Unexposed filters and exposed samples were kept in individual Petri dishes and sealed with Teflon tape. Filters and samples were shipped between the United States and India using ice-coolers with blue-ice packets to ensure that the temperature of the filters during shipment (3-5 days) would remain cool to prevent sample degradation. All PTFE filters were gravimetrically analyzed at Georgia Tech by the same operator by repeated weighing before and after the experiment on a Mettler Toledo microbalance maintained in a temperature- and humidity-

controlled environment (20.5 ± 0.2°C, 39 ± 2% RH). Once weighing was completed, samples were stored in freezers until chemical analysis.

One of each pair of PTFE filter samples was analyzed by ion chromatography (Dionex Corp, Model 2020i) for the anions NO_3^-, SO_4^{2-}, and Cl^- [Mulik, 1976, Derrick and Moyers, 1981] and by an indophenol colorimetric procedure for NH_4^+ [Bolleter, 1976] using an Alpkem rapid flow analyzer (Model RFA-300). The second set of each of these sample sets was analyzed for trace elements using X-Ray Fluorescence (XRF) by the Desert Research Institute (DRI). Quartz fiber substrates were analyzed for elemental and organic carbon content using the thermal-optical carbon analysis method of Huntzicker et al. [1982] as modified by Birch and Cary [1996]. In the thermal evolution and combustion method of Birch and Cary [1996], elemental carbon is defined as carbon that resists volatilization up to a temperature of 900°C in an inert atmosphere in a manner similar to graphite, and also is black. In this paper, we will use the term Elemental Carbon (EC) to define the carbon detected by this method. Variations in elemental carbon values between alternative methods can arise due to differences in the way that alternative methods correct for charring of the samples during analysis. Table 3.2 lists the analytical methods being used to analyze the various samples.

Table 3.2. Analytical methods used for physical and for chemical analysis of the filter substrates.

Species of Interest	Instrument Used	Method Used
Mass	Mettler model M-55-A mechanical microbalance	Gravimetric Analysis by repeated weighing before and after the experiment. Microbalance maintained in a temperature and humidity-controlled environment ($21.0 \pm 0.2^{o}C$, $39 \pm 3\%$ RH)
Sulfate Ion Chloride Ion Nitrate Ion	Dionex Corporation, Model 2020i	Ion Chromatography described by Mulik et al., 1976
Ammonium Ion	Alpkem rapid flow analyzer (Model RFA-300)	Indophenol Colorimetric Procedure described in Bolleter et al., 1961
Elemental Carbon Organic Carbon	Carbon Analyzer	Thermal-optical carbon analysis method of Huntzicker et al. [1982] as modified by Birch and Cary [1996]
Trace Elements	XRF	X-Ray Fluorescence Analysis by Desert Research
Organic Speciation	GCMS	Schauer et al., 1996 and 2000; Zheng et al., 2002; Sheesley et al., 2003

3.4. Results and Discussion

3.4.1. Regional Meteorology and Particulate Matter Concentrations:

Monsoon winds and rains control the extent of pollution seen over many of the South and East Asian countries like India and China. Monsoon winds, which come from the Southwest during the months of June, July, August, and part of September, are characterized by heavy rain

and winds. The monsoon gathers moisture over the Indian Ocean and releases it over South and Southeast Asia. Conversely, the predominant wind direction during the winter is from the Northeast, and is characterized by a dry air mass producing almost no rain as the air mass travels over continental landmass. Because of this regional wind pattern, rain scavenging during the summer causes a decrease in concentrations of fine particulate matter. This trend of decreasing aerosol mass during the summer monsoon has been captured in the present study and can be seen in Figures 3.4 and 3.5 which show the seasonal variations of the fine particle mass and chemical composition over Mumbai, Delhi, Kolkata, and Chandigarh.

Figure 3.4. Fine particulate mass concentrations in Delhi, Mumbai, Kolkata, and Chandigarh (2001). The dashed line represent the standards set by the US EPA.

Average fine particle mass concentrations during summer were 49 ± 0.6 μg m^{-3} in Delhi, 21 ± 1.4 μg m^{-3} in Mumbai, 27 ± 0.5 μg m^{-3} in Kolkata, and 29 ± 0.7 μg m^{-3} in Chandigarh. It was surprising to see summertime ambient fine particulate matter concentrations in Chandigarh exceeding those of Mumbai and Kolkata. Both Mumbai and Kolkata are located near the Arabian Sea and the Bay of Bengal respectively; whereas Delhi and Chandigarh are located in the middle of the Indian subcontinent. Five years (Jan 1995 to Dec 1999) of backwind trajectory analysis conducted by NOAA revealed that 62% of all trajectories arriving at Delhi during that time period experienced stagnation (personal communication, Joyce M. Harris, NOAA). Heavy rains and proximity to the ocean with the influence of diurnal land and sea breezes aiding in the dilution of the aerosol concentration reduce levels in Mumbai and Kolkata (as seen in the results section, significant amount of Na$^+$ is present signifying presence of sea salts). Of the locations monitored, Delhi records the highest fine particle mass concentrations throughout the year except for the month of December when Kolkata's fine particle mass concentrations exceed those observed in Delhi.

Figure 3.5. Chemical composition and seasonal variations in fine particle mass in (a) Delhi, (b) Mumbai, and (c) Kolkata.

The highest concentrations of aerosol mass are seen during the month of December, representing the winter season in all of the three cities sampled (no sample was taken in Chandigarh during winter). Average fine particle mass concentrations during the winter were 231 ± 1.6 μg m^{-3} in Delhi, 89 ± 0.5 μg m^{-3} in Mumbai, and 305 ± 1.1 μg m^{-3} in Kolkata. During the winter month of December, more stagnation and less rain scavenging occurs in cities like Delhi,

causing aerosol particles to remain suspended over the city for an extended period of time. Also, the lower solar insolation rates during the winter months lead to lower atmospheric inversion layers where pollutants become trapped close to the ground, further increasing fine particle concentrations.

India has yet to set a fine particle standard. In the absence of a fine particle standard, the US EPA's 24-hour $PM_{2.5}$ standard of 65 μg m^{-3} can be used to show the severity of the particulate pollution in India. The current study shows that most of the observed $PM_{2.5}$ concentrations in Delhi and the wintertime $PM_{2.5}$ concentrations in both Mumbai and Kolkata exceed the daily EPA $PM_{2.5}$ standard. Table 3.3 shows the US EPA's pollutant standard index for $PM_{2.5}$ which can be used for general assessment of health risks from existing air quality. 24-hr average of $PM_{2.5}$ concentration in the range of 40.5-65.4 μg m^{-3} is considered as unhealthy for sensitive groups, 65.5-150.4 μg m^{-3} as unhealthy, 150.5-250.4 μg m^{-3} as very unhealthy, and above 250 μg m^{-3} as hazardous.

Table 3.3. Health risks from air quality in Delhi, Mumbai, and Kolkata using EPA's pollutant standard index.

	Unhealthy for Sensitive Groups[*1]	Unhealthy[*2]	Very Unhealthy[*3]	Hazardous[*4]
Delhi (21 samples)	Jul 2, 8	March 4, 10, 16, 22, 28 June 8, 14 Oct 11, 17	Oct 5 Dec 17, 23, 29 Jan 10, 16	Jan 4
Mumbai (25 samples)	Mar 4, 19 Dec 23	Oct 17, 23, 29 Nov 4, 10 Dec 5, 11, 17, 29 Jan 4, 10		
Kolkata (19 samples)	Mar 22, 28 Apr 3 Oct 11, 23	Mar 16		Dec 5, 11, 17, 23, 29

[*1] Unhealthy for Sensitive Groups: Increasing likelihood of respiratory symptoms in sensitive individuals, aggravation of heart of lung disease and premature mortality in persons with cardiopulmonary disease and the elderly.

[*2] Unhealthy: Increased aggravation of heart or lung disease and premature mortality in persons with cardiopulmonary disease and the elderly; increased respiratory effects in general population

[*3] Very Unhealthy: Significant aggravation of heart or lung disease and premature mortality in persons with cardiopulmonary disease and the elderly; significant increase in respiratory effects in general population.

[*4] Hazardous: Serious aggravation of heart or lung disease and premature mortality in persons with cardiopulmonary disease and the elderly; serious risk of respiratory effects in general population.

Wintertime air quality in Kolkata, Delhi, and Mumbai can be considered to be hazardous, very unhealthy, and unhealthy, respectively. Out of 21 samples collected in Delhi, the $PM_{2.5}$ concentrations from 16 samples are in the "unhealthy" or worse than "unhealthy" range. $PM_{2.5}$ is responsible for respiratory problems such as asthma and bronchitis, as well as reduction in visibility (Dockery et al., 1993). In a local Indian newspaper, Ms. Anumita Roy Chowdhury, a researcher at the Delhi-based Center for Science and Environment (CSE), mentioned that each year, air-pollution-related diseases claim some 52,000 lives in 36 Indian cities, including the

capital New Delhi where the toll is 10,000. Particle pollution is so widespread that many visitors landing in Delhi by air during the winter time observe the thick haze over the city. Because of low visibility, flights to and from Delhi may be cancelled during the wintertime.

3.4.2. Fine Particle Chemical Analysis Results:

Organic matter is the highest contributor to the fine particle concentrations for all four cities sampled. Organic matter has been calculated by multiplying organic carbon by 1.4 to account for the H, O, N, and other elements typically found in organic matter. Seasonal variations in organic matter (OM) and elemental carbon (EC) were observed. OM and EC concentrations increase during the winter season compared to the rest of the year (see Figure 3.5 and Table 3.4).

Table 3.4. Seasonal chemical composition and percentage contribution to fine particle mass in (a) Delhi, (b) Mumbai, (c) Kolkata, and (d) Chandigarh.

(a)

Delhi	Spring	1σ	% of PM$_{2.5}$	Summer	1σ	% of PM$_{2.5}$	Fall	1σ	% of PM$_{2.5}$	Winter	1σ	% of PM$_{2.5}$
Unidentified	12.9	N/A	11.3%	5.49	N/A	11.1%	29.9	N/A	18.8%	7.63	N/A	3.3%
Nitrate	2.50	0.16	2.2%	1.51	0.14	3.1%	3.63	0.26	2.3%	16.8	0.76	7.3%
Chloride	8.81	0.16	7.7%	0.50	0.08	1.0%	1.44	0.13	0.9%	15.3	0.46	6.6%
Ammonium	7.22	1.89	6.3%	1.96	0.05	4.0%	4.42	0.10	2.8%	12.1	0.31	5.3%
Sulfate	9.61	0.14	8.4%	5.16	0.12	10.4%	10.06	0.22	6.3%	18.8	0.65	8.1%
Sodium	0.25	0.16	0.2%	0.29	0.17	0.6%	0.10	0.31	0.1%	0.08	0.33	0.0%
Potassium	1.97	0.08	1.7%	0.65	0.03	1.3%	3.34	0.17	2.1%	2.09	0.11	0.9%
Non-Crustal Metals	1.28	0.84	1.1%	1.04	0.95	2.1%	1.99	1.29	1.3%	2.05	1.24	0.9%
Crustal Oxides	7.65	0.61	6.7%	6.28	0.55	12.7%	12.4	0.92	7.8%	4.52	0.65	2.0%
Organic Matter	52.9	2.65	46.3%	22.6	1.14	45.6%	80.3	4.03	50.5%	134.1	6.71	58.1%
Elemental Carbon	9.11	0.46	8.0%	4.04	0.21	8.2%	11.5	0.58	7.2%	17.4	0.88	7.5%
Avg PM2.5	114.2	2.76	100.0%	49.5	0.64	100.0%	159.1	0.63	100.0%	230.9	1.60	100.0%

(b)

Mumbai	Spring	1σ	% of PM$_{2.5}$	Summer	1σ	% of PM$_{2.5}$	Fall	1σ	% of PM$_{2.5}$	Winter	1σ	% of PM$_{2.5}$
Unidentified	4.16	N/A	11.6%	5.47	N/A	26.1%	9.98	N/A	15.6%	4.55	N/A	5.1%
Nitrate	0.68	0.11	1.9%	0.93	0.17	4.4%	1.88	0.14	2.9%	2.87	0.16	3.2%
Chloride	0.11	0.05	0.3%	2.43	0.09	11.6%	0.60	0.07	0.9%	0.65	0.08	0.7%
Ammonium	1.18	0.04	3.3%	0.40	0.07	1.9%	2.33	0.06	3.6%	4.17	0.06	4.7%
Sulfate	5.58	0.12	15.5%	3.13	0.15	14.9%	7.90	0.16	12.4%	10.9	0.26	12.3%
Sodium	0.33	0.06	0.9%	1.38	0.13	6.6%	0.23	0.12	0.4%	0.22	0.18	0.2%
Potassium	0.59	0.03	1.6%	0.19	0.01	0.9%	0.85	0.05	1.3%	1.21	0.06	1.4%
Non-Crustal Metals	0.39	0.70	1.1%	0.29	0.71	1.4%	0.76	0.82	1.2%	1.05	0.84	1.2%
Crustal Oxides	5.88	0.43	16.4%	3.36	0.40	16.0%	5.69	0.50	8.9%	8.09	0.57	9.1%
Organic Matter	13.3	0.67	37.1%	2.30	0.13	11.0%	28.1	1.41	44.0%	47.0	2.36	52.8%
Elemental Carbon	3.71	0.19	10.3%	1.09	0.06	5.2%	5.57	0.28	8.7%	8.22	0.42	9.2%
Avg PM2.5	35.9	2.33	100.0%	21.0	1.38	100.0%	63.9	2.40	100.0%	88.9	0.54	100.0%

(c)

Kolkata	Spring	1σ	% of PM$_{2.5}$	Summer	1σ	% of PM$_{2.5}$	Fall	1σ	% of PM$_{2.5}$	Winter	1σ	% of PM$_{2.5}$
Unidentified	1.99	N/A	3.6%	0.80	N/A	3.0%	1.17	N/A	2.6%	15.9	N/A	5.2%
Nitrate	1.07	0.12	2.0%	0.83	0.14	3.2%	0.51	0.12	1.1%	9.09	0.36	3.0%
Chloride	0.37	0.06	0.7%	0.20	0.07	0.7%	0.19	0.06	0.4%	8.69	0.29	2.9%
Ammonium	2.18	0.05	4.0%	0.52	0.05	2.0%	1.32	0.05	3.0%	10.2	0.14	3.4%
Sulfate	8.70	0.14	15.9%	3.00	0.12	11.4%	3.98	0.10	8.9%	13.2	0.31	4.3%
Sodium	0.31	0.10	0.6%	0.27	0.08	1.0%	0.12	0.15	0.3%	0.02	0.35	0.0%
Potassium	1.08	0.06	2.0%	0.38	0.02	1.4%	0.75	0.04	1.7%	3.75	0.19	1.2%
Non-Crustal Metals	0.48	0.93	0.9%	0.44	0.87	1.7%	1.08	1.00	2.4%	3.76	1.54	1.2%
Crustal Oxides	6.17	0.49	11.3%	2.54	0.35	9.6%	1.85	0.41	4.1%	7.99	1.00	2.6%
Organic Matter	26.3	1.32	48.0%	10.9	0.55	41.1%	24.7	1.24	55.1%	205.3	10.27	67.4%
Elemental Carbon	6.08	0.31	11.1%	6.59	0.33	24.9%	9.09	0.46	20.3%	26.5	1.33	8.7%
Avg PM2.5	54.7	1.63	100.0%	26.5	0.45	100.0%	44.7	0.56	100.0%	304.5	1.13	100.0%

(d)

Chandigarh	Spring	1σ	% of PM$_{2.5}$	Summer	1σ	% of PM$_{2.5}$	Fall	1σ	% of PM$_{2.5}$	Winter	1σ	% of PM$_{2.5}$
Unidentified	N/A	N/A	N/A	4.63	N/A	15.8%	N/A	N/A	N/A	N/A	N/A	N/A
Nitrate	N/A	N/A	N/A	0.72	0.15	2.5%	N/A	N/A	N/A	N/A	N/A	N/A
Chloride	N/A	N/A	N/A	0.15	0.08	0.5%	N/A	N/A	N/A	N/A	N/A	N/A
Ammonium	N/A	N/A	N/A	1.95	0.06	6.7%	N/A	N/A	N/A	N/A	N/A	N/A
Sulfate	N/A	N/A	N/A	4.73	0.13	16.2%	N/A	N/A	N/A	N/A	N/A	N/A
Sodium	N/A	N/A	N/A	0.16	0.24	0.5%	N/A	N/A	N/A	N/A	N/A	N/A
Potassium	N/A	N/A	N/A	0.58	0.03	2.0%	N/A	N/A	N/A	N/A	N/A	N/A
Non-Crustal Metals	N/A	N/A	N/A	1.06	1.48	3.6%	N/A	N/A	N/A	N/A	N/A	N/A
Crustal Oxides	N/A	N/A	N/A	3.89	0.57	13.3%	N/A	N/A	N/A	N/A	N/A	N/A
Organic Matter	N/A	N/A	N/A	10.0	0.51	34.4%	N/A	N/A	N/A	N/A	N/A	N/A
Elemental Carbon	N/A	N/A	N/A	1.32	0.07	4.5%	N/A	N/A	N/A	N/A	N/A	N/A
Avg PM2.5	N/A	N/A	N/A	29.2	0.70	100.0%	N/A	N/A	N/A	N/A	N/A	N/A

The percentage of OM and EC in the fine particle mass are 46% OM and 8.2% EC in Delhi during the summer and 58% OM and 7.5% EC in Delhi during the winter; 11% OM and 5.2% EC in Mumbai during the summer and 53% OM and 9.2% EC during the winter; 41% OM and 25% EC in Kolkata during the summer and 67% OM and 8.7% EC in Kolkata during the winter; and 34% OM and 4.5% EC in Chandigarh for the summer. Approximately half of all measured $PM_{2.5}$ is organic in nature and the concentrations of both OM and EC increase during the winter. To explain this seasonality in OM and understand the sources of this organic matter, it is important to conduct organic speciation and observe target organic compounds individually by season. The results of the organic speciation work will be presented in a future paper.

Elemental carbon (EC) and organic matter (OM) are emitted mostly from burning fossil fuels and biomass [Andreae, 1995]. From previous source testing, it has been found that biomass burning in India has a lower ratio of EC to OC compared to fossil fuel burning [Sheesley, 2003; Chowdhury et al., 2004]. The ratio of EC to OC is highest during the month of June for all the three sites. This ratio reaches unity during June in both Mumbai and Kolkata, whereas in Delhi this ratio is approximately 0.3. However, the EC to OC ratio decreases to 0.2 to 0.4 during the remainder of the year in all three sites. A high EC to OC ratio signifies the dominance of fossil fuel burning over biomass burning. From this ratio analysis, it appears biomass burning increases during the winter leading to a lower EC to OC ratio during the winter.

Of the fine particle mass, sodium and potassium contribute 0.03-0.60% and 0.9-2.1% respectively in Delhi, 0.2-6.6% and 0.9-1.6% respectively in Mumbai, 0.01-1.0% and 1.2-2.0% respectively in Kolkata, and 0.5% and 2.0% in Chandigarh. High sodium concentrations are

predominantly seen during the summer, indicating presence of marine aerosol (sea salts in the form of NaCl) in all of the cities, especially in Mumbai where 6.6% of the fine particle mass during June is from sodium ion. The Southwest monsoon carry sea salts from both the Bay of Bengal and the Arabian Sea. Presence of potassium has traditionally been linked to biomass burning; however, potassium can also come from marine aerosol and soil dust. According to Stumm and Morgan [1996, pg 308], the concentration ratio of K^+ to Na^+ in sea water is approximately 0.03. In this study, ratios of K^+ to Na^+ in the ambient samples were in the range of 2 to 32 for Delhi, 0.1 to 5 for Mumbai, 1 to 156 for Kolkata, and 4 for summer time Chandigarh. The higher ratios were typically seen during the colder months. From this ratio analysis it appears that biomass burning occurs in all four cities peaking during the colder period.

Crustal oxide has been calculated by adding the oxides of aluminum, silicon, calcium, titanium, iron, and phosphorus. Relative contributions of crustal oxides or dust to the fine particle mass reach a peak during the spring and summer in all of the cities. During this time, contributions of dust to the fine particle mass are 6-13% in Delhi, 16% in Mumbai, 10-11% in Kolkata, and 13% in Chandigarh. These crustal elements are probably emitted principally in the form of fugitive dust. Al and Si are used as markers for dust as they are present as alumino-silicates or clay minerals. Carrico et al. [2003] conclude that in Nepal, long range transport of desert dust from arid regions is observed to the Indian subcontinent. They hypothesize that this dust comes from West India, the Middle East and perhaps as far as the Sahara. Saharan dust production peaks in March [Marticorena et al., 1997]. African dust transported eastward into the Middle East peaks in April [Ganor, 1994, Moulin et al., 1998]. Effects of long range transport of desert dust may be present in these samples during peak dust seasons. However, Mumbai seems

to experience high dust concentration throughout the year, possibly because of the heavy roads and buildings construction in the city.

Non-crustal metals (e.g., V, Cr, Mn) contribute only about 1% to the fine particle mass in all of the three cities. Concentrations of trace metals, as measured by XRF, can be found in Table 3.5.

Table 3.5. Trace metal concentrations in μg m^{-3} in the ambient fine particle in Delhi, Mumbai, and Kolkata during the year 2001.

	Delhi		Mumbai		Kolkata	
	Annual Avg	Std Dev	Annual Avg	Std Dev	Annual Avg	Std Dev
Mg	0.1161	0.0997	0.1627	0.0349	0.0613	0.1206
Al	0.6126	0.0395	0.4808	0.0314	0.4041	0.0309
Si	1.7444	0.0902	1.3428	0.0699	1.1916	0.0627
P	0.0000	0.0246	0.0019	0.0192	0.0008	0.0208
K	1.7613	0.0900	0.7880	0.0415	1.4908	0.0763
Ca	0.6123	0.0346	0.7331	0.0387	0.3667	0.0224
Ti	0.0472	0.0550	0.0487	0.0531	0.0434	0.0521
V	0.0040	0.0340	0.0066	0.0298	0.0037	0.0290
Cr	0.0134	0.0068	0.0082	0.0058	0.0032	0.0057
Mn	0.0516	0.0039	0.0234	0.0025	0.0307	0.0030
Fe	0.6665	0.0338	0.7142	0.0361	0.5013	0.0256
Co	0.0000	0.0110	0.0000	0.0116	0.0001	0.0085
Ni	0.0057	0.0017	0.0131	0.0014	0.0023	0.0025
Cu	0.0845	0.0047	0.0638	0.0038	0.0492	0.0030
Zn	0.4476	0.0227	0.1606	0.0087	0.2783	0.0144
Ga	0.0041	0.0088	0.0027	0.0056	0.0061	0.0118
As	0.0074	0.0924	0.0022	0.0247	0.0127	0.1368
Se	0.0033	0.0052	0.0026	0.0038	0.0030	0.0063
Br	0.0503	0.0040	0.0222	0.0020	0.0235	0.0043
Rb	0.0043	0.0030	0.0021	0.0029	0.0041	0.0024
Sr	0.0051	0.0026	0.0069	0.0016	0.0032	0.0026
Y	0.0050	0.0075	0.0020	0.0045	0.0065	0.0099
Zr	0.0034	0.0048	0.0028	0.0047	0.0026	0.0053
Mo	0.0037	0.0105	0.0047	0.0093	0.0041	0.0105
Pd	0.0011	0.0237	0.0005	0.0224	0.0009	0.0234
Ag	0.0084	0.0289	0.0217	0.0239	0.0052	0.0293
Cd	0.0108	0.0301	0.0040	0.0278	0.0154	0.0253
In	0.0066	0.0347	0.0047	0.0316	0.0042	0.0337
Sn	0.0138	0.0439	0.0081	0.0434	0.0146	0.0442
Sb	0.0149	0.0553	0.0039	0.0511	0.0104	0.0525
Ba	0.0480	0.1960	0.0646	0.1688	0.0503	0.1945
La	0.0787	0.2814	0.0514	0.2704	0.0483	0.2858
Au	0.0147	0.0184	0.0079	0.0102	0.0083	0.0155
Hg	0.0040	0.0085	0.0044	0.0072	0.0023	0.0092
Tl	0.0001	0.0182	0.0008	0.0089	0.0004	0.0256
Pb	0.5769	0.0300	0.1371	0.0093	0.8586	0.0443
U	0.0037	0.0080	0.0035	0.0072	0.0031	0.0079

It is interesting to note that the annual average lead concentrations were 0.58 ± 0.03 μg m^{-3}, 0.14 ± 0.01 μg m^{-3} and 0.86 ± 0.04 μg m^{-3} in Delhi, Mumbai, and Kolkata respectively. Lead concentrations seem to increase during the colder months leading to concentrations as high as 2.4 μg m^{-3} in Delhi (January 4, 2002), 0.5 μg m^{-3} in Mumbai (December 11, 2001), and 3.4 μg m^{-3} in Kolkata (December 17, 2001). In 1992, Shahandra in Delhi recorded the highest annual average of 8.5 μg m^{-3} [Aggarwal, 1999]. Lead has been added traditionally to petrol as anti-knock agents to raise its octane level. Removing the lead from petrol can virtually eliminate the largest source of lead in the cities using leaded fuel since it is the primary source of airborne lead emissions in such Indian cities. Unleaded petrol was introduced in Delhi and by September 1, 1998 Delhi became lead free. However, our results show that lead is still present in these cities, probably from re-entrainment of lead-laden dust, from smelter activities, or from residual lead in automobile systems.

Vehicular traffic in most Indian cities is disproportionately dominated by extremely polluting vehicles [Aggarwal et al., 1999]. In December 1998, Saifuddin Soz, then the Union Minister for Environment and Forests, issued a white paper on Delhi's pollution mentioning that while the relative contribution of industries and domestic sources to total air pollution load in Delhi has been steadily declining since 1970, the contribution of automobile emissions has been increasing dramatically. Under Supreme Court orders, the Ministry of Petroleum and Natural Gas (MPNG) introduced diesel with a 500 ppm wt sulfur content in the severely polluted cities of Delhi, Mumbai, and Kolkata. Table 3.6 describes the changes in sulfur specifications that took place during the year 2001 in all of the three Indian megacities.

Table 3.6. Diesel sulfur specifications in Delhi, Kolkata, and Mumbai.

City	Private diesel vehicles	All diesel vehicles
Delhi	2500 ppm wt until April 2000, 500 ppm wt thereafter	2500 ppm wt until March 2001, 500 ppm wt thereafter
Kolkata	2500 ppm wt until July 2001, 500 ppm wt thereafter	2500 ppm wt until October 2001, 500 ppm wt thereafter
Mumbai	2500 ppm wt until January 2001, 500 ppm wt thereafter	2500 ppm wt until October 2001, 500 ppm wt thereafter

All three Indian cities have switched sulfur content for all vehicles from 2500 ppm wt to 500 ppm wt at different months during the year 2001. As seen in Figure 3.6, reduction in sulfur content of diesel fuel appears to have decreased the ambient measured sulfate in all three. Continuation of similar measurements would support the validity of this finding.

Figure 3.6. Particulate sulfate trend in Indian cities in 2001 and changes in diesel sulfur specifications. The vertical dashed lines represent the timeline when fuel specification changes occurred in each of the four cities.

3.5. Conclusions

Chemically-detailed particulate matter characterization for Delhi, Mumbai, Kolkata, and Chandigarh were also conducted during the year 2001. For the period studied, average fine particle mass concentration during the winter season in Delhi was 231 ± 1.6 μg m^{-3}, in Mumbai was 89 ± 0.5 μg m^{-3}, and in Kolkata was 305 ± 1.1 μg m^{-3} and average fine particle mass

concentration during the summer in Delhi was 50 ± 0.6 μg m^{-3}, in Mumbai was 21 ± 1.4 μg m^{-3}, in Kolkata was 27 ± 0.5 μg m^{-3}, and in Chandigarh was 9 ± 0.7 μg m^{-3}. Most of the observed $PM_{2.5}$ concentrations in Delhi and the wintertime $PM_{2.5}$ concentrations in both Mumbai and Kolkata exceeded the U.S. EPA 24-hour average $PM_{2.5}$ standard of 65 μg m^{-3} signifying unhealthy air quality. Organic matter (OM), elemental carbon (EC), NO_3^-, SO_4^{2-}, Cl^-, NH_4^+, and trace metals were also analyzed, and OC and sulfate dominate total mass. These measurements provide important information about the seasonal and spatial distribution of fine particle-phase inorganic compounds in India.

3.6. Acknowledgement

3.7. References

Aggarwal, A. L., N. Sunita, and S. Sen (Eds.) (1999), *The citizens' fifth report*, Centre for Science and Environment, New Delhi, India.

Andrea, M. O. 1995. *Future climates of the world*, edited by A. Henderson-Sellers, Elsevier, New York.

Birch, M. E., and R. A. Cary (1996), Elemental carbon-based method for monitoring occupational exposures to particulate diesel exhaust, *Aerosol Sci. Technol.*, 25, 221-241.

Bolleter, W.T., C. T. Bushman, and P. W. Tidwell (1961), Spectrophotometric determinations of ammonium as indophenol, *Anal. Chem., 33*, 592-594.

Carrico, C.M., Bergin, M.H., Shrestha, A.B., Dibb, J.E., Gomes, L., Harris, J.M., Th e importance of carbon and desert dust to seasonal aerosol properties in the Nepal Himalaya, *Atmos. Environ.*, in press, 2003.

Chowdhury, Zohir ; L. S. Hughes, L. S. Salmon, G. R. Cass (2001), Atmospheric particle size and composition measurements to support light extinction calculations over the Indian Ocean, J. Geophys. Res., *Vol. 106 (D22)*, p. 28,597.

Chowdhury Zohir; Schauer, James J.; Cass, Glen R.; and Adel Serefin (2004), Size Distribution and Chemical Composition from Chinese, Indian, and Bangladeshi Coal Smoke, manuscript in preparation.

Christoforou, C. S., Salmon, L. S., Hannigan, M. P., Solomon, P. A., and Cass, G. R. (2000), Trends in Fine Particle Concentration and Chemical Composition in Southern California, Journal of the Air and Waste Management Association, *50*, 43-53.

Derrick, M. and Moyers, J.L. (1981), Precise and sensitive water soluble ion extraction method for aerosol samples collected on polytetrafluoroethylene filters. Analyt. Lett., *9*, 1637.

Dockery, D.W., C. A. Pope, X. P. Xu, J. D. Spengler, J. H. Ware, M. E. Fay, B. G. Ferris, and F. E. Speizer (1993), An association between air-pollution and mortality in 6 United-States cities, *New England Journal of Medicine, 329,* 1753-1759.

Ganor, E. (1994), The frequency of Saharan dust episodes over Tel Aviv, *Atmos. Environ., 28,* 17, 2867-2871.

Huntzicker, J. J., R. L. Johnson, J. J. Shah, and R. A. Cary (1982), Analysis of organic and elemental carbon in ambient aerosols by a thermal-optical method, *Particulate Carbon, Atmospheric Life Cycle*, edited by G. T. Wolff and R. L. Klimisch, pp. 79-88, Plenum, New York.

John, W. and G. Reischl (1980), A cyclone for size-selective sampling of ambient air, *J. Air Pollut. Control Assoc., 30,* 872-876.

Kowalczyk, G. S., C. E. Choquette, and G. E. Gordon (1978), Chemical element balances and identification of air pollution sources in Washington, DC., *Atmos. Environ.*, 12, 1143-1154.

Marticorena, B., G. Bergametti, B. Aumont, Y. Callot, C. N'Doume', and M. Legrand (1997), Modeling the atmospheric dust cycle. 2. Simulation of Saharan dust sources, *J. Geophys. Res., 102* (D4) 4,387-4,404.

Moulin, C., C. E. Lambert, U. Dayan, V. Masson, M. Ramonet, P. Bousquet, M. Legrand, Y. J. Balkanaski, W. Guelle, B. Marticorena, G. Begametti, and F. Dulac (1998), Satellite climatology of African dust transport in the Mediterranean atmosphere, *J. Geophys. Res*., *103* (D11), 13,137-13,144.

Mulik, J., R. Puckett, D. Williams, and E. Sawicki (1976), Ion chromatographic analysis of sulfate and nitrate in ambient aerosols, *Anal. Lett., 9*, 653-663.

NEERI (2000), Ambient Air Quality Status for Ten Cities of India, *Report*, National Environmental Engineering Research Institute, Nagpur, India, October 2000.

Pope, C. A. III, R. T. Burnett, M. J. Thun, et al., 2002, "Lung cancer, cardiopulmonary mortality, and long-term exposure to fine particulate air pollution," *JAMA, 287*, 1,132-1,141.

Ramanathan, V. , P. J. Crutzen, J. Lelieveld, A. P. Mitra, D. Althausen, J. Anderson, M. O. Andreae, W. Cantrell, G. R. Cass, C. E. Chung, A. D. Clarke, J. A. Coakley, W. D. Collins, W. C. Conant, F. Dulac, J. Heintzenberg, A. J. Heymsfield, B. Holben, S. Howell, J. Hudson, A. Jayaraman, J. T. Kiehl, T. N. Krishnamurti, D. Lubin, G. McFarquhar, T. Novakov, J. A. Ogren, I. A. Podgorny, K. Prather, K. Priestley, J. M. Prospero, P. K. Quinn, K. Rajeev, P. Rasch, S. Rupert, R. Sadourny, S. K. Satheesh, G. E. Shaw, P. Sheridan, and F. P. J. Valero (2001), Indian Ocean Experiment: An integrated analysis of the climate forcing and effects of the great Indo-Asian haze, *J. Geophys. Res. Vol. 106* (D22) p. 28,371-28,398.

Schauer, J. J. W. F. Rogge, L. M. Hildemann, M. A. Mazurek, and G. R. Cass (1996), Source apportionment of airborne particulate matter using organic compounds as tracers, *Atmospheric Environment,* 30 (22), 3837-3855.

Schauer, J. J. and G. R. Cass (2000), Source apportionment of wintertime gas-phase and particle-phase air pollutants using organic compounds as tracers, *Environmental Science and Technology*, 34 (9), 1821-1832.

Stumm, W and Morgan, J. J. (1996). Aquatic Chemistry: chemical equilibria and rates in natural waters, third edition, John Wiley & Sons, Inc., New York.

Venkataraman, C., C. K. Reddy, S. Josson, and M. S. Reddy (2002), Aerosol Chemical and Size Characteristics at Mumbai, India, during the INDOEX-IFP (1999), *Atmospheric Environment, 36* (12)*, 1979-1991*.

Zheng, M., G. R. Cass, J. J. Schauer, E. S. Edgerton (2002), Source apportionment of PM2.5 in the Southeastern United States using solvent-extractable organic compounds as tracers," *Environmental Science and Technology*, 36, 2361-2371.

CHAPTER-4

Size distributed chemical composition of fine particles emitted from burning Indian subcontinent biomass

4.1. Abstract

A pair of micro-orifice uniform deposit impactors (MOUDIs) was used to measure the fine and ultrafine aerosol size distributions and chemical composition from many of the important biomass combustion sources found in the Indian subcontinent. A dilution source sampling system was used to collect the exhaust, and to cool and dilute the source emissions before measurement. The sources tested in this study were dried cowdung patties, ricestraw, coconut branches, jackfruit wood, and synthetic biomass fuel originating from Bangladesh. The particle mass distributions from the five biomass samples have a single mode that peaks at 0.18-0.32 μm particle aerodynamic diameter. Particles emitted from biomass burning are mostly organic matter (57-62%) and elemental carbon (2-8%) in nature with significant amount of chloride ion (2-9%)

present. Size distribution from several trace elements (Na, Cl, K, Al, Cr, Mn, Co, Zn, Br, Cd, La, Ce, Cs, Eu, Th, Nd, As, Mg, Sb) has also been shown. The purpose of these experiments was to examine the emissions that occur when biomass is burned under conditions similar to a chula which is typically used in the Indian subcontinent. The data obtained from these source tests will prove useful in constructing and evaluating regional emission inventory and assessing source impacts on air quality.

4.2. Introduction

Biomass burning has a significant impact on global atmospheric chemistry since it provides large sources of particulate matter as well as carbon monoxide, nitrogen oxides, and hydrocarbons, primarily in the tropics [*Crutzen et al.*, 1979, *Logan et al.*, 1981]. Two notable components of biomass burning are the incineration of wood, charcoal and agricultural waste as household fuel, and the combustion of crop residue in open fields. As the developing world population continues to rise, the contributions from these types of biomass burning increase [*Woods and Hall*, 1994]. The work of Woods and Hall [1994] has been seminal in shifting the focus of study of biomass combustion in the developing world from the use of fuelwood to a more comprehensive picture of "biofuels" combustion including the burning of crop residues and dung as fuels. Rural areas of developing countries depend primarily on biomass for fuel [*Smil*, 1979; *Cecelski et al.*, 1979; *Meyers and Leach*, 1989; *Leach and Gowen*, 1987]. The amount of biofuel consumed varies as climate (higher consumption for colder climates) [*Leach*, 1988], and with the plenitude of fuel resource; where fuel is easily obtained, more is consumed

[*Meyers and Leach*, 1989]. The choice of biofuel consumed depends on availability, local customs, and season [*Meyers and Leach*, 1989]. Asia is the largest contributor to the burning of biofuels and agricultural residue in the developing world, because of the dominance of China and India. A variety of detailed studies and reviews are available for Asia. Biomass as rural energy is discussed in country-specific reports in a compendium by *Islam et al.* (1984); the report on Bangladesh, for example, analyzes the results of eight major surveys. *Ebinger* (1981) presents the results of a government survey that documents the fuel use patterns throughout Pakistan. *Leach* [1987] cites these studies and other surveys in his book describing household energy in South Asia. In South Asia all types of biofuels, like fuelwood, agricultural residues, and animal wastes, are used [*Cecelski et al.*, 1979, *Meyers and Leach*, 1989]. Fuelwood includes firewood, brushwood, twigs, branches, and cut branches [*Openshaw*, 1986]. On the other hand, billions of tons of agricultural wastes are generated each year in the developing and developed countries. Agricultural residue includes all leaves, straw and husks left in the field after harvest, hulls and shells removed during processing of crop at the mills, as well as animal dung. According to Logan et al. [1981], the amount of total biofuel burned in the developing world is distributed as 61% fuelwood, 30% crop residue, and about 7% dung.

Emissions from biomass burning include a wide range of gases and particles, in quantities that in some cases can be significant not only on the local scale but also on the global scale. This type of burning can have major effects seasonally on a regional scale, for example, during the months of rice straw burning in southeast Asia. Reliable

74

estimates of particle emissions from biomass burning depend not only on good estimates of the amount of matter burned, but also on good estimates of emission factors from burning of household fuels together with comprehensive assessments of the conditions of domestic fuel use throughout the developing world. The scale of biomass burning is difficult to comprehend and little information exists in either quantities or characteristics of the emissions. Several tests in order to understand the mass emissions from Indian sub continental biomass combustion have been conducted in our laboratory. In the present paper, the size distribution and chemical composition of fine particulate matter emitted from combustion of five types of biomass from Bangladesh will be determined and discussed. The purpose of these experiments was to examine the emissions that occur when biomass are burned under conditions similar to a small chula typically used in many developing countries.

4.3. Experimental Methods

4.3.1. Biomass Selection:

Biomass fuel samples including coconut leaves, rice straw, jackfruit branches, dried cow dung patties, and biomass briquettes manufactured from compressed biomass material were obtained from several local markets near Dhaka, Bangladesh. Sheesley et al. [2003] describes these biomass fuels in details and Table 4.1 of this paper summarizes the specifics of the fuel acquisition. The samples are representative of the biomass fuel

available in the Indian subcontinent. The fuel was transported to the United States for testing during May of 1999.

Table 4.1. Fuel Sample Acquisition Information.

Biomass Sample	Market Location	Source
Coconut Leaves	N/A	Backyard of a household, Mirpur-2, Dhaka
Rice Straw	Amin Bazar, Gabtali, Dhaka	Savar, Dhaka
Cowdung Patties	Amin Bazar, Gabtali, Dhaka	Savar, Dhaka
Biomass Briquettes	Chiriakhana Road, Mirpur-2, Dhaka	N/A
Jackfruit Branches	Mirpur-1 Bus Terminal, Dhaka	Savar, Dhaka

The purchased cow dung patties were compacted by hand and dried under the Sun. The diet of the cows consisted of mostly rice straw and grasses. Biomass briquettes are made of rice husk, a local crop residue. The rice husk is heated and compacted in locally manufactured briquetting machines. Biomass briquettes are used as a fuel for heating urban hotels and tea shops, and for melting bitumen used in road paving operations.

Cow dung patties and rice straw are two of the most common fuels used in rural areas all over South Asia. Coconut leaves and branches are used mostly in the coastal areas where the trees grow well. Jackfruit branches are mostly used in Bangladesh and some parts of India including West Bengal. The biomass briquette burned in this study is used solely in Bangladesh; Indian biomass briquettes are composed with different raw materials and would be expected to have different emission profiles when burned.

Dung use increases from South to North, agricultural residue use increases from North to South, and fuelwood consumption reaches its highest levels in the Eastern plateau and Eastern Himalayan Zones [*Joshi et al.*, 1992]. Crop residues are especially important as cattle feed in the semi-arid regions where much of the land is cultivated and little grassland and pasture land remains [*Rao*, 1985]. In the northwest, the rice straw is mixed with cow dung for use as fuel. However, residue is burned in the fields in India; for example, in Punjab [*Meelu, et al.*, 1991; *Jenkins et al.*, 1992; *Salour et al.*, 1989; *Desai*, 1985]. Rice straw in the central region around Hyderabad is also burned in the fields.

4.3.2. Source Sampling Procedures:

For the source testing, a Vermont Castings, Inc., Encore Model #2190 catalyst-equipped wood stove was used. The procedure has been described previously in the dissertation by Fine, but will be summarized briefly here [Fine, 2002]. A wood stove was used for burning the biomass in order to provide efficient collection of the smoke. The

stove has a 0.076 m^3 firebox. The primary air control lever was used to maintain an oven temperature between 150 and 250^{0}C during the main segment of the biomass burning tests. The maximum oven temperature for each biomass test and their burn rates are included in Table 4.2.

Table 4.2. Combustion Parameters.

	Burn Rate (kg/hr)	Maximum Stove Temperature (^{o}C)
Coconut Leaves	2.3	220
Rice Straw	9.0	150
Cowdung Patties	3.5	220
Biomass Briquettes	2.0	200
Jackfruit Branches	2.2	180

The damper, which directs the emissions through the catalyst, was not used for this test. The biomass was placed in the firebox with approximately 5–10 stalks of rice straw for ignition. Approximately 0.5–2.0 kg of biomass was consumed with a burn time of around 2 hours, except for the coconut leaves and rice straw, which burned over a period of 30 min. Collection of emission samples began before ignition and continued until no particles were emitted. Calorific values were not measured for these biomass samples; however, Sinha et al. [1998] reported values of 3800 kcal/kg for agricultural residues and

78

3140 kcal/kg for dried cow dung (dung cake). The sample was taken from the flue, 3 m above the stove. The dilution source sampler used in this study has been described previously by Hildemann et al. [1989] with the specific configuration detailed by Fine et al. [2001]. The conditions in the dilution source sampler have been optimized for collection of particulate matter. The emissions are diluted 20 to 30 times with activated carbon- and HEPA filtered air and travel in the residence chamber long enough to allow condensation of vapors onto particles. This is done at ambient temperature to simulate gas-particle partitioning as occurs in the atmosphere downstream of the emission source.

The dilution exhaust then passes through an AIHL-design cyclone separator which eliminates particles larger than 1.8 μm aerodynamic diameter. The remaining fine particles are collected on PTFE Teflon filters and quartz fiber filters for subsequent chemical analysis. In this study two additional sampling trains each connected to a 10-stage microorifice uniform deposit impactor (MOUDI, MSP Corp., Model 100) [Marple et al., 1991] were simultaneously operated in parallel downstream of the residence time chamber of the source sampling system. The impactors are seen as the most practical way to measure bulk particle chemical composition as a function of particle size. For collection of particles, air was drawn at a rate of 30 L min^{-1} through a stainless steel inlet line extending from the body of the residence chamber to a Teflon-coated AIHL-design cyclone separator [John and Reischl, 1980] which removed large particles according to a collection efficiency curve having a 50% aerodynamic cutoff diameter at 1.8 μm before the air passed through the impactors. The AIHL cyclone was used to suppress particle bounce from the upper stages of the impactors. Particles over the size range 0.056–1.8

μm particle diameter were collected on impaction stages 5 through 10 of the impactors. All 10 stages of the impactors were in place during the experiment but only the lower 6 stages collected meaningful samples because of the presence of the cyclone separator upstream of the impactors. One of the two impactors was loaded with aluminum foil substrates (MSP Corp., 47 mm diameter) and a quartz fiber afterfilter (Pallflex, 2500 QAO, 47 mm diameter). The second impactor was operated with PTFE impaction substrates and afterfilters (Gelman Sciences, 47 mm diameter, Teflo material, 2.0 μm pore size). The foil impaction substrates and quartz fiber filters were baked before use in order to lower their carbon blank values, since these materials were dedicated to the analysis of carbonaceous aerosol species; foil substrates were baked for 48 hours at $550^{o}C$, and quartz fiber filters were baked for 12 hours at $550^{o}C$. To avoid contamination by organic compounds, no grease or oil was applied to the impaction substrates. Following sample collection, filter samples and samples on impaction substrates were placed in petri dishes, sealed with Teflon tape, then frozen immediately until subsequent analysis.

4.3.3. Chemical Analysis:

All foil and PTFE impaction substrates and PTFE filters were gravimetrically analyzed by repeated weighing before and after the experiment on a Mettler model M-55-A mechanical microbalance maintained in a temperature and humidity-controlled environment ($21.0 \pm 0.2^{o}C$, $39 \pm 3\%$ RH). PTFE impactor substrates were cut in half before chemical analysis to allow the use of several different chemical analysis

techniques. One half of the each of the PTFE impactor substrates and one of each pair of PTFE fine particle filter samples were analyzed by ion chromatography (Dionex Corp, Model 2020i) for NO_3^-, SO_4^{2-}, and Cl^- [Mulik et al., 1976] and by an indophenol colorimetric procedure for NH_4^+ [Bolleter, 1961] using an Alpkem rapid flow analyzer (Model RFA-300). The second half of each of these sample sets was analyzed for trace elements using neutron activation analysis [Olmez, 1989]. Foil and quartz fiber substrates were analyzed for elemental and organic carbon content using the thermal-optical carbon analysis method of Huntzicker et al. [1982] as modified by Birch and Cary [1996]. Correction for pyrolytic formation of elemental carbon during organic carbon determination from the impactor samples was accomplished using the methodology described in the paper by Kleeman et al. [1999].

4.4. Results and Discussion:

As seen in Figure 4.1, most of the combustion particles are carbonaceous in nature with organic matter dominating over elemental carbon. Organic matter has been computed by multiplying organic carbon by 1.4 to account for the H, O, N, and other elements typically found in organic compounds.

Figure 4.1. Percent contribution of individual chemical species to the fine particulate matter (Da<1.8 μm) emitted from burning coconut leaves, rice straw, jackfruit wood, synthetic log, and cow dung from Bangladesh. The size of the pie chart represent the total fine particle concentration in the residence chamber.

For almost all of the biomass samples, the organic mass is >57% of the total mass of identified species present in the particulate matter emissions. Coconut leaves and cow dung had the highest percentage at 62% and 61% respectively, while rice straw emission had the lowest at 57%. Traditionally, a value of 1.2 to 1.4 [Countess et al., 1980; Japar et al., 1984; White and Roberts, 1977] has been used to estimate organic matter from organic carbon, however, Turpin and Lim [2001] suggest that a higher ratio of 2.2 to 2.6

can be expected in aerosol impacted by wood smoke. If we use a higher organic carbon to organic matter ratio, the unidentified mass (19% to 37%) can be explained.

The elemental carbon emission values show little variability among the biomass samples except for the coconut leaves. At 8%, the coconut leaf emission of elemental carbon is a factor of 2-3 times higher than the emission of the other biomass samples. The emission of the ionic species is also quite similar for all samples. Again, the coconut leaves show the highest emission for all the ionic species. Chlorine is the second highest single element emitted from coconut leaves, rice straw, and cowdung, after organic matter, but the fraction emitted by coconut leaves is about twice that of any other sample in this study. Regarding the high chlorine emission of the coconut leaves, it has been shown that salt (NaCl and/or KCl) applied by growers to enhance production increases the chlorine and sodium content of coconut leaves and decreases the potassium content [Remison et al., 1988]. Since chlorine content depends upon the amount of salt applied to a particular plant, it varies among coconut leaves combustion emission samples. There is good agreement between the INAA (instrumental neutron activation analysis) chlorine measurements and the ion chromatography chloride measurements. This agreement indicates that all of the chlorine is water soluble.

Typical of combustion from diesel and gasoline, biomass combustion also have a single peak between 0.18-0.32 μm of the MOUDI as seen in Figure 4.2. Rice straw seems to have a broader peak between 0.18-0.56 μm compared to the rest of the samples combusted in this experiment.

Figure 4.2. Size and chemical species distribution of 1 μg of fine particulate matter emitted from burning coconut leaves, rice straw, jackfruit wood, synthetic log, and cow dung from Bangladesh as measured by MOUDI impactor.

Fine particle emissions from rice straw and cow dung appear to be more than the emissions from the other three biomass samples. When burning rice straw, the straw quickly produced flames and progressed towards the smoldering phase with high amount of black smoke. This long smoldering phase probably causes a lot of particle emissions and conversion of gas to particle thus increasing the particle mass concentrations for all species sampled. On the other hand, coconut leaves and the synthetic fuel have lower

particle emissions. The synthetic fuel is compressed and seem to burn slowly but steadily and also cause less particle emissions.

Measurements of particle-phase chemical species concentrations made using the MOUDI impactors can be summed across all stages to calculate bulk fine particle concentrations for each source test. These values may then be compared to fine particle filter-based measurements taken at the same time in order to evaluate the performance of the impactors and related analysis methods. The sum of the mass concentrations from the MOUDI filters gives the total mass for all particle smaller than 1.8 micron. When comparing this sum with the $PM_{2.5}$ filter mass concentrations, there seem to be good agreement. See Figure 4.3 for this comparison. Filter-based measurements are collected from the dilution source sampling using 47 mm diameter quartz fiber (Pallflex Tissuequartz 2500 QAO and Teflon membrane (Gelman Teflo, 1 μm pore size) filters operating downstream of a fine particle cyclone separator.

Figure 4.3. Comparison of filter to MOUDI mass concentrations in the dilution chamber from burning five Bangladeshi biomass samples.

The sum of the MOUDI mass concentrations is approximately 65-76% of the mass acquired in the filter. At least part of this small discrepancy could be due to the fact that the particle size ranges sampled by the impactor (0-1.8 micron particle diameter) is smaller than the size range covered by the filter samples (0-2.5 micron particle diameter). Also, the high pressure in the MOUDI may have caused the high volatile particles to vaporize and lead to a low mass.

The particulate phase metal concentrations were analyzed by INAA. Several of the metals analyzed were above detection after blank subtraction and are shown in Figures 4.4 to 4.8. Potassium emissions were measured in all five biomass samples at significant levels with peaks around 0.18-0.32 μm. Potassium emission from coconut leaves combustion seems to quite different from the other four samples. Potassium has been proposed as a potential molecular marker for biomass combustion emission. However, as for coconut leaves, growing conditions may have too much of an impact on the final concentration of potassium in any given plant for it to be successfully predicted in the combustion emissions of that species, let alone throughout biomass in general. It has also been reported that the emission of potassium from meat cooking is significant enough to be a confounding factor when apportioning ambient concentrations [Hildemann et al., 1991; Rogge et al., 1991; Schauer et al., 1999a]. Although the emission fraction of potassium in smoke from meat charbroiling is significantly less than the fraction emitted in biomass smoke, smoke from both meat charbroiling and biomass combustion contribute appreciably to ambient particulate matter concentrations in some locations [Schauer and Cass, 2000]. The sodium levels of coconut leaf emissions are also significant in comparison to the total mass, but lower than chlorine despite their both resulting in part from salting of the plants by the growers, as discussed previously. As for trace metals, cowdung smoke has measurable quantities of zinc and bromine. There is also a small amount of bromine present in the other biomass emission. Trace metals are not a significant contributor to the total particulate emissions from the combustion of these biomass sources.

Figure 4.4. Size and chemical distribution of individual trace species emitted from coconut leaves smoke as measured by MOUDI impactor. Error bars represent one standard deviation.

Figure 4.5. Size and chemical distribution of individual trace species emitted from rice straw smoke as measured by MOUDI impactor. Error bars represent one standard deviation.

Figure 4.6. Size and chemical distribution of individual trace species emitted from dried cow dung smoke as measured by MOUDI impactor. Error bars represent one standard deviation.

Figure 4.7. Size and chemical distribution of individual trace species emitted from synthetic fuel smoke as measured by MOUDI impactor. Error bars represent one standard deviation.

Figure 4.8. Size and chemical distribution of individual trace species emitted from jackfruit wood smoke as measured by MOUDI impactor. Error bars represent one standard deviation.

A few trace elements were not measured by the INAA technique including silicon, phosphorus, and sulfur. However, previous biomass combustion emission profiles indicate that these are present only in trace amounts, not exceeding 1.00 weight percent of the total particulate mass emissions [Fine et al., 2001, 2002; Schauer et al., 2001].

4.5. Conclusions

The particle mass distributions from the five biomass samples have a single mode that peaks at 0.18-0.32 μm particle aerodynamic diameter. From other work by Hildemann et al. (1991a, 1991b), it appears that combustion generated particles appear to

peak at this size range. Particles emitted from biomass burning are mostly organic matter (57-62%) and elemental carbon (2-8%) in nature with significant amount of chloride ion (2-9%) present.

4.6. Acknowledgements

4.7. References

Birch, M. E., and R. A. Cary, Elemental carbon-based method for monitoring occupational exposures to particulate diesel exhaust, Aerosol Sci. Technol., 25, 221-241, 1996.

Bolleter, W.T., C. T. Bushman, and P. W. Tidwell, Spectrophotometric determinations of ammonium as indophenol, Anal. Chem., 33, 592-594, 1961.

Cecelski, E.,J.Dunkerley, and W. Ramsay, *Household Energy and the Poor in the Third World*, Resources for the Future, Inc., Washington, D.C., 1979.

Countess, R. J., G. T. Wolff, and S. H. Cadle, The Denver winter aerosol: A comprehensive chemical characterization., J. Air Pollut. Control Assoc., 30, 1194–1200, 1980.

Crutzen, P.J., L.E. Heidt, J.P. Krasnec, W.H. Pollock, and W. Seiler, Biomass burning as a source of atmospheric gases CO, H2, N2O, NO, CH3Cl and COS, *Nature, 282,* 253-256, 1979.

Desai, A.V., Ends and means in rural energy surveys, Report for the International Development Research Centre, IDRC-MR112e, June 1985.

Ebinger, C.K., *Pakistan: Energy Planning in a Strategic Vortex*, 155pp., Indiana University Press, Bloomington, Indiana, 1981

Fine, P. M., G. R. Cass, and B. R. T. Simoneit, Chemical characterization of fine particle emissions from fireplace combustion of woods grown in the northeastern United States, Environ. Sci. Technol., 35(13), 2665–2675, 2001.

Fine, P. M., The contribution of biomass combustion to ambient fine particle concentrations in the United States, Ph.D. thesis, Calif. Inst. of Technol., Pasadena, Calif., 2002.

Hildemann, L. M., G. R. Cass, and G. R. Markowski, A dilution stack sampler for collection of organic aerosol emissions - design, characterization and field-tests, Aerosol Sci. Technol., 10(1), 193– 204, 1989.

Hildemann, L. M., G. R. Markowski, and G. R. Cass, Chemical-composition of emissions from urban sources of fine organic aerosol, Environ. Sci. Technol., 25(4), 744– 759, 1991.

Huntzicker, J. J., R. L. Johnson, J. J. Shah, and R. A. Cary, Particulate Carbon, Atmospheric Life Cycle, edited by G. T. Wolff and R. L. Klimisch, pp. 79-88, Plenum, New York, 1982.

Islam, M.N., Energy and rural development: critical assessment of the Bangladesh situation, in *Rural Energy to Meet Development Needs: Asian Village Approaches*, M.N. Islam, R. Morse, and M.H. Soesastro (Eds.), 561pp., Westview Press, Inc., Boulder, 1984.

Islam, M.N., R. Morse, and M.H. Soesastro (Eds.), *Rural Energy to Meet Development Needs: Asian Village Approaches*, 561pp., Westview Press, Inc., Boulder, 1984.

Japar, S. M., A. C. Szkarlat, R. A. Gorse, E. K. Heyerdahl, R. L. Johnson, J. A. Rau, and J. J. Huntzicker, Comparison of solvent-extraction and thermal optical carbon analysis-methods—Application to diesel vehicle exhaust aerosol, Environ. Sci. Technol., 18(4), 231–234, 1984.

Jenkins, B., S.Q. Turn, and R.B. Williams, Atmospheric emissions from agricultural burning in California: determination of burn fracgions, distribution factors, and crop-specific contributions, *Agr., Ecosystems., and Env., 38*, 313-30, 1992.

John, W., and G. Reischl, A cyclone for size-selective sampling of ambient air, J. Air Pollut. Control Assoc., 30, 872-876, 1980.

Joshi, V., C. Venkataraman, D.R. Ahuja, Emissions from Burning Biofuels in Metal Cookstoves, *Environmental Management 13*, 763-772, 1989.

Joshi, V., C.S. Sinha, M. Karuppasamy, K.K. Srivastava, and P.B. Singh, Rural energy database, Final Report submitted to Ministry of Non-conventional Energy Sources, Tata Energy Research Institute, New Delhi, September, 1992.

Kleeman MJ, Schauer JJ, Cass GR. 1999. Size and composition distribution of fine particulate matter emitted from wood burning, meat charbroiling, and cigarettes. *Environmental Science & Technology*. 33: 3516-3523.

Leach, G., *Household Energy in South Asia*, 111pp., Elsevier Applied Science, London and New York, 1987.

Leach, G., Residential energy in the Third World, *Ann. Rev. Energy 1988, 13*, 47-65, 1988.

Leach, G., and M. Gowen, *Household energy handbook: an interim guide and reference manual*, World Bank Technical Paper No. 67, The World Bank, Washington, D.C., 1987.

Logan, J.A., Prather, M.J., Wofsy, S.C. and McElroy,. M.B. Tropospheric Chemistry: A global perspective. *J. Geophys. Res., 86*, 7210-7254, 1981.

Marple, V. A., K. L. Rubow, and S. M. Behm. A microorifice uniform deposit impactor (MOUDI), description, calibration, and use, Aerosol Sci. Technol., 14, 434-446, 1991.

Meelu, O.P., Y. Singh, and B. Singh, Green manure and crop residue management in rice-wheat rotation, in *Extended Summary, Proceedings International Symposium Rice Research: New Frontiers, 15-18 November, 1990*, K. Muralidharan, K.V. Rao, K. Satyanarayana, G.S.V. Prasad, and E.A. Siddiq, (eds.), Directorate of Rice Research, Hyderabad, India, 1991.

Meyers, S., and G. Leach, Biomass fuels in the developing countries: an overview, Lawrence Berkeley Laboratory (LBL-27222), Berkeley, CA, 1989.

Mulik, J., R. Puckett, D. Williams, and E. Sawicki, Ion chromatographic analysis of sulfate and nitrate in ambient aerosols, Anal. Lett., 9, 653-663, 1976.

Olmez, I., Instrumental neutron activation analysis of atmospheric particulate matter, in Methods of Air Sampling and Analysis, edited by J. J. P. Lodge, pp. 143– 150, Lewis Publishers, Chelsea, Mich., 1989.

Openshaw, K.O., Concepts and methods for collecting and compiling statistics on biomass used as energy, paper prepared for N.W. Statistical Office Workshop, Rome, September 29- October 3, 1986.

Rao, P.P., Marketing of fodder in rural and urban areas of India, in *Agricultural Markets in the Semi-Arid Tropics*, Proceedings of the International Workshop at ICRISAT Center,

India, 24-28 October 1983, International Crops Research Institute for the Semi-Arid Tropics (ICRISAT), Patancheru, A.P., India, 1985.

Rogge, W. F., L. M. Hildemann, M. A. Mazurek, G. R. Cass, and B. R. T. Simoneit, Sources of fine organic aerosol. 1. Charbroilers and meat cooking operations, Environ. Sci. Technol., 25(6), 1112–1125, 1991.

Salour, D., B.M. Jenkins, M. Vafaei, M. Kayhanian, Combustion of Rice Straw and

Straw/Wood Fuel Blends in a Fluidized Bed Reactor, Paper No. 89-6574 of the 1989 International Winter Meeting of ASAE, published by the ASAE, St. Joseph, MI, 1989.

Schauer, J. J., and G. R. Cass, Source apportionment of wintertime gasphase and particle-phase air pollutants using organic compounds as tracers, Environ. Sci. Technol., 34(9), 1821– 1832, 2000.

Schauer, J. J., M. J. Kleeman, G. R. Cass, and B. R. T. Simoneit, Measurement of emissions from air pollution sources, 1, C1 through C29 organic compounds from meat charbroiling, Environ. Sci. Technol., 33(10), 1566–1577, 1999.

Schauer, J. J., M. J. Kleeman, G. R. Cass, and B. R. T. Simoneit, Measurement of emissions from air pollution sources, 3, C-1 –C-29 organic compounds from fireplace combustion of wood, Environ. Sci. Technol., 35(9), 1716–1728, 2001.

Sheesley, Rebecca J.; Schauer, James J.; Chowdhury, Zohir; and Cass, Glen R. (2003) "Characterization of Organic Aerosols Emitted from the Combustion of Biomass

Indigenous to the Indian *Subcontinent,"* Journal of Geophysical Research*, 108*, No. D9, AAC 8-1 to AAC 8-15.

Sinha, C. S., S. Sinha, and V. Joshi, Energy use in the rural areas of India: Setting up a rural energy data base, Biomass Bioenerg., 14(5–6), 489–503, 1998.

Smil, V., Energy flows in the Developing World, *Am. Scientist 67*, 522-531, 1979.

Turpin, B. J., and H. J. Lim, Species contributions to PM2 5 mass concentrations: Revisiting common assumptions for estimating organic mass, Aerosol Sci. Technol., 35(1), 602– 610, 2001.

White, W. H., and P. T. Roberts, On the nature and origins of visibilityreducing aerosols in the Los Angeles air basin, Atmos. Environ., 11, 803–812, 1977.

Woods, J., and D.O. Hall, Bioenergy for development: technical and environmental dimensions, FAO Environment and Energy Paper No. 13, Food and Agriculture Organization of the United Nations, Rome, 1994.

CHAPTER-5

Size distributed chemical composition of fine particles emitted from burning Asian coals

5.1. Abstract

Two micro-orifice uniform deposit impactors (MOUDIs) were used to collect diluted exhaust emissions from the combustion of three Asian coals in a batch underfire air grate furnace. Prior to sample collection, the hot exhaust emissions were diluted in the Caltech dilution source sampler (Hildemann et al., 1989). The three Asian coals were from Meghalaya (India), Dinajpur (Bangladesh), and Datong (China). The particle mass distributions from the three coals have a single mode that peaks at 0.18-0.32 μm particle aerodynamic diameter. Particles emitted from coal burning were mostly elemental carbon in nature. Organic matter was the next largest contributor. Size distributions from several trace elements (sodium, magnesium, aluminum, chlorine, scandium, vanadium, cobalt, arsenic, bromine, antimony, lanthanum, neodymium, samarium, europium, and mercury) were measured using instrumental neutron activation analysis. The purpose of these

experiments was to examine the emissions that occur when chunks of coal, on the order of 2-3 cm in diameter, are burned under conditions similar to a small industrial or commercial hand-stoked furnace. The data obtained from these source tests will prove useful in constructing and evaluating regional emission inventory and assessing source impacts on air quality.

5.2. Introduction

Much of the energy demand in the densely populated Asian countries, particularly India and China, is met by coal and bio fuel combustion. Residential or domestic combustion of coal takes place in homes for heating or cooking purposes and is thought to contribute heavily to global or regional burdens of carbonaceous particles [Cooke et al., 1999]. In India, according to Reddy and Venktaraman [2002], 54% of the energy demand is met by the usage of coal in power plants to generate electricity, and they estimate that 92% of the fine particle in India is emitted from such coal combustion. Streets et al. [2001], on the other hand, attribute 45% of the carbon emissions in China to residential coal burning. However, little information exists in either quantities or characteristics of the emissions.

Moreover, in order to construct and exercise advanced mechanistic air quality models that seek to predict the evolution of the size and composition distribution of fine particles in the atmosphere, it is necessary to be able to specify both the size distribution and the chemical

composition of the direct particle emissions as they occur at the source [Kleeman and Cass, 2001; Bhave et al., 2002]. The size and composition of particles found in the atmosphere also determine much of the visibility reduction observed in large cities. Source-oriented models have been developed to understand the air pollutant effects on visibility that can compute light scattering, light extinction, and estimate visual range directly from data on gas phase and primary particle phase air pollutant emissions from sources [Eldering and Cass, 1996]. On the other hand, regional models as well as climate models can have extensive use of the size distribution and chemical composition data from different emission sources. Hildemann et al. [1991a, 1991b] conducted a series of source tests using a dilution source sampling system designed to measure the size distribution and chemical composition of particulate emissions from major urban sources in southern California. No test on fine particle emissions from coal combustion has been conducted in these source tests. During these source tests, the source effluent was diluted with pre-cooled purified air prior to sample collection in order to simulate the condensation of organic vapors onto pre-existing solid particles that will occur as hot exhaust plumes are released to the atmosphere. Several tests in order to understand the mass emissions from Asian coals and Indian sub continental biomass combustion have been conducted in our laboratory using this dilution tunnel system by including two Micro-Orifice Uniform Deposit Impactors (MOUDIs). In the present paper, the size distribution and chemical composition of fine particulate matter emitted from the low temperature combustion of three types of coals from Asia will be determined and discussed. The three Asian coals were from Meghalaya (India), Dinajpur (Bangladesh), and Datong (China). The purpose of these experiments was to examine the emissions that occur when chunks of coal are burned under conditions similar to a small industrial or commercial hand-stoked furnace.

102

5.3. Experimental Methods

5.3.1. Coal Selection:

Three types of Asian coals were tested for this experiment. Meghalaya coal originates in the north-eastern region of India, Barapukuria coal originates at Dinajpur, Bangladesh, and Datong coal comes from China. The Meghalaya coal is used in a large number of industries in North-East India whereas, the Bangladeshi coal is used at brick kilns. The composition of the three coals is described in Table 5.1.

Table 5.1. Chemical composition of raw coals used in the analysis of coal combustion emission.

Coal Type	Bangladeshi Coal	Indian Coal	Chinese Coal
Ash (%)	8.16	6.44	3.85
Sulfur (%)	0.56	3.04	1.18
Carbon (%)	76.5	72.0	80.8
Hydrogen (%)	4.64	5.54	4.64
Nitrogen (%)	1.50	1.32	1.10
Oxygen (%)	8.33	11.66	8.41

Note: The analyses were done on dry weight basis.

5.3.2. Combustion Conditions:

The present experiment was conducted at the Utah Combustion Research Group facility at the University of Utah. Coal combustion occurred in a Brick Kiln Furnace. The Brick Kiln Furnace is designed to accept wall or floor-mounted burners so that a variety of firing configurations, and interactions between burners, can be studied. Banks of fluid- or air-cooled tubes are hung from the roof of the furnace to simulate a chemical process heater. The reactor, without its gas train, exhaust duct, and electrical system, is 3.6 m tall. The front width is 1.5 m, and the side length is 2.1 m. The inner cavity is 0.9 m wide, 1.5 m long, and 3 m tall. The facility is insulated with a 12.7 cm layer of fiberboard, next to the steel shell, and a 10.2 cm in layer of castable refractory. Temperatures of 1100 to 1200°C were maintained at the Brick Kiln Furnace during this experiment. Lumps of coal of typical size were burned on an open grate with combustion air supplied from below the grate.

5.3.3. Source Sampling Procedures:

The operation of the dilution source sampling system used in this experiment has been described by Hildemann et al. (1991a, 1991b) and Schauer et al. (1999a, 1999b). A schematic diagram of the dilution sampler is shown in Figure 1a of Hildemann et al. (1991a) and in Figure 1 of Schauer et al. (1999a). As part of the standard source testing procedure, a sample stream from the exhaust of the coal combustion is drawn through a 10 μm size cut in the stack cyclone, followed by passage through a treated teflon inlet

line. From the inlet line the sample stream is mixed with air which causes semi-volatile compounds in the sample to condense onto the solid particles in the exhaust stream as will occur in the plume downwind of the source. The dilution exhaust then passes through an AIHL-design cyclone separator which eliminates particles larger than 1.8 μm aerodynamic diameter. The remaining fine particles are collected on PTFE Teflon filters and quartz fiber filters for subsequent chemical analysis. In this study two additional sampling trains each connected to a 10-stage microorifice uniform deposit impactor (MOUDI, MSP Corp., Model 100) (Marple et al., 1991) were simultaneously operated in parallel downstream of the residence time chamber of the source sampling system. The impactors are seen as the most practical way to measure bulk particle chemical composition as a function of particle size. For collection of particles, air was drawn at a rate of 30 L min^{-1} through a stainless steel inlet line extending from the body of the residence chamber to a Teflon-coated AIHL-design cyclone separator (John and Reischl, 1980) which removed large particles according to a collection efficiency curve having a 50% aerodynamic cutoff diameter at 1.8 μm before the air passed through the impactors. The 15% and 85% particle collection cut points for this cyclone at this flowrate are at approximately 1.7 μm and 2.2 μm aerodynamic diameter respectively based on visual extrapolation of the collection efficiency curves presented by John and Reischl (1980). The AIHL cyclone was used to suppress particle bounce from the upper stages of the impactors. Particles over the size range 0.056–1.8 μm particle diameter were collected on impaction stages 5 through 10 of the impactors. All 10 stages of the impactors were in place during the experiment but only the lower 6 stages collected meaningful samples because of the presence of the cyclone separator upstream of the impactors. One of the

105

two impactors was loaded with aluminum foil substrates (MSP Corp., 47 mm diameter) and a quartz fiber afterfilter (Pallflex, 2500 QAO, 47 mm diameter). The second impactor was operated with PTFE impaction substrates and afterfilters (Gelman Sciences, 47 mm diameter, Teflo material, 2.0 μm pore size). The foil impaction substrates and quartz fiber filters were baked before use in order to lower their carbon blank values, since these materials were dedicated to the analysis of carbonaceous aerosol species; foil substrates were baked for 48 hours at 550°C, and quartz fiber filters were baked for 12 hours at 550°C. To avoid contamination by organic compounds, no grease or oil was applied to the impaction substrates. Following sample collection, filter samples and samples on impaction substrates were placed in petri dishes, sealed with Teflon tape, then frozen immediately until subsequent analysis.

All foil and PTFE impaction substrates and PTFE filters were gravimetrically analyzed by repeated weighing before and after the experiment on a Mettler model M-55-A mechanical microbalance maintained in a temperature and humidity-controlled environment (21.0 $\pm$ 0.2^{o}C, 39 $\pm$ 3% RH). PTFE impactor substrates were cut in half before chemical analysis to allow the use of several different chemical analysis techniques. One half of the each of the PTFE impactor substrates and one of each pair of PTFE fine particle filter samples were analyzed by ion chromatography (Dionex Corp, Model 2020i) for NO_3^-, SO_4^{2-}, and Cl^- [Mulik et al., 1976] and by an indophenol colorimetric procedure for NH_4^+ [Bolleter, 1961] using an Alpkem rapid flow analyzer (Model RFA-300). The second half of each of these sample sets was analyzed for trace elements using neutron activation analysis [Olmez, 1989]. Foil and quartz fiber substrates

were analyzed for elemental and organic carbon content using the thermal-optical carbon analysis method of Huntzicker et al. [1982] as modified by Birch and Cary [1996]. Correction for pyrolytic formation of elemental carbon during organic carbon determination from the impactor samples was accomplished using the methodology described in the paper by Kleeman et al. [1999].

5.4. Results and Discussion:

The coal was broken into chunks of diameter of at least 2-3 cm. Among the three Asian coals tested in here, the Bangladeshi and the Indian coal seemed to have the highest mass concentrations of particles compared to the Chinese coal. As seen in Figure 5.1, for all three types of coal combustion, carbonaceous particles are the largest contributors of fine particle concentration.

Figure 5.1. Percent contribution of individual chemical species to the fine particulate matter (Da<1.8 μm) emitted from Bangladeshi, Indian, and Chinese coals. The size of the pie chart represent the total fine particle concentration in the residence chamber.

Coal is composed of carbon and other organic compounds which when burned emit these carbonaceous particles. This carbonaceous fraction may be PAH and soot, dominated by the cracking of the tars in the pyrolysis products. As predicted, most of the fine particle concentration is elemental carbon (EC) in nature with significant amount of organic matter (OM). Coal burned in this manner produces more black carbon (soot) than the black carbon emission from diesel vehicles although the organic carbon content seems to be less during coal burning than that from diesel vehicles. To account for the hydrogen and oxygen content of the organic compounds, organic compound concentrations are calculated from organic carbon measurements multiplied by a factor of 1.2. The 1.2 factor was chosen because of the more reducing environment present during coal combustion compared to the normal ambient conditions. The Bangladeshi and the Indian coals appear to emit more carbonaceous particles (77-82% EC and 15-17% OM) than the Chinese coal (54% EC and 39% OM).

Combustion from all three types of coal tested in this experiment emit sulfate. It appears that the Bangladeshi coal contains less sulfur than the Indian and the Chinese coals since the Bangladeshi coal emits less sulfate (1% of fine particles) compared to the Indian (4%) and the Chinese (3.6%) coals. SO_2, which is a precursor to sulfate, is produced from the sulfur containing compounds present in the coal which reacts with the oxygen of the combustion air. Chloride emission is significant from the Chinese coal combustion (2.2% of fine particle concentrations) and ammonium emission is significant for the Indian coal (1.3% of fine particle concentrations). By burning the coals in this manner, it appears that the amount of small fly ash particles is negligible. Usually small

fly ash particles are carried by the moving flue gases and eventually become transported

out in the atmosphere.

The fine particle size and composition distributions of particles emitted from the

Bangladeshi, Indian, and Chinese coal combustion are shown in Figure 5.2.

Figure 5.2. Size and chemical species distribution of 1 µg of fine particulate matter emitted from Bangladeshi, Indian, and Chinese coal smoke as measured by MOUDI impactor.

Results shown in this figure have been normalized to display the size distribution of 1 µg

of particulate matter emitted from the coal being tested. A single mode peaking at 0.18-

0.32 µm particle aerodynamic diameter is observed for all three coals. This characteristic

is typical of combustion generated particle size distribution. However, the size and

composition distribution in coal combustion emissions is quite different from other

contributors to urban air pollution including automobiles, wood combustion, meat smoke,

paved road dust, food frying, and natural gas combustion (Hildemann, et al., 1991b;

Kleeman, et al., 1999 and 2000). Because of the submicron size, particles in this size range will be transported great distance once airborne from their sources.

Measurements of particle-phase chemical species concentrations made using the MOUDI impactors can be summed across all stages to calculate bulk fine particle concentrations for each source test. These values may then be compared to fine particle filter-based measurements taken at the same time in order to evaluate the performance of the impactors and related analysis methods. The sum of the mass concentrations from the MOUDI filters gives the total mass for all particle smaller than 1.8 micron. When comparing this sum with the $PM_{2.5}$ filter mass concentrations, there seem to be good agreement. See Figure 5.3 for this comparison. Filter-based measurements are collected from the dilution source sampling using 47 mm diameter quartz fiber (Pallflex Tissuequartz 2500 QAO and Teflon membrane (Gelman Teflo, 1 μm pore size) filters operating downstream of a fine particle cyclone separator. The sum of the MOUDI mass concentrations is approximately 60-75% of the mass acquired in the filter. At least part of this small discrepancy could be due to the fact that the particle size ranges sampled by the impactor (0-1.8 micron particle diameter) is smaller than the size range covered by the filter samples (0-2.5 micron particle diameter). Also, the high pressure in the MOUDI may have caused the high volatile particles to vaporize and lead to a low mass.

Figure 5.3. Comparison of filter to MOUDI mass concentrations in the dilution chamber from burning three Asian coals.

The size distributions of trace species measured in particles emitted from Bangladeshi coal are shown in Figure 5.4 and from Indian coal in Figure 5.5.
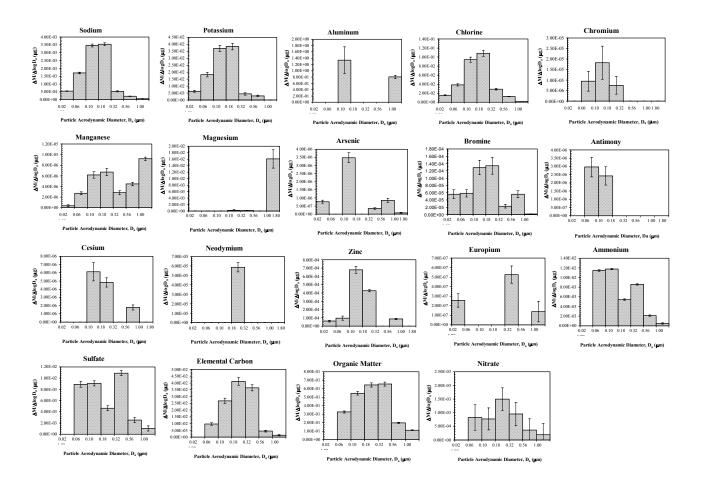
Figure 5.4. Size and chemical distribution of individual trace species emitted from Bangladeshi coal smoke as measured by MOUDI impactor. Error bars represent one standard deviation.
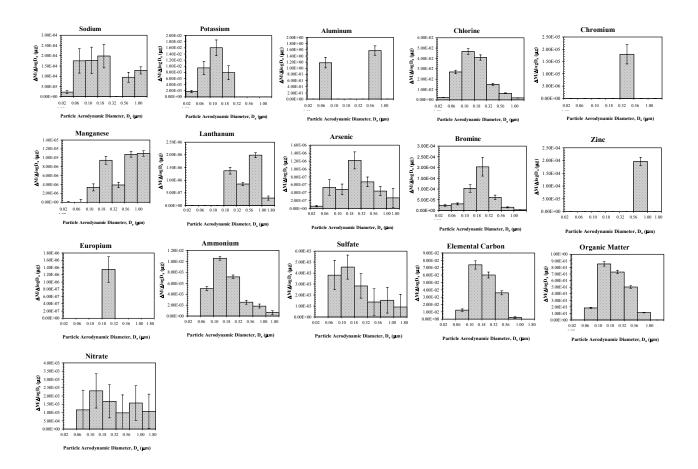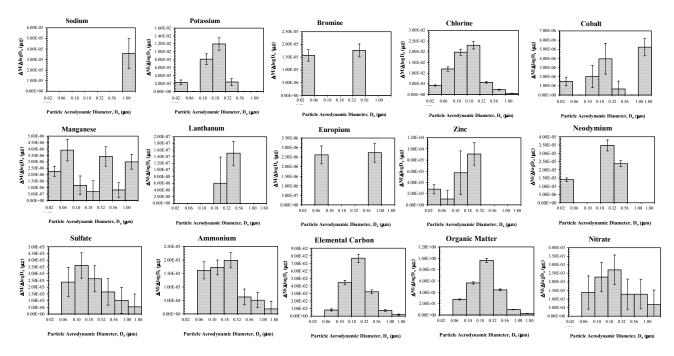
112

Figure 5.5. Size and chemical distribution of individual trace species emitted from Indian coal smoke as measured by MOUDI impactor. Error bars represent one standard deviation.

113

Out of the 34 trace species measured by Neutron Activation, only those elements which are significantly higher than the calculated uncertainties are presented in these figures to more clearly explain the overall trends. These figures depict the trace elements distribution relative to 1 μg of the whole fine particle sample (D_a<1.8 μm) as defined by summing up the masses from each stage of the MOUDI. At high flame temperature particles are formed with volatilization of ash components and then condensation and coagulation of the volatile material in the dilution sampling system with cool condition (McElroy, et al., 1982; Quann, et al., 1982; Markowski and Filby, 1985; Amdur, et al., 1986; Kauppinen and Pakkanen, 1990). Na, Mg, Al, Cl, Sc, V, Co, As, Br, Sb, La, Nd, Sm, Eu, and Hg—these 15 metals have been detected from the Bangladeshi coal sample, whereas Na, Cl, Sc, V, Cr, Co, As, Br, Sb, La, Sa, Eu, Hg—these 13 metals have been detected for the Indian coal through Neutron Activation analysis. For the Bangladeshi coal, Mg, Cl, V, Co, As, Sb, Hg and Nd have a bimodal size distribution with one peak at the supramicron range and another one at the submicron range (between 0.10 and 0.18 μm). For the Indian coal, Hg, Co, and Cl display a bimodal size distribution with a supramicron and a submicron peak. This may indicate that these elements experienced some volatilization and recondensation to form fine particles during the combustion process. In contrast, for the Bangladeshi coal, Na, Al, Sc, La, and Sm peak at the higher size range of the MOUDI (1.0 to 1.8 μm) and for the Indian coal Na, Sc, La, Sm, Sb, and V peak at the supramicron range. These elements tend to follow the size distribution of particulate matter mass. This may indicate that these elements were relatively refractory during combustion process and thus the non-vaporized part of coal fly ash was predominant in the chemical size distribution above 0.56 μm. In other words,

incombustible mineral component of the coal fly ash were carried over. More volatile elements such as Cl, Br, Sc, Sb, As, Co, NH_4^+, SO_4^{-2} were strongly observed at after filter (< 0.06 µm). SO_4^{-2} displays particle mass for all the size ranges of the MOUDI. Interestingly, As and in some degree Hg showed a increment tendency as the size range decreases. The presence of arsenic in the coal smoke emission confirms its origin in Bangladesh and Meghalaya as groundwater and soil in that region is known to be contaminated by arsenic, which may contaminate the coal.

5.5. Conclusions

The particle mass distributions from the three coals also have a single mode that peaks at 0.18-0.32 µm particle aerodynamic diameter. Particles emitted from coal burning were mostly elemental carbon in nature. Organic matter was the next largest contributor.

5.6. Acknowledgements

5.7. References

Amdur MO, Sarofim AF, Neville M, Quann RJ, Mccarthy JF, Elliott JF, Lam HF, Rogers AE, Conner MW. 1986. Coal Combustion Aerosols and SO_2 - an Interdisciplinary Analysis. *Environmental Science & Technology*. 20: 138-145.

Bhave, P. V., Kleeman, M. J., Allen, J. O., Hughes, L. S., and Cass, G. R. (2002). Evaluation of an air quality model for the size and composition of source-oriented particle classes. Environ. Sci. Technol., 36, 2154-2163.

Birch, M. E., and R. A. Cary, Elemental carbon-based method for monitoring occupational exposures to particulate diesel exhaust, Aerosol Sci. Technol., 25, 221-241, 1996.

Bolleter, W.T., C. T. Bushman, and P. W. Tidwell, Spectrophotometric determinations of ammonium as indophenol, Anal. Chem., 33, 592-594, 1961.

Bond, Tami C., David S. Covert, John C. Kramlich, Timothy V. Larson, Robert J. Charlson, *J. Geophys. Res.*, 107(D21), 8347, doi:10.1029/2001JD000571, 2002.

Cooke, W. F., C. Liousse, H. Cachier, and J. Feichter, Construction of a $1^0 X 1^0$ fossil fuel emission data set for carbonaceous aerosol and implementation and radiative impact in the ECHAM4 model, J. Geophys. Res., 104(18), 22,137– 22,162, 1999.

Eldering, A. and Cass, G. R. (1996). Source-oriented model for air pollutant effects on visibility, J. Geophys. Research, 101, D14, 19343-19369.

Hildemann LM, Markowski GR, Cass GR. 1991a. Chemical-Composition of Emissions from Urban Sources of Fine Organic Aerosol. *Environmental Science & Technology*. 25: 744-759.

Hildemann LM, Markowski GR, Jones MC, Cass GR. 1991b. Submicrometer aerosol mass distributions of emissions from boilers, fireplaces, automobiles, diesel trucks, and meat cooking operations. *Aerosol Science and Technology*. 14: 138-152.

Huntzicker, J. J., R. L. Johnson, J. J. Shah, and R. A. Cary, Particulate Carbon, Atmospheric Life Cycle, edited by G. T. Wolff and R. L. Klimisch, pp. 79-88, Plenum, New York, 1982.

John, W., and G. Reischl, A cyclone for size-selective sampling of ambient air, J. Air Pollut. Control Assoc., 30, 872-876, 1980.

Kleeman MJ, Schauer JJ, Cass GR. 1999. Size and composition distribution of fine particulate matter emitted from wood burning, meat charbroiling, and cigarettes. *Environmental Science & Technology*. 33: 3516-3523.

Kleeman MJ, Schauer JJ, Cass GR. 2000. Size and composition distribution of fine particulate matter emitted from motor vehicles. *Environmental Science & Technology*. 34: 1132-1142.

Kleeman, M. J. and Cass, G. R. (2001). A 3D Eulerian source-oriented model for an externally mixed aerosol. Environ. Sci. Technol., 35, 4834-4848.

Kauppinen EI, Pakkanen TA. 1990. Coal Combustion Aerosols - a Field-Study. *Environmental Science & Technology*. 24: 1811-1818.

Markowski GR, Filby R. 1985. Trace-Element Concentration as a Function of Particle-Size in Fly-Ash from a Pulverized Coal Utility Boiler. *Environmental Science & Technology*. 19: 796-804.

Marple, V. A., K. L. Rubow, and S. M. Behm. A microorifice uniform deposit impactor (MOUDI), description, calibration, and use, Aerosol Sci. Technol., 14, 434-446, 1991.

McElroy MW, Carr RC, Ensor DS, Markowski GR. 1982. Size Distribution of Fine Particles from Coal Combustion. *Science*. 215: 13-19.

Mulik, J., R. Puckett, D. Williams, and E. Sawicki, Ion chromatographic analysis of sulfate and nitrate in ambient aerosols, Anal. Lett., 9, 653-663, 1976.

Olmez, I., in Methods of Air Sampling Analysis, 3rd ed., edited by J. P. Lodge, pp. 143-150, Lewis, Chelsea, Mich., 1989.

Quann RJ, Neville M, Janghorbani M, Mims CA, Sarofim AF. 1982. Mineral Matter and Trace-Element Vaporization in a Laboratory-Pulverized Coal Combustion System. *Environmental Science & Technology*. 16: 776-781.

Schauer J. J., Kleeman MJ, Cass GR, Simoneit BRT. 1999a. Measurement of emissions from air pollution sources. 1. C-1 through C-29 organic compounds from meat charbroiling. *Environmental Science & Technology*. 33: 1566-1577.

Schauer J. J., Kleeman MJ, Cass GR, Simoneit BRT. 1999b. Measurement of emissions from air pollution sources. 2. C-1 through C-30 organic compounds from medium duty diesel trucks. *Environmental Science & Technology*. 33: 1578-1587.

Streets, D. G., S. Gupta, S. T.Waldhoff, M. Q.Wang, T. C. Bond, and Y. Bo, Black carbon emissions in China, Atmos. Environ., 35, 4281– 4296, 2001.

Venkataraman, C.; Reddy, C. K.; Josson, S.; and Reddy, M.S. (2002). Aerosol Chemical and Size Characteristics at Mumbai, India, during the INDOEX-IFP (1999), *Atmospheric Environment, 36(12), 1979-1991.*

CHAPTER-6

Detailed speciation of ambient fine organic carbon particles and source apportionment of $PM_{2.5}$ in Indian cities

6.1. Abstract

The fine particle organic carbon in Delhi, Mumbai, Kolkata, and Chandigarh has been speciated in order to identify and quantify five major sources to the fine particle pollution in those cities using chemical mass balance modeling with organic compounds as tracers. Fifty-five organic compounds were quantified using GC/MS techniques, including n-alkanes, polycyclic aromatic hydrocarbons (PAHs), hopanes, steranes, and levoglucosan. Annual average concentrations for four seasonal periods were determined for three out of the four sites. Summertime concentrations for levoglucosan, picene, and the sum of hopanes and

steranes were respectively 210±42 ng/m^3, 0.30±0.06 ng/m^3, and 8.5±1.7 ng/m^3 (for Delhi); 75±15 ng/m^3, 0.30±0.06 ng/m^3, 15±3 ng/m^3 (for Kolkata); 140±28 ng/m^3, 0.20±0.04 ng/m^3, and 41±8 ng/m^3 (for Chandigarh). Wintertime concentrations for the same compounds were respectively 5300±1100 ng/m^3, 5.1±1.0 ng/m^3, and 80±16 ng/m^3 (for Delhi); 5500±1100 ng/m^3, 7.1±1.4 ng/m^3, 110±22 ng/m^3 (for Kolkata); 910±180 ng/m^3, 1±0.2 ng/m^3, 23±5 ng/m^3 (for Mumbai). These measured concentrations of organic carbon from the four sampling sites were used in a molecular marker source apportionment model to quantify the primary source contributions to the PM$_{2.5}$ mass concentrations at those sites. Five important sources were identified and quantified: diesel exhaust, gasoline exhaust, road dust, coal combustion, and biomass combustion. Important trends in the seasonal and spatial patterns of the impact of these five sources were observed. Primary emissions from fossil fuel combustion (coal, diesel, and gasoline) were responsible for 22-33% of PM$_{2.5}$ mass in Delhi, 23-29% in Mumbai, 37-70% in Kolkata, and 24% in Chandigarh. These figures can be compared to the biomass combustion contributions to ambient PM$_{2.5}$ of 9-28% for Delhi, 12-21% for Mumbai, 15-31% for Kolkata, and 9% for Chandigarh. These measurements provide important information about the seasonal and spatial distribution of fine particle-phase organic compounds in Indian cities as well as quantifying source contributions leading to the fine particle air pollution in those cities.

6.2. Introduction

Urban areas in India typically experience very high concentrations of airborne particulate matter [Aggarwal et al., 1999]. Studies have shown that $PM_{2.5}$ contributes to the visibility problem and are likely responsible for respiratory and cardio-pulmonary diseases like asthma, bronchitis, and heart disease [Pope et al, 2002, Dockery et al., 1993], but the actual concentrations and mixture of sources that produce the problem in a particular area will remain undetermined until detailed measurements can be made. Over the past several decades, a series of methods have been developed for diagnosing the relative importance of the various emissions sources that together accumulate to create fine particle air pollution problems in urban areas. Source-oriented methods of analysis exist that rely on atmospheric transport models driven by detailed emissions inventories. However, lack of detailed measurements, detailed emission inventories, and appropriate emission factors for South Asian-city specific sources, quantitative identification of major anthropogenic sources leading to fine particle air pollution in key Indian cities has been difficult to achieve using this method. A different approach to identifying sources is to use receptor-based techniques which rely on identification of key tracers in sampling sites (receptors). This method uses the differences in chemical composition of particulate matter emitted from different sources to identify the presence of particles from specific sources when they are present in atmospheric samples. The receptor-based method has been widely used as a tool in air pollution source apportionment studies and has been successfully applied in many US cities to understand the source contribution to the ambient air pollution [Chow et al., 1992, Kowalczyk, 1978, Zeng and Hopke, 1989]. These methods are particularly attractive for application in regions that

have not been studied previously because they are able to yield rapid insights into the causes of a local air pollution problem before the completion of an accurate emissions inventory. In the Indian subcontinent, such a receptor-based source apportionment model has been carried in Bangladesh using inorganic elemental analysis of $PM_{2.5}$ [Begum et al, 2004]. In India, no such work has been published. Models using primarily inorganic elements have limitations when examining fine particulate mass since a significant fraction of the fine particulate mass in the urban atmosphere is from combustion sources. These sources emit fine particles largely comprised of organic carbon with only trace levels of inorganic elements. The trace elements present in the fine particle emissions from several important urban air pollution sources are not sufficient to provide unique fingerprints that can be used to properly distinguish the sources in a receptor-based model. The organic compounds present in fine particles emitted from burning wood, combustion of automotive fuels, and combustion of coal are very different. These differences can be exploited by receptor models to determine their respective contributions to the atmospheric concentrations of fine particulate matter [Schauer et al., 1996]. Such a receptor model based on the use of organic tracers was developed by Schauer et al. [1996] and has been successfully applied in the study of fine particle sources in the Los Angeles area and in the San Joaquin Valley of California [Schauer et al., 2000] as well as in the Southeast USA [Zheng et al., 2002]. In the present paper, this method has been used to quantify the sources that contribute to $PM_{2.5}$ at four cities in India.

6.3. Experimental Setup

Ambient sampling over one year was conducted in Delhi, Mumbai, and Kolkata--three of the megacities located in India. Four months from the entire year were selected to represent the seasonal pattern observed in the region. Five samples every six days were taken for each of the four months sampled. The selected four months were: March to represent spring, June to represent summer, October to represent autumn, and December to represent winter. A fourth site, Chandigarh, upwind of Delhi was selected to represent more regional background conditions in India. After analyzing five years of backwind trajectories from NOAA, Chandigarh appeared to be suitable as a background site upwind to Delhi. It is a smaller city with a population of 809,000 located in the northern side of India. Suitable power supplies, availability of trained personnel, cost of transportation, and ease of communication were limiting factors in selecting Chandigarh as the background site. In spite of efforts to take samples for four seasons, only five samples during the summer season were obtained; the rest of the sampling protocol could not be completed.

Figure 6.1 shows the location of the four cities in the Indian subcontinent where the samples were taken and Table 6.1 describes the sites.

Table 6.1. Description of the sampling sites.

City	Site Address	Location Type	Site Description	Source of Pollution
Mumbai	NEERI Zonal Laboratory 89/B, Dr. Annie Basen Rd. Worli, Mumbai-400018 India	Urban Residential	Sampler placed 3 m above ground on a rooftop. A four-story building and slum areas near-by.	City traffic typically seen in residential and business areas, and cooking by slum dwellers.
Delhi	National Physical Lab Dr. K. S. Krishnan Marg New Delhi – 110012 India	Urban Residential	Sampler placed 5 m above ground on an office building rooftop in the NPL campus. Unobstructed space around.	City traffic typically seen in residential and business areas, and cooking by slum dwellers.
Kolkata	NEERI Zonal Laboratory I-8, Sect-C, East Kolkata P.O. Box Haltu, Kolkata 700078 India	Urban Residential	Sampler on a 2 meter platform located in an open field. Ruby General Hospital and a diesel truck garage nearby.	City traffic typically seen in residential and business areas, cooking by slum dwellers, and some emission from combustion by diesel trucks parked in nearby garage.

Figure 6.1. Location of the four sampling sites: Delhi, Mumbai, Kolkata, and Chandigarh.

The sites at Delhi, Mumbai, and Kolkata were carefully selected to avoid undue influence of emissions coming from heavy city traffic or industrial work, yet they were located within the metropolitan cities, thus enabling the capture of the cities' emissions throughout the day and the night. In each location, the samplers were placed either on rooftops or in the middle of open fields to ensure that the sampler inlet was able to sample wind coming from all directions. The Chandigarh site needed to be outside the limit of the main town and thus was located at the Postgraduate Institute of Medical Education and Research on a rooftop on the fourth floor. Sampling started on March 4, 2001 and continued until January 16, 2002. Samples were collected at ambient temperatures and relative humidities for 24 hours starting at midnight local time every sixth day for each of the months sampled. After the completion of the sampling campaign, there were 21 samples for Delhi, 25 samples for Mumbai, 20 samples for Kolkata, and 5 samples for Chandigarh. These samples were chemically analyzed, and the results from the organic speciation are described in this paper. A second paper will be presented with findings from the inorganic speciation work.

A Caltech-built, $PM_{2.5}$ filter sampler was used at each of the four sites. Sampling equipment is shown schematically in Figure 6.2. Fine particulate matter was collected on one quartz fiber filter (Pallflex, 2500 QAO, 47 mm diameter), two pre-washed Nylon Filters (Gelman Sciences, Nylasorb, 47 mm diameter), and on two PTFE filters (Gelman Sciences, Teflo, 1.0 μm pore size).

Figure 6.2. Schematic diagram of the sampling unit. TU1 and TU2 are teflon filters, NU1 and ND1 are undenuded nylon filter and denuded nylon filter respectively, and QU1 is a quartz fiber filter.

Ambient air was drawn at a rate of approximately 22.5 lpm through an acid-washed Pyrex glass

inlet line to a Teflon-coated Air and Industrial Hygiene Laboratory (AIHL)-design cyclone

separator [John and Reischl, 1980], which removed large particles with a collection efficiency curve having a 50% aerodynamic cutoff diameter at 2.5 μm before the air passed through the filters. The nylon filter located downstream of the MgO-coated diffusion denuder was used in conjunction with the nylon filter downstream of the cyclone alone to measure gas-phase nitric acid, hydrochloric acid, and fine particle nitrate by the denuder difference method. The air flowrate through each filter was measured before and after each 24-hour sampling period with a calibrated rotameter.

Extraction of particle-phase organic compounds collected on quartz fiber filters was based on the methods described by Mazurek et al. [1987] and further refined by Schauer et al. [1996] and Zheng et al. [2002]. Samples were combined by season and extracted in annealed glass jars with Teflon-lined lids. Mumbai summertime samples did not contain enough organic carbon (OC) for acceptable GC/MS analysis and thus were not analyzed. In addition, filter blanks as well as lab blanks were analyzed. Filter blanks were prepared, stored, shipped in the same manner as the samples, and lab blanks were used to identify possible contaminants from handling samples in the laboratory. Results from both field and lab blanks were carefully analyzed and subtracted before reporting the final results. In total, 23 samples were analyzed including field and laboratory quality assurance/quality control (QA/QC) blanks.

The samples were first spiked with an internal standard mix containing 16 deuterated compounds. These deuterated internal standards as well as standard mixtures were provided by the Wisconsin State Hygiene Laboratory. The deuterated internal standards were:

dodecane-*d*26, hexadecane-*d*34, eicosane-*d*42, octacosane-*d*58, hexatriacontane-*d*74, benzaldehyde-*d*6, decanoic acid-*d*19, heptadecanoic acid-*d*33, phthalic acid-3,4,5,6-*d*4, acenaphthene-*d*10, 4,4′-dimethoxybenzophenone-*d*8, dibenz(ah)anthracene-*d*14, chrysene-*d*12, ααα-20R-cholestane-*d*4, cholesterol-2,2,3,4,4,6-*d*6, and levoglucosan-13C6. These internal standards provided internal quantification references for the key particle phase organic compounds covering their range of mass spectral fragmentations, polarity, and reactivitiy with derivatization reagents. About 250 μL of the internal standard mix was spiked per milligram of OC. The amount of spiked internal standard mix was proportional to the amount of the OC present in the sample. Samples were extracted under mild sonication (20 minutes) twice with hexane (Fischer Optima Grace), followed by three successive extractions using a 2:1 mixture of benzene and isoproponal (benzene—high purity lots of E&M Scientific Omnisolv; isopropanal—Burdick & Jackson). High purity benzene was further distilled in the laboratory to remove the small fraction of impurities and tested for purity by GC/MS prior to use. The extract was filtered to remove loose filter materials, and the volume was reduced to about 5 mL using a rotary evaporator. Finally, it was blown down close to the volume of injected internal standard using ultrapure N_2. The extract was split into two fractions. One fraction was derivatized with diazomethane to convert organic acids to their methyl ester analogues which are better identitied and quantified using GC/MS.

A Hewlett-Packard GC/MSD (6890 GC and 5973MSD) equipped with a 30 m l. x 0.25 mm i.d. x 0.25 μm film thickness HP 5 MS capillary column was used. The operation conditions were: isothermal hold at 65°C for 2 min, temperature ramp of 10°C min^{-1} to 300°C, isothermal hold at 300°C for 22 min, GC/MS interface temperature 300°C. The flow of the

carrier gas, He, was 1 mL min^{-1}. The injection volume was 1 μL for each sample. The scan range was 50-500 amu, and the sample was analyzed under electron ionization mode (70 eV). These same instrumental settings were used by Zheng et al. [2002]. Not all organic compounds were solvent extractable, nor were they all elutable from a GC column. Hundreds of authentic standards have been prepared for the positive identification and quantification of the organic compounds available from the Wisconsin Hygene Laboratory. Estimated measurement uncertainties of the measured organic compounds by GC/MS techniques as found by Schauer et al [1999a] used in the present study were ±20% (1 sigma).

Chemical Mass Balance (CMB 8.0) [Watson et al., 1998] modeling was used to apportion PM$_{2.5}$ particles to various sources. The CMB model combines the chemical and physical characteristics of particles or gases measured at the sources and the receptors to quantify the source contributions to the receptor [Miller et al., 1972]. Chemical Mass Balance (CMB 8.0) (Watson et al., 1998) modeling was used to apportion PM$_{2.5}$ particles to various sources. The CMB receptor model consists of a solution to linear equations that express each receptor chemical concentration as a linear sum of products of source profile abundances and source contributions. The source profile abundances (i.e., the mass fraction of a chemical or other property in the emissions from each source type) and the receptor concentrations, with appropriate uncertainty estimates, serve as input data to the CMB model. In order to distinguish among source type contributions, the measured chemical and physical characteristics must be such that they are present in different proportions in different source emissions and changes in these proportions between source and receptor are negligible or can

131

be approximated. The CMB calculates values for the contributions from each source and the uncertainties of those values.

The CMB is applicable to multi-species data sets, the most common of which are chemically characterized particulate matter (PM) and volatile organic compounds (VOCs). Although not perfect, source apportionment modeling is a powerful tool for inferring sources of atmospheric PM given a high quality set of observations and the needed source profiles. Refer to Watson et al. (1998) for the mathematics involved in CMB modeling. Model assumptions, as described by Watson et al. (1998) are:

1) Compositions of source emissions are constant over the period of ambient and source sampling

2) Chemical species do not react with each other, rather they add linearly

3) All sources with a potential for contributing to the receptor have been identified and have had their emissions characterized

4) The number of sources or source categories is less than or equal to the number of species

5) The source profiles are linearly independent of each other, and

6) Measurement uncertainties are random, uncorrelated, and normally distributed.

CMB can tolerate reasonable deviations from these assumptions, though deviations increase the stated uncertainties of the source contribution estimates (Cheng and Hopke, 1989).

In the present study, CMB was conducted using organic compounds as molecular markers. An important aspect of molecular marker source apportionment is the selection of organic compounds that can be properly used as tracer species in the model. Fifty-five organic compounds, along with Al, Si, and elemental carbon (EC) have been quantified in this study by using the methods described by Mazurek et al. [1987] and further refined by Schauer et al. [1996]. These compounds have been selected carefully so they can be used as tracer species in the CMB model. These species do not form, do not significantly react, nor have other selective removal processes (i.e. volatilization) in the atmosphere. After repeated analysis, out of the fifty-five identified organic compounds, thirty-two were selected as fitting species. Source profiles are other key parameters used in CMB modeling. Eighteen source profiles, as described in Table 6.2, were selected for this study. These source profiles were put together at California Institute of Technology using the same laboratory procedures described previously for atmospheric samples and using the same quantification standards as used in this study. Whenever possible, source profiles from the Indian Subcontinent were selected. Five source profiles selected from Bangladesh were: coconut leaves, rice straw, cow dung, jackfruit wood, and biomass briquette. Sheesley et al. [2003] describes in detail these five sources from Bangladesh. Source profiles for diesel engine exhaust, gasoline-powered vehicle exhaust, road dust, and natural gas combustion were obtained from previous studies in North America and applied to this study [Hildemann et al., 1991, Rogge 1993a, Rogge et al., 1993b, Schauer et al., 1999b, Schauer et al., 2001, Schauer et al., 2002b]. The coal source profile was obtained from the analysis of fine particulate matter emitted from the burning of Datong coal in China [Zheng et al., in preparation].

Table 6.2. List of source profiles used in this study.

SN	Source Profile Name	Description	Used in Final Analysis
1	Medium Duty Diesel Trucks		Yes
2	Non-Catalyst Gasoline Powered Motor-Vehicle		No
3	Catalyst Equipped Gasoline Powered Motor-Vehicle		No
4	Average of Gasoline Vehicle: 83% Non-Catalytic, 17% Catalytic	Weighted average of #2 and #3	Yes
5	Meat Cooking		No
6	Road Dust from Fresno, CA		No
7	Road Dust from Bakersfield, CA		No
8	Road Dust from Kern Wildlife Refuge, CA		No
9	Average of Road Dust	Average of #6 to 8	Yes
10	Fuel Oil		No
11	Beijing Coal		Yes
12	Natural Gas		No
13	Coconut Leaves from Bangladesh		No
14	Rice Straw from Bangladesh		No
15	Cow Dung from Bangladesh		No
16	Biomass Briquette from Bangladesh		No
17	Jackfruit Branches from Bangladesh		No
18	Average of Bangladeshi Biomass	Average of #13 to 17	Yes

Figure 6.3 shows the emissions from each of these source profiles. Given that not all of the source profiles have been directly measured in India, the model inputs serve as best estimates of the actual emission profiles based on available data. However, tracer species are limited to a few characteristic tracers per source and so they are more specific to the sources than to the locations. It should be noted in here that the identification of sources carries a lot less uncertainties than the quantification since CMB can over quantify source contributions. The results and uncertainties in the modeling work are explained in the following sections in more details.

Figure 6.3. Fine particle emission pattern from diesel combustion, gasoline combustion, road dust, coal combustion, and biomass combustion.

6.4. Results and Discussion

6.4.1. Organic Speciation Results:

136

The organic component of ambient particles in both polluted and remote areas is a complex mixture of hundreds of organic compounds [Hahn, 1980; Cass et al., 1982; Simoneit and Mazurek, 1982; Rogge et al., 1993abc]. Compounds identified in the ambient aerosol include n-alkanes, n-alkanoic acids, aliphatic, retene, aromatic polycarboxylic acids, polycyclic aromatic hydrocarbons, steranes, and so forth [Mazurek et al., 1989; Hildemann et al., 1993; Rogge et al., 1993abc]. Most of these compounds have also been identified in the current study. Results from organic speciation for all four cities are displayed in Figure 6.4, and are further analyzed and presented with key organic tracers in Figure 6.5.

Figure 6.4. Concentrations of organic species in fine particles for four Indian cities as identified by Gas Chromatography Mass Spectrometry.

Organic speciation for the summertime Mumbai samples could not be conducted because of the low organic carbon levels since the organic carbon mass for this composited sample did not contain enough mass to meet the detection limit for the target organic compounds analyzed by GC/MS. Hopanes and steranes are organic markers that are present in heavy petroleum distillates such as lubricating oil [Simoneit, 1985, Simoneit, 1999a]. In the southern California atmosphere, these compounds have been shown to be predominately from the exhaust emissions of gasoline and diesel-powered motor vehicles and result from the presence of lubricating oil in PM emissions [Schauer et al, 2000, Rogge 1993a, Rogge et al., 1993b, Rogge et al., 1996, Schauer et al., 2002]. Wood smoke contributes to carbonaceous aerosol concentrations but not to hopane and sterane concentrations. Diesel vehicles are important sources of both elemental carbon and hopanes and steranes, while gasoline-powered vehicles are important sources of hopanes and steranes and smaller contributors to elemental carbon concentrations. On the other hand, levoglucosan is a major component of wood smoke aerosol and has been shown to be a good tracer for wood burning (Schauer et al., 1996, Schauer et al., 2002, Simoneit et al., 1999b], whereas silicon and aluminum are markers for road dust.

Figure 6.5. Seasonal variations of elemental carbon, organic carbon, levoglucosan, picene, hopanes and steranes, and alkanes for Delhi, Mumbai, Kolkata, and Chandigarh.

Summertime levoglucosan concentrations for Delhi, Kolkata, and Chandigarh are 210 ± 42 ng/m^3, 75 ± 15 ng/m^3, and 140 ± 28 ng/m^3 respectively; whereas wintertime levoglucosan concentrations for the Delhi, Kolkata, and Mumbai are, respectively, 5300 ± 1100 ng/m^3, 5500 ± 1100 ng/m^3, 910 ± 180 ng/m^3. Summertime Mumbai and wintertime Chandigarh measurements were not available. Ratios for levoglucosan to the sum of hopanes and steranes follow a seasonal trend: ratios are at least three to ten times higher during the colder months compared to the warmer months for all the cities in this study. This seasonal trend in levoglucosan, a proven biomass smoke marker, may suggest increased amount of

wood used for home heating. Also, stigmasterol, a suggested marker for cowdung combustion smoke, has been detected in all cities. Very low income households use cowdung patties along with tree leaves and branches to cook or heat their surroundings.

Picene concentrations in the summer in Delhi, Kolkata, and Chandigarh were 0.30 ± 0.06 ng/m^3, 0.30 ± 0.06 ng/m^3, 0.20 ± 0.04 ng/m^3, respectively, and wintertime concentrations in Delhi, Kolkata, and Mumbai are 5.1 ± 1.0 ng/m^3, 7.1 ± 1.4 ng/m^3, 0.9 ± 0.2 ng/m^3 respectively. Concentrations of picene, which is a coal marker, increased during the winter, particularly because of air stagnation and because of a decrease in wet deposition. Three thermal power plant stations are present in Delhi: Indraprastha (284 MW capacity, burning 11,50,000 MT/yr of pulverized coal with 39.4% ash and 0.36% sulfur content in the coal), Rajghat (135 MW capacity, burning 876,000 MT/yr of pulverized coal with a 35-42% ash and 0.50% sulfur content in the coal), and Badarpur (720 MW capacity, burning 3,940,000 MT/yr of pulverized coal with a 28-32% ash and 0.35% sulfur content) (Varma, 1999). Although electrostatic precipitators (ESPs) are present in each of these power generating facilities, poor maintenance has been blamed for high loads of fly ash [Aggarwal et al., 1999].

Cholesterol concentrations were below the instrument detection limit in almost all the samples suggesting that the amount of meat cooking is minimum and negligible. This is consistent with most Indians being vegetarian and thus meat consumption is low in the country compared to other countries.

6.4.2. CMB Results:

Results from CMB modeling (Figure 6.6) show that there is no single dominant source of $PM_{2.5}$ and a number of sources contribute to the fine particle concentrations. Gasoline combustion is primarily from mobile sources, but the diesel contribution is from both stationary and mobile sources. It is not possible to attribute secondary sulfates, nitrates, and ammonium to specific primary sources using CMB, though sulfates can likely be linked to the sulfur in fossil fuels. Secondary particulate formation comprised approximately one-tenth to one-fifth of $PM_{2.5}$. Broadly, mobile sources and biomass combustion appear to contribute substantially and in several cases approximately in equal proportions. Road dust can also be significant. Predictably, the contributions of biomass and coal, presumably used for heating, are high in winter in Delhi and Kolkata. Out of the 12 samples that underwent CMB analysis, road dust was the largest contributor in three, whereas, biomass combustion in two, and unidentified sources in the remaining three. Unidentified hydrocarbons and water are two potential sources of the unidentified mass. Diesel exceeds gasoline in all cases, which is not surprising, given the relatively higher emission rates for diesel compared to gasoline and the higher consumption of diesel compared to gasoline in India. It should be pointed out that although the source profile for diesel is from medium-duty diesel trucks, it is not possible to distinguish between diesel exhaust from vehicles and diesel emissions from stationary sources. The use of diesel in small power generators is not insignificant in the Indian cities studied because of frequent power outage. Therefore, not all diesel-derived $PM_{2.5}$ is from mobile sources. Gasoline, in contrast, is used almost exclusively in vehicles, and can be attributed to mobile sources with little error. By summing the contributions from diesel,

141

gasoline, and coal, we find that in most cases fossil fuel combustion exceeds biomass combustion. It is interesting to note that the sum of the identified sources from the CMB results from spring (107%), summer (130%), and autumn (120%) seasons in Kolkata exceeded the measured mass of $PM_{2.5}$. Total mass concentrations from identified sources should equal approximately 100%, although values ranging from 80 to 120% are acceptable [Watson et al., 1998]. If the measured mass is very low (< 5 to 10 $\mu g/m^3$), percent mass may be outside of this range because the precision of the mass measurement is on the order of 1 to 2 $\mu g/m^3$. Also, higher levels can be due to larger ratios of total $PM_{2.5}$ to specific tracers than are actually present, or propagation of the various uncertainties involved in this process [Zheng et al., 2002]. It has often been found that CMB can lead to greater mass apportioned than measured.

Results obtained by using the organic compounds in CMB have been used to reconstruct the mass of the inorganic portion of ambient fine particle. The results are shown in Figures 6.7 to 6.9. The mass compares very well for sulfate, nitrate, chloride, ammonium, organic matter, elemental carbon, as well as the aluminum and silicon since these were used as fitting species in the model. For the remaining trace species like Zn, Fe, Pb, Mn, Mg, Ti the mass reconstructed is significantly less than the concentrations found in the atmosphere. It is interesting to note that Fe, Mg, and Ti are found in the soil. Also, Pb which has been phased out from the Indian fuel recently, it can be resuspended from the soil and become airborne. In the absence of a fine particle soil profile from Indian cities, the trace metal emissions found in the soil profiles conducted by Chow et al. [2004] have been used in the mass reconstruction. Chow et al. [2004] report fine particle emissions from paved road dust from San Antonio and

Laredo, Texas, USA.   Typical Fe, Mn, and Zn content of Indian soil from Pune, Maharashtra, ranges from 4.2 to 17.6 mg kg^{-1}, 6.2 to 27.6 mg kg^{-1}, and 0.8 to 4.6 mg kg^{-1} respectively [Mali et al., 1999] which are higher than the same species found in the soil from San Antonio and Laredo, Texas. [Chow et al., 2004].

.Figure 6.6. Source contribution to the ambient fine particles in Delhi, Mumbai, Kolkata, and Chandigarh.

Figure 6.7. Inorganic mass reconstruction for Delhi by using CMB source apportionment results.

Figure 6.8. Inorganic mass reconstruction for Mumbai by using CMB source apportionment results.

Figure 6.9. Inorganic mass reconstruction for Kolkata by using CMB source apportionment results.

Figure 6.10. Seasonal and Spatial Variation of the Predominant Sources in Delhi, Mumbai, Kolkata, and Chandigarh.

6.4.3. Fuel-Based Particulate Matter Emissions:

An initial confirmation of the CMB-based source apportionment was conducted by comparing the results here for fuel oil, diesel, and gasoline emissions to the results obtained from National Environmental Engineering Research Institute (NEERI)'s yearly fuel usage and fuel-based emissions factors in Mumbai for the year 2001. Emission factors were obtained from Reddy and Venkataraman [2002]. The emission factor for gasoline vehicles is a

weighted average between the emission factor for non-catalytic vehicles using unleaded gasoline reported by Reddy and Venkataraman [2002] and for motorcycles [EPA, 2002]. As seen from Table 6.3, a first order approximation, it appears that diesel contribution to fine particle emission in Mumbai is an order of magnitude higher than gasoline and fuel oil.

Table 6.3. First order approximation of particulate emission from Mumbai using a fuel-based approach. The estimate for gasoline is sensitive to the assumed fraction of fuel use by motorcycles and the emissions factor for that source.

	Yearly Consumption	Emission Factor	Density	Fuel-Based PM Emission	CMB PM Emission	Reddy and Venkataraman
	10^6 l	g/kg	kg/l	Kg/Day	% of Fine	Entire India
Furnace Oil	424	0.65	0.95	620	Negligible	Negligible
LSHS	1845	0.3	0.95	1400	Negligible	Negligible
Diesel (automotive + industrial)	1140	4.2	0.85	11,000	22%	10%
Gasoline	565	0.6	0.75	700	3%	Negligible

This is comparable to our results obtained from CMB. In addition, gasoline and diesel emissions from vehicular activity are directly emitted at ground level and thus have a proportionally greater effect on urban air quality. Reddy and Venkataraman [2002] find that utility coal burning has the largest emissions nationally in India. Such emissions are not concentrated as much in cities as are motor vehicle emissions. Further, those emissions, along

with the emissions from burning fuel oil are often injected into the atmosphere well above the mixed layer. Thus, one expects fuel oil and coal sources to have smaller impact, relative to their total emissions rate, on urban, ground level particulate measurements as apportioned here

It is also of interest to conduct an order of magnitude approximation of the expected levels of PM from the various sources. Using an approximate size of greater Mumbai of 50 x 50 km, an average mixing height of 200 m, and an average wind speed of 2 m/s, and assuming instant mixing in to the whole airshed, the above emissions estimates would suggest PM levels from the three sources would be <u>about</u> 5 $\mu g/m^3$ for diesels, 0.3 $\mu g/m^3$ for gasoline fueled vehicles and 0.2 $\mu g/m^3$ for furnace oil. While all of these values appear low (due to the approximations in the calculation and possible underestimates in the emissions factors for the various sources), it does suggest that it is not surprising that our source apportionment does not find significant levels of PM coming from furnace oil, kerosene and other liquid and gaseous fuel used in industrial, external combustion boilers. Again, gasoline fueled vehicles emit near the ground, similar to where the monitors are sampling air, and will have a greater impact, particularly at night when the mixing depths are much lower.

6.5. Uncertainties

Receptor modeling of the type performed here is open to uncertainties, albeit not so large as other approaches relying on less detailed information. Indeed, the use of organic molecular markers provides significant extra information than is typically available. Further,

the agreement with other approaches of estimating sources of PM$_{2.5}$ conducted above is also encouraging, as is the agreement with other studies [Reddy and Venkataraman, 2002]. Still, it is important to recognize the uncertainties and possible sources of error.

First, as a receptor modeling approach, errors in the measurements will manifest themselves directly in the source apportionments, and possibly be magnified if the source profiles are similar. It can be shown that if two source profiles are similar, small variations of the measurements in the source profiles can lead to large uncertainties in the source apportionment results. Second, errors, omissions and/or variations in the source profiles will impact the source apportionment. For example, in this study, it was found that using all of the available, and possibly applicable biomass burning profiles led to the CMB model giving erroneous results (some of the sources had negative strengths), so a single profile for the various biomass burning sources had to be used. This involved judgment as to what mixture of profiles for biomass burning would be best. More subtle is that a source in one location can have a different profile than ostensibly the same source in another location, for example, diesel trucks. The source profile used was developed in the United States. The engine type, age, condition, duty cycle, additional controls, maintenance, fuel type and lubricating oil can all impact the source profile. The profile for coal was taken from a Chinese coal. Subtler still is the assumed uncertainties in the measurements and profiles can impact results. Parameters chosen for the CMB application can affect results. Finally, the measurements taken were for a limited period. Without additional monitoring it is difficult to say if the analysis is representative over longer periods.

While the above list seems daunting, it is important to remember that even without applying the CMB, one can look at the measured organics and identify which sources are most likely to have a major impact because emissions from fossil fuel combustion in internal combustion (IC) engines has certain characteristics very distinct from biomass burning, which is distinct from meat cooking, all of which are distinct from road dust. Thus, the uncertainties within, say, apportioning the amount of PM from compression ignition versus spark ignition engines may be relatively large, organic carbon from biomass burning has distinctly different compounds, so the uncertainty between fossil fuel and biomass combustion is not so uncertain. Thus, while it is more difficult to say with great confidence how much PM is coming from gasoline-fueled automobiles vs. diesel vehicles, one can say with greater confidence how much is coming from IC engines. A formal error analysis is beyond the scope of this work. Again, it is reassuring the consistency of the results from the receptor modeling with those from the fuel-based estimates and other estimates for India.

Reducing the uncertainties requires significant effort. In particular, it would be very beneficial to measure source profiles for the various sources specific to India, e.g., measure the source profiles for Indian diesels, automobiles, two wheelers and coal. Second, monitoring for another year or two would be useful to assess the representativeness of the current observations. Such monitoring could be limited to less detailed organic speciation. Third, more detailed emissions inventory work, and/or comparison with other available estimates would be useful. Ultimately, the emissions inventory will be used for policy setting and control strategy development, so it is important that the sources and resulting impacts on air quality be reconciled.

6.6. Conclusions

Detailed source apportionment for Delhi, Mumbai, Kolkata, and Chandigarh were conducted using receptor-based chemical mass balance modeling. Measured concentrations of organic carbon species, elemental carbon, and metals from the four sampling sites were used in a molecular marker source apportionment model to quantify the primary source contribution to the $PM_{2.5}$ mass concentrations at those sites. Five important sources of primary $PM_{2.5}$ were quantified: diesel exhaust, gasoline exhaust, road dust, coal combustion, and biomass combustion. Important trends in the seasonal and spatial patterns of the impact of these five sources were observed. Primary emissions from fossil fuel combustion (coal, diesel, and gasoline) were 22-33% in Delhi, 23-29% in Mumbai, 37-70% in Kolkata, and 24% in Chandigarh. These figures can be compared to the biomass combustion of 9-28% for Delhi, 12-21% for Mumbai, 15-31% for Kolkata, and 9% for Chandigarh. Road dust was also significant.

There is a need to conduct several source tests for diesel and gasoline combustion using vehicles representing the local vehicle fleet (diesel trucks, three-wheel auto-rickshaws). Coal source tests using Indian and Bangladeshi coals have been conducted, however, organic speciation work from the Indian coal results have not yet been completed. Emissions from local soil profiles (paved road dust as well as non-paved road dust) are necessary to refine the results from this work. Additional fine particle sampling is needed to identify the magnitude of seasonal variability. Finally, it is important to reconcile the observations and source

apportionment work done here with results that would be achieved using a source-based model in order to evaluate the emissions inventories developed for the various regions. Our order of magnitude calculation for Mumbai suggests that the two will give consistent results, though may differ quantitatively. This latter work is important for identifying possible missing sources and to provide a defensible, more first-principles, approach to policy-makers that can directly link specific sources to their air quality and health impacts.

6.7. Acknowledgement

6.8. References

Aggarwal, A. L.; Sunita, N.; Sen, S. (Editors), The citizens' fifth report, Centre for Science and Environment, New Delhi, 1999.

Begum, B. A., Eugene, K., Biswas, S. K., Hopke, P. K., 2004, "Investigation of sources of atmospheric aerosol at urban and semi-urban areas in Bangladesh", *Atmos. Env.,* in press.

Cheng, M.D. and Hopke, P. K., 1989, "Identification of markers for chemical mass balance receptor model," *Atmos. Environ*., 23, 1373-1384.

Cass, G. R.; Boone, P. M.; and Macias, E. S. (1982). Emissions and air quality relationships for atmospheric carbon particles in Los Angeles air in Particulate Carbon: Atmospheric Life Cycle, edited by G. T. Wolff and R. L. Klimisch. Plenum Press, New York, pp. 207-240.

Chow, J. C.; Watson, J. G.; Lowenthal, D. H.; Solomon, P. A.; Magliano, K. L.; Ziman, S. D.; Richards, L. W. (1992) PM_{10} source apportionment in California's San Joaquin Valley, Atmos. Environ., 26A, 3,335-3,354.

Chow, J. C.; Watson, J. G.; Kuhns, H.; Etyemezian, V.; Lowenthal, D. H.; Crow, D.; Kohl, S. D.; Engelbrecht, J. P., and Green, M. C. (2004). Source profiles for industrial, mobile, and area sources in the Big Bend Regional Aerosol Visibility and Observational study, Chemosphere, 54, 185-208.

Dockery, D.W., Pope, C.A., Xu, X. P., Spengler, J. D., Ware, J. H., Fay, M. E., Ferris, B. G., Speizer, F. E., 1993, "An association between air-pollution and mortality in 6 United-States cities," *New England Journal of Medicine,* 329, 1753-1759.

EPA. (2002) Exhaust Emission Factors for Nonroad Engine Modeling-Spark Ignition. EPA420-P-02-015, November 2002, NR-010c.

Hahn, J. (1980). Organic constituents of natural aerosols, Ann. N. Y. Acad. Sci., 338, 359-379.

Hildemann, L.M., Markowski, G.R., Cass, G.R., 1991. Chemical composition of emissions from urban sources of fine organic aerosol. Environmental Science and Technology, 25, 744-759.

Hildemann, L. M.; Cass, G. R.; Mazurek, M. A.; and Simoneit, B. R. T. (1993). Mathematical modeling of urban organic aerosols: properties measured by high-resolution gas chromatography, Environmental Science and Technology, 27, 2045-2055.

John, W. and Reischl, G., 1980, "A cyclone for size-selective sampling of ambient air," *J. Air Pollut. Control Assoc.,* 30*,* 872-876.

Kowalczyk, G. S., C. E. Choquette, and G. E. Gordon, Chemical element balances and identification of air pollution sources in Washington, DC. Atmospher. Environ., 12, 1143-1154, 1978.

Pope, C. A. III, Burnett, R. T., Thun, M. J., 2002, "Lung cancer, cardiopulmonary mortality, and long-term exposure to fine particulate air pollution," *J. of Amer. Med. Ass.,* 287, 1,132-1,141.

Mali, V. S.; Zenda, N. A., and Verma, U.K. (1999). Correlation between soil physico-chemical properties and available micronutrients in salt affected soils. Proceedings of the second International Workshop on Foliar Fertilization, Paper No. 2220, April 1999, Bangkok, Thailand.

Mazurek, M. A., Simoneit, B. R. T., Cass, G. R. and Gray, H. A., 1987, "Quantitative high-resolution gas chromatography and high-resolution gas chromatography/mass spectrometry analysis of carbonaceous fine aerosol particles," *Intern. J. Environ. Anal. Chem*., 29, 119-139.

Mazurek, M. A.; Cass, G. R.; and Simoneit, B. R. T. (1989). Interpretation of high resolution gas chromatography and high resolution gas chromatography/mass spectrometry data acquired from atmospheric organic aerosol samples, Aerosol Sci. Technol., 10, 408-420.

Miller, M. S., Friedlander, S. K., and Hidy, G. M. (1972) A chemical element balance for the Pasadena aerosol, J. Colloid Interface Sci., 39, 165-176.

Reddy, M.S; and Venkataraman, C. (2002). Inventory of Aerosol and Sulphur Dioxide Emissions from India: I – Fossil Fuel Combustion, Atmospheric Environment, 36 (4), 677-697.

Rogge, W. F.; Mazurek, M. A.; Hildemann, L. M.; Cass, G. R.; Simoneit, B. R. T. Quantification of Urban Organic Aerosols at a Molecular Level—Identification, Abundance and Seasonal-Variation; Atmos. Environ. Part A—General Topics, 1993a, 27, 1,309-1,330.

Rogge, W. F.; Hildemann, L. M.; Mazurek, M.A.; Cass, G. R.; Simoneit, B. R. T. Sources of Fine Organic Aerosol. 2. Noncatalyst and Catalyst-Equipped Automobiles and Heavy-Duty Diesel Trucks; Environ. Sci. Technol. 1993b, 27, 636-651.

Rogge, W. F.; Hildemann, L. M.; Mazurek, M.A.; Cass, G. R.; Simoneit, B. R. T. Sources of Fine Organic Aerosol. 4. Particulate abrasion products from leaf surfaces or urban plants, Environ. Sci. Technol. 1993c, 27, 2700-2711.

Rogge, W. F.; Hildemann, L. M.; Mazurek, M.A.; Cass, G. R.; Simoneit, B. R. T. Mathematical Modeling of Atmospheric Fine Particle-Associated Primary Organic Compound Concentrations. J. Geophys. Res.—Atmospheres, 1996, 101, 19,379-19,394.

Schauer, J. J., Rogge, W. F., Hildemann, L. M., Mazurek, M. A., and Cass, G. R., 1996. "Source apportionment of airborne particulate matter using organic compounds as tracers," *Atmospheric Environment,* 30 (22), 3837-3855.

Schauer, J. J., M. J. Kleeman, G. R. Cass, and B. R. T. Simoneit, Measurement of emissions from air pollution sources. 1. C1 through C29 organic compounds from meat charbroiling, Environmental Science & Technology, 33 (10), 1566-1577, 1999a.

Schauer, J. J., M. J. Kleeman, G. R. Cass, and B. R. T. Simoneit, Measurement of emissions from air pollution sources. 2. C1 through C30 organic compounds from medium duty diesel trucks, Environmental Science & Technology, 33 (10), 1578-1587, 1999b.

Schauer, J. J. and G. R. Cass, Source apportionment of wintertime gas-phase and particle-phase air pollutants using organic compounds as tracers, Environmental Science and Technology, 34 (9), 1821-1832, 2000.

Schauer, J. J., M. J. Kleeman, G. R. Cass, and B. R. T. Simoneit, Measurement of emissions from air pollution sources. 3. C1 through C29 organic compounds from fireplace combustion of wood, Environmental Science & Technology, 35 (9), 1716-1728, 2001.

Schauer, J. J., M. P. Fraser, G. R. Cass, and B. R. T. Simoneit, Source reconciliation of atmospheric gas-phase and particle-phase pollutants during a severe photochemical smog episode, Submitted to Environmental Science & Technology, 2002a.

Schauer, J. J., M. J. Kleeman, G. R. Cass, and B. R. T. Simoneit, Measurement of emissions from air pollution sources. 5. C1 through C32 organic compounds from gasoline-powered motor vehicles, Environmental Science & Technology, 36 (6), 1169-1180, 2002b.

Sheesley, Rebecca J.; Schauer, James J.; Chowdhury, Zohir; and Cass, Glen R. (2003) "Characterization of Organic Aerosols Emitted from the Combustion of Biomass Indigenous to the Indian Subcontinent," *Journal of Geophysical Research*, 108, No. D9, AAC 8-1 to AAC 8-15.

Simoneit, B. R. T. and Mazurek, M. A. (1982). Organic matter in the troposphere II. Natural background of biogenic lipid matter in aerosols over the rural Western United States, Atmos. Environ., 16, 2139-2159.

Simoneit, B. R. T. (1985) Application of Molecular Marker Analysis to Vehicular Exhaust for Source Reconciliations; Int. J. Environ. Anal. Chem., 1985, 22, 203-233.

Simoneit, B. R. T. (1999a) A Review of Biomarker Compounds as Source Indicators and Tracers for Air Pollution; Environ. Sci. Pollut. Res., 1999, 6, 159-169.

Simoneit, B. R. T.; Schauer, J. J.; Nolte, C. G.; Oros, D. R.; Elias, V.O.; Fraser, M. P.; Rogge, W. F.; Cass, G. R. (1999b). Levoglucosan, A Tracer for Cellulose in Biomass Burning and Atmospheric Particles; Atmos. Environ. 1999, 33, 173-182.

Varma, C. V. J. (Ed.) (1999). Compendium of Thermal Power Stations in India (Vol. I and II) Publication No. 253, Central Board of Irrigation and Power.

Watson, J.G., Robinson, N.F., Fujita, E.M., Chow, J.C., Pace, T.G., Lewis, C., Coulter, T., 1998. CMB8 applications and validation protocol for PM2.5 and VOCs. Report No. 1808.2D1. Prepared for U.S. Environmental Protection Agency, Research Triangle Park, NC, Desert Research Institute, Reno, NV.

Zeng, Y. and Hopke, P. K. (1989). Three-mode factor analysis: a new multivariate method for analyzing spatial and temporal composition variation, in *Receptor Models in Air Resources Management*, edited by J. G. Watson, APCA Transactions No. 14, Air Pollution Control Association, Pittsburgh, PA, pp. 173-189.

Zheng, M., Cass, G.R., Schauer, J.J., Edgerton, E.S., 2002. Source apportionment of PM2.5 in the Southeastern United States using solvent-extractable organic compounds as tracers, Environmental Science and Technology, 36, 2361-2371.

Zheng, M., Salmon, L.G., Schauer, J.J., Zeng L., Zhang Y., Kiang, C.S., Cass G.R. Source Apportionment of PM2.5 in Beijing, China by Chemical Mass Balance, manuscript in preparation.

CHAPTER-7

Summary and Future Work

The size distribution and chemical composition of the atmospheric aerosol at the Kaashidhoo Climate Observatory (KCO) in the Republic of Maldives was determined during February 1999 to aid in determining the light scattering and light absorption properties of the aerosol particles in that region. Fine particle concentrations (D_a<1.8 μm) averaged 17.7±0.2 μg m^{-3} and varied between 8.4±0.3–24.7±0.2 μg m^{-3} over the period studied. Sulfate ion and carbonaceous aerosols were the largest contributors to the fine particle mass concentration, accounting for 33-37% and 26-27% of the fine mass, respectively. Black elemental carbon particles contributed 6–11% of the fine particle mass concentration and dominate light absorption in the atmosphere at KCO [Eldering et al., 2002]. These fine particle concentrations are comparable to those found in major cities in the United States, and are surprisingly high for a remote location such as the Maldive Islands, which is located downwind of the Indian subcontinent.

Chemically-detailed particulate matter characterization for Delhi, Mumbai, Kolkata, and Chandigarh were also conducted during the year 2001. For the period studied, average

fine particle mass concentration during the winter season in Delhi was 231 ± 1.6 μg m^{-3}, in Mumbai was 89 ± 0.5 μg m^{-3}, and in Kolkata was 305 ± 1.1 μg m^{-3} and average fine particle mass concentration during the summer in Delhi was 50 ± 0.6 μg m^{-3}, in Mumbai was 21 ± 1.4 μg m^{-3}, in Kolkata was 27 ± 0.5 μg m^{-3}, and in Chandigarh was 9 ± 0.7 μg m^{-3}. Most of the observed $PM_{2.5}$ concentrations in Delhi and the wintertime $PM_{2.5}$ concentrations in both Mumbai and Kolkata exceeded the U.S. EPA 24-hour average $PM_{2.5}$ standard of 65 μg m^{-3} signifying unhealthy air quality. Organic matter (OM), elemental carbon (EC), NO_3^-, SO_4^{2-}, Cl^-, NH_4^+, and trace metals were also analyzed, and OC and sulfate dominate total mass. These measurements provide important information about the seasonal and spatial distribution of fine particle-phase inorganic compounds in India.

The results from the biomass and coal source tests were indispensable in understanding the emission characteristics of local air pollution sources. The particle mass distributions from the five biomass samples have a single mode that peaks at 0.18-0.32 μm particle aerodynamic diameter. From other work by Hildemann et al. (1991a, 1991b), it appears that combustion generated particles appear to peak at this size range. Particles emitted from biomass burning are mostly organic matter (57-62%) and elemental carbon (2-8%) in nature with significant amount of chloride ion (2-9%) present. The particle mass distributions from the three coals also have a single mode that peaks at 0.18-0.32 μm particle aerodynamic diameter. Particles emitted from coal burning were mostly elemental carbon in nature. Organic matter was the next largest contributor.

Detailed source apportionment for Delhi, Mumbai, Kolkata, and Chandigarh were conducted using receptor-based chemical mass balance modeling. Measured concentrations of organic carbon species, elemental carbon, and metals from the four sampling sites were used in a molecular marker source apportionment model to quantify the primary source contribution to the $PM_{2.5}$ mass concentrations at those sites. Five important sources of primary $PM_{2.5}$ were quantified: diesel exhaust, gasoline exhaust, road dust, coal combustion, and biomass combustion. Important trends in the seasonal and spatial patterns of the impact of these five sources were observed. Primary emissions from fossil fuel combustion (coal, diesel, and gasoline) were 22-33% in Delhi, 23-29% in Mumbai, 37-70% in Kolkata, and 24% in Chandigarh. These figures can be compared to the biomass combustion of 9-28% for Delhi, 12-21% for Mumbai, 15-31% for Kolkata, and 9% for Chandigarh. Road dust was also significant.

There is a need to conduct several source tests for diesel and gasoline combustion using vehicles representing the local vehicle fleet (diesel trucks, three-wheel auto-rickshaws). Coal source tests using Indian and Bangladeshi coals have been conducted, however, organic speciation work from the Indian coal results have not yet been completed. Emissions from local soil profiles (paved road dust as well as non-paved road dust) are necessary to refine the results from this work. Additional fine particle sampling is needed to identify the magnitude of seasonal variability. Finally, it is important to reconcile the observations and source apportionment work done here with results that would be achieved using a source-based model in order to evaluate the emissions inventories developed for the various regions. Our order of magnitude calculation for Mumbai suggests that the two will give consistent results,

though may differ quantitatively. This latter work is important for identifying possible missing sources and to provide a defensible, more first-principles, approach to policy-makers that can directly link specific sources to their air quality and health impacts.

APPENDIX

TABLE A-I. Trace Metal Concentration in the Ambient Fine Particle in Delhi During the Year 2001.

	Mar 04, '01	Mar 10, '01	Mar 16, '01	Mar 22, '01	Mar 28, '01	Jun 08, '01	Jun 14, '01	Jun 20, '01	Jun 26, '01	Jul 02, '01	Jul 08, '01	Jul 14, '01	Oct 05, '01	Oct 11, '01	Oct 17, '01	Dec 05, '01	Dec 17, '01	Dec 23, '01	Dec 29, '01	Jan 04, '02	Jan 10, '02
Mg	0.076	0.083	0.047	0.162	0.255	0.294	0.061	0.376	0.017	0.121	0.000	0.059	0.074	0.095	0.445	0.000	0.047	0.122	0.002	0.103	0.000
Mg Std	0.102	0.094	0.127	0.031	0.037	0.038	0.111	0.038	0.075	0.026	0.140	0.062	0.128	0.101	0.073	0.115	0.110	0.124	0.105	0.305	0.153
Al	0.447	0.530	0.544	0.480	1.321	1.606	0.247	1.159	0.178	0.377	0.252	0.261	0.419	1.172	1.711	0.260	0.425	0.433	0.108	0.695	0.240
Al Std	0.030	0.035	0.034	0.032	0.071	0.085	0.027	0.063	0.016	0.025	0.020	0.020	0.036	0.065	0.094	0.022	0.030	0.032	0.019	0.047	0.026
Si	1.387	1.600	1.598	1.497	3.780	4.070	0.787	3.286	0.509	1.018	0.730	0.708	1.158	3.013	4.734	0.771	1.136	1.229	0.610	2.145	0.867
Si Std	0.071	0.082	0.082	0.078	0.190	0.203	0.048	0.165	0.028	0.053	0.040	0.038	0.065	0.152	0.242	0.041	0.061	0.065	0.035	0.110	0.048
P	0.000	0.000	0.000	0.000	0.000	0.000	0.000	0.000	0.000	0.000	0.000	0.000	0.000	0.000	0.000	0.000	0.000	0.000	0.000	0.000	0.000
P Std	0.023	0.022	0.021	0.023	0.022	0.024	0.030	0.018	0.015	0.019	0.021	0.012	0.038	0.022	0.031	0.023	0.027	0.027	0.027	0.042	0.031
K	1.628	4.271	0.925	1.340	1.682	1.148	0.801	0.714	0.438	0.658	0.546	0.262	2.518	2.214	5.279	1.338	2.253	2.076	1.270	3.528	2.099
K Std	0.082	0.213	0.048	0.069	0.085	0.058	0.046	0.037	0.023	0.034	0.029	0.015	0.131	0.112	0.268	0.068	0.116	0.105	0.065	0.176	0.109
Ca	0.567	0.412	0.503	0.444	1.263	1.264	0.205	1.259	0.108	0.305	0.179	0.309	0.503	1.004	2.376	0.181	0.360	0.429	0.191	0.516	0.483
Ca Std	0.031	0.031	0.027	0.025	0.065	0.064	0.018	0.064	0.008	0.017	0.011	0.017	0.032	0.053	0.124	0.013	0.023	0.026	0.015	0.033	0.029
Ti	0.071	0.038	0.007	0.012	0.101	0.139	0.028	0.082	0.000	0.006	0.035	0.022	0.000	0.103	0.160	0.014	0.053	0.025	0.000	0.082	0.015
Ti Std	0.018	0.057	0.059	0.058	0.018	0.020	0.129	0.021	0.062	0.056	0.046	0.050	0.117	0.022	0.025	0.063	0.061	0.082	0.088	0.027	0.077
V	0.012	0.000	0.000	0.000	0.005	0.010	0.013	0.000	0.000	0.000	0.008	0.001	0.000	0.000	0.014	0.000	0.005	0.000	0.000	0.012	0.004
V Std	0.022	0.036	0.025	0.037	0.022	0.024	0.054	0.038	0.040	0.023	0.019	0.021	0.048	0.040	0.030	0.040	0.025	0.051	0.055	0.033	0.032
Cr	0.013	0.013	0.005	0.009	0.007	0.013	0.007	0.000	0.003	0.005	0.018	0.003	0.002	0.016	0.025	0.013	0.004	0.000	0.000	0.121	0.005
Cr Std	0.002	0.004	0.005	0.011	0.002	0.002	0.011	0.011	0.012	0.005	0.002	0.004	0.010	0.004	0.003	0.004	0.005	0.015	0.016	0.007	0.007
Mn	0.021	0.067	0.034	0.028	0.049	0.067	0.009	0.024	0.028	0.026	0.054	0.010	0.044	0.063	0.124	0.081	0.027	0.026	0.022	0.261	0.022
Mn Std	0.002	0.003	0.002	0.003	0.004	0.002	0.009	0.004	0.003	0.002	0.003	0.001	0.004	0.004	0.007	0.005	0.002	0.003	0.003	0.014	0.002
Fe	0.616	0.532	0.531	0.542	1.257	1.197	0.284	1.047	0.180	0.422	0.329	0.257	0.577	1.016	1.867	0.398	0.429	0.601	0.277	1.129	0.509
Fe Std	0.031	0.027	0.027	0.028	0.063	0.060	0.016	0.052	0.009	0.021	0.017	0.013	0.030	0.051	0.095	0.020	0.022	0.030	0.014	0.056	0.026
Co	0.000	0.000	0.000	0.000	0.000	0.000	0.000	0.000	0.000	0.000	0.000	0.000	0.000	0.000	0.000	0.000	0.000	0.000	0.000	0.000	0.000
Co Std	0.011	0.009	0.009	0.009	0.020	0.019	0.007	0.016	0.004	0.007	0.006	0.005	0.011	0.016	0.029	0.007	0.007	0.010	0.006	0.018	0.009
Ni	0.016	0.005	0.002	0.003	0.005	0.005	0.000	0.003	0.002	0.003	0.006	0.001	0.006	0.009	0.008	0.009	0.005	0.008	0.004	0.015	0.005
Ni Std	0.001	0.001	0.003	0.001	0.001	0.001	0.006	0.003	0.003	0.001	0.001	0.002	0.002	0.001	0.001	0.001	0.001	0.001	0.001	0.002	0.001
Cu	0.096	0.039	0.030	0.093	0.194	0.050	0.161	0.012	0.058	0.071	0.132	0.007	0.088	0.030	0.254	0.052	0.038	0.062	0.023	0.229	0.055
Cu Std	0.005	0.002	0.002	0.005	0.010	0.003	0.009	0.001	0.004	0.007	0.009	0.001	0.005	0.002	0.013	0.003	0.002	0.004	0.002	0.012	0.003
Zn	0.358	0.323	0.320	0.402	0.353	0.412	0.676	0.052	0.212	0.443	0.425	0.062	0.547	0.408	0.850	0.988	0.368	0.390	0.309	1.046	0.455
Zn Std	0.018	0.016	0.016	0.021	0.018	0.021	0.035	0.003	0.011	0.022	0.022	0.003	0.028	0.021	0.043	0.049	0.019	0.020	0.016	0.052	0.023
Ga	0.002	0.002	0.002	0.001	0.005	0.002	0.002	0.000	0.002	0.000	0.011	0.004	0.000	0.007	0.011	0.004	0.004	0.004	0.003	0.013	0.007
Ga Std	0.006	0.005	0.010	0.005	0.007	0.006	0.011	0.005	0.007	0.006	0.012	0.004	0.011	0.002	0.016	0.010	0.008	0.009	0.008	0.026	0.012
As	0.011	0.002	0.005	0.005	0.012	0.005	0.000	0.001	0.007	0.006	0.016	0.000	0.001	0.009	0.030	0.003	0.008	0.008	0.000	0.023	0.006
As Std	0.051	0.037	0.133	0.040	0.072	0.043	0.040	0.008	0.069	0.051	0.170	0.009	0.055	0.066	0.229	0.118	0.094	0.097	0.044	0.377	0.139
Se	0.003	0.003	0.001	0.003	0.002	0.005	0.007	0.004	0.000	0.002	0.000	0.003	0.011	0.004	0.000	0.003	0.004	0.006	0.000	0.004	0.005
Se Std	0.004	0.004	0.005	0.004	0.004	0.001	0.009	0.004	0.004	0.004	0.006	0.003	0.003	0.004	0.009	0.006	0.005	0.006	0.006	0.013	0.007
Br	0.066	0.189	0.041	0.062	0.051	0.032	0.021	0.008	0.008	0.017	0.008	0.007	0.039	0.033	0.071	0.037	0.039	0.068	0.051	0.137	0.073
Br Std	0.004	0.010	0.003	0.004	0.003	0.002	0.003	0.001	0.002	0.002	0.009	0.001	0.004	0.003	0.006	0.003	0.003	0.004	0.004	0.009	0.005
Rb	0.003	0.011	0.003	0.003	0.005	0.004	0.000	0.004	0.002	0.001	0.002	0.001	0.003	0.005	0.008	0.002	0.007	0.007	0.003	0.011	0.004
Rb Std	0.004	0.003	0.004	0.004	0.001	0.001	0.006	0.001	0.003	0.003	0.003	0.002	0.006	0.001	0.002	0.004	0.001	0.002	0.005	0.003	0.005
Sr	0.004	0.004	0.004	0.005	0.012	0.011	0.004	0.012	0.001	0.003	0.001	0.005	0.003	0.007	0.014	0.001	0.003	0.005	0.005	0.003	0.002
Sr Std	0.001	0.001	0.001	0.001	0.001	0.001	0.007	0.001	0.003	0.003	0.003	0.001	0.006	0.001	0.002	0.003	0.004	0.002	0.005	0.005	0.004
Y	0.003	0.002	0.003	0.002	0.004	0.002	0.009	0.002	0.001	0.003	0.009	0.001	0.006	0.005	0.012	0.007	0.007	0.005	0.001	0.018	0.004
Y Std	0.005	0.004	0.009	0.004	0.006	0.005	0.010	0.004	0.006	0.005	0.010	0.004	0.009	0.006	0.014	0.008	0.007	0.008	0.006	0.022	0.010
Zr	0.002	0.002	0.003	0.003	0.003	0.005	0.005	0.005	0.003	0.001	0.002	0.001	0.004	0.006	0.005	0.004	0.002	0.005	0.002	0.008	0.001
Zr Std	0.004	0.004	0.005	0.004	0.004	0.002	0.011	0.002	0.005	0.005	0.004	0.004	0.009	0.002	0.006	0.005	0.005	0.006	0.007	0.002	0.006
Mo	0.001	0.003	0.003	0.005	0.000	0.004	0.000	0.001	0.006	0.000	0.003	0.006	0.004	0.002	0.005	0.006	0.002	0.008	0.006	0.006	0.007
Mo Std	0.008	0.008	0.009	0.008	0.008	0.009	0.020	0.009	0.009	0.009	0.007	0.008	0.018	0.009	0.012	0.009	0.010	0.012	0.013	0.013	0.012
Pd	0.000	0.000	0.000	0.000	0.000	0.000	0.018	0.000	0.000	0.000	0.000	0.000	0.000	0.003	0.000	0.001	0.000	0.000	0.000	0.001	0.000
Pd Std	0.018	0.019	0.020	0.019	0.018	0.020	0.047	0.019	0.020	0.019	0.018	0.019	0.040	0.021	0.026	0.021	0.023	0.027	0.028	0.029	0.029
Ag	0.085	0.000	0.009	0.011	0.000	0.017	0.021	0.000	0.000	0.000	0.000	0.000	0.000	0.000	0.000	0.007	0.000	0.007	0.000	0.018	0.002
Ag Std	0.010	0.023	0.025	0.023	0.023	0.025	0.059	0.025	0.025	0.024	0.022	0.024	0.051	0.025	0.032	0.026	0.028	0.034	0.035	0.036	0.034
Cd	0.000	0.021	0.019	0.023	0.008	0.014	0.003	0.000	0.000	0.005	0.015	0.000	0.035	0.012	0.010	0.003	0.004	0.000	0.000	0.033	0.023
Cd Std	0.024	0.024	0.025	0.024	0.023	0.025	0.057	0.025	0.025	0.025	0.022	0.023	0.053	0.025	0.034	0.026	0.028	0.034	0.036	0.037	0.036
In	0.000	0.000	0.000	0.011	0.000	0.005	0.040	0.001	0.004	0.000	0.018	0.023	0.000	0.000	0.000	0.004	0.004	0.019	0.005	0.000	0.005
In Std	0.028	0.026	0.029	0.028	0.026	0.029	0.069	0.029	0.030	0.029	0.025	0.027	0.060	0.030	0.037	0.030	0.032	0.040	0.042	0.042	0.041
Sn	0.008	0.005	0.046	0.015	0.019	0.005	0.006	0.022	0.003	0.004	0.000	0.000	0.012	0.015	0.057	0.012	0.011	0.000	0.003	0.015	0.033
Sn Std	0.039	0.037	0.014	0.037	0.036	0.040	0.091	0.038	0.039	0.039	0.035	0.035	0.080	0.041	0.017	0.040	0.044	0.051	0.056	0.056	0.057
Sb	0.000	0.019	0.027	0.000	0.007	0.000	0.038	0.000	0.026	0.018	0.000	0.000	0.000	0.000	0.033	0.031	0.034	0.007	0.000	0.050	0.006
Sb Std	0.044	0.044	0.048	0.044	0.043	0.047	0.108	0.045	0.047	0.046	0.041	0.043	0.093	0.047	0.062	0.049	0.053	0.062	0.066	0.067	0.066
Ba	0.000	0.000	0.143	0.061	0.079	0.000	0.000	0.045	0.000	0.108	0.000	0.000	0.223	0.012	0.006	0.049	0.044	0.026	0.127	0.000	0.085
Ba Std	0.152	0.154	0.172	0.156	0.149	0.168	0.388	0.162	0.167	0.164	0.139	0.150	0.344	0.168	0.212	0.168	0.183	0.222	0.236	0.232	0.229
La	0.000	0.096	0.062	0.159	0.066	0.046	0.152	0.127	0.261	0.000	0.000	0.000	0.058	0.000	0.117	0.000	0.146	0.190	0.000	0.000	0.000
La Std	0.228	0.228	0.256	0.235	0.223	0.249	0.576	0.238	0.084	0.241	0.202	0.219	0.497	0.248	0.311	0.252	0.269	0.326	0.348	0.339	0.340
Au	0.010	0.000	0.007	0.013	0.009	0.013	0.027	0.003	0.009	0.011	0.016	0.009	0.000	0.015	0.029	0.033	0.017	0.014	0.015	0.037	0.023
Au Std	0.015	0.014	0.014	0.016	0.014	0.017	0.031	0.008	0.011	0.018	0.017	0.003	0.026	0.017	0.031	0.036	0.018	0.018	0.016	0.041	0.007
Hg	0.003	0.004	0.000	0.000	0.003	0.004	0.008	0.003	0.001	0.002	0.005	0.000	0.012	0.001	0.006	0.006	0.005	0.010	0.004	0.000	0.005
Hg Std	0.007	0.007	0.008	0.007	0.006	0.007	0.016	0.007	0.007	0.007	0.007	0.006	0.014	0.007	0.011	0.009	0.008	0.003	0.010	0.014	0.010
Tl	0.000	0.000	0.000	0.000	0.000	0.000	0.000	0.002	0.000	0.000	0.000	0.000	0.000	0.000	0.000	0.000	0.000	0.000	0.000	0.000	0.000
Tl Std	0.011	0.009	0.023	0.009	0.013	0.010	0.017	0.007	0.013	0.011	0.029	0.006	0.017	0.013	0.039	0.021	0.017	0.019	0.012	0.063	0.025
Pb	0.318	0.226	0.839	0.242	0.453	0.262	0.220	0.031	0.430	0.315	1.081	0.038	0.327	0.411	1.452	0.746	0.586	0.604	0.263	2.395	0.876
Pb Std	0.017	0.012	0.043	0.013	0.023	0.014	0.014	0.004	0.022	0.017	0.055	0.004	0.019	0.021	0.074	0.038	0.031	0.031	0.015	0.119	0.046
U	0.001	0.004	0.003	0.001	0.004	0.005	0.004	0.002	0.001	0.003	0.002	0.001	0.009	0.002	0.006	0.005	0.003	0.008	0.007	0.007	0.003
U Std	0.006	0.007	0.007	0.006	0.006	0.007	0.015	0.006	0.007	0.007	0.006	0.006	0.013	0.007	0.009	0.007	0.008	0.009	0.010	0.011	0.009

TABLE A-II. Trace Metal Concentration in the Ambient Fine Particle in Mumbai During the Year 2001.

	Mar 04, '01	Mar 10, '01	Mar 16, '01	Mar 19, '01	Mar 22, '01	Mar 28, '01	Jun 08, '01	Jun 14, '01	Jun 20, '01	Jun 26, '01	Jul 02, '01	Oct 11, '01	Oct 17, '01	Oct 23, '01	Oct 29, '01	Nov 04, '01	Nov 10, '01	Dec 05, '01	Dec 11, '01	Dec 17, '01	Dec 23, '01	Dec 29, '01	Jan 04, '02	Jan 10 '02
Mg	0.138	0.118	0.130	0.140	0.216	0.177	0.270	0.413	0.178	0.151	0.193	0.094	0.317	0.139	0.159	0.062	0.106	0.116	0.067	0.208	0.045	0.095	0.283	0.092
Mg Std	0.025	0.022	0.025	0.024	0.027	0.023	0.063	0.038	0.028	0.026	0.027	0.019	0.039	0.027	0.028	0.074	0.026	0.025	0.087	0.033	0.059	0.031	0.036	0.023
Al	0.583	0.458	0.320	0.455	0.746	0.343	0.481	0.235	0.206	0.081	0.149	0.168	1.384	0.479	0.403	0.454	0.647	0.402	0.294	0.821	0.280	0.594	1.293	0.263
Al Std	0.035	0.028	0.024	0.029	0.043	0.023	0.046	0.021	0.018	0.012	0.016	0.015	0.075	0.031	0.028	0.030	0.038	0.026	0.022	0.048	0.021	0.037	0.071	0.021
Si	1.650	1.272	0.951	1.358	2.340	1.088	1.244	0.746	0.694	0.285	0.591	0.540	3.674	1.410	1.075	1.024	1.352	0.908	0.811	2.787	0.696	1.414	3.516	0.804
Si Std	0.084	0.065	0.051	0.070	0.120	0.057	0.071	0.041	0.037	0.017	0.032	0.030	0.185	0.074	0.056	0.054	0.070	0.048	0.043	0.141	0.038	0.073	0.178	0.043
P	0.000	0.000	0.000	0.000	0.000	0.000	0.000	0.000	0.000	0.000	0.000	0.000	0.000	0.000	0.000	0.006	0.015	0.008	0.000	0.001	0.017	0.000	0.000	0.000
P Std	0.018	0.015	0.018	0.016	0.013	0.014	0.039	0.017	0.013	0.011	0.012	0.012	0.023	0.021	0.023	0.022	0.021	0.021	0.021	0.022	0.018	0.025	0.026	0.020
K	1.090	0.793	0.356	0.594	0.411	0.292	0.239	0.187	0.194	0.158	0.169	0.208	1.551	0.999	0.791	1.028	1.396	1.304	0.881	0.863	0.941	2.019	1.562	0.890
K Std	0.055	0.041	0.021	0.032	0.022	0.016	0.020	0.013	0.012	0.010	0.010	0.012	0.079	0.052	0.041	0.054	0.071	0.067	0.045	0.045	0.049	0.102	0.080	0.046
Ca	0.523	0.445	0.486	0.497	0.766	0.716	0.580	0.609	0.281	0.174	0.317	0.222	1.646	0.657	0.404	0.585	0.597	0.469	0.454	3.284	0.440	0.775	2.218	0.451
Ca Std	0.028	0.024	0.027	0.027	0.040	0.037	0.036	0.033	0.016	0.011	0.018	0.013	0.084	0.035	0.022	0.032	0.032	0.026	0.025	0.165	0.024	0.041	0.112	0.025
Ti	0.066	0.044	0.000	0.045	0.064	0.027	0.047	0.000	0.000	0.010	0.019	0.000	0.113	0.065	0.045	0.017	0.025	0.022	0.049	0.255	0.044	0.070	0.112	0.030
Ti Std	0.017	0.052	0.071	0.054	0.017	0.053	0.191	0.065	0.054	0.050	0.055	0.050	0.022	0.018	0.070	0.059	0.071	0.060	0.057	0.025	0.057	0.019	0.023	0.065
V	0.006	0.005	0.000	0.011	0.000	0.000	0.006	0.000	0.000	0.002	0.000	0.000	0.009	0.017	0.021	0.008	0.004	0.008	0.020	0.011	0.007	0.022	0.000	0.000
V Std	0.021	0.021	0.029	0.022	0.032	0.033	0.079	0.027	0.022	0.021	0.023	0.021	0.040	0.022	0.029	0.025	0.042	0.025	0.024	0.027	0.024	0.024	0.042	0.041
Cr	0.006	0.002	0.005	0.011	0.000	0.000	0.005	0.003	0.000	0.002	0.001	0.000	0.009	0.011	0.020	0.014	0.007	0.011	0.019	0.020	0.019	0.020	0.013	0.001
Cr Std	0.002	0.005	0.006	0.002	0.009	0.010	0.016	0.006	0.005	0.004	0.005	0.004	0.012	0.002	0.003	0.002	0.012	0.002	0.002	0.003	0.002	0.002	0.013	0.012
Mn	0.021	0.009	0.007	0.011	0.011	0.006	0.015	0.004	0.007	0.006	0.003	0.005	0.045	0.032	0.040	0.027	0.038	0.024	0.045	0.059	0.027	0.045	0.053	0.023
Mn Std	0.002	0.001	0.002	0.002	0.002	0.002	0.004	0.004	0.001	0.001	0.004	0.001	0.003	0.002	0.003	0.002	0.003	0.002	0.003	0.004	0.002	0.003	0.004	0.002
Fe	0.661	0.460	0.407	0.466	0.754	0.377	0.519	0.301	0.287	0.156	0.213	0.218	1.366	0.716	0.638	0.646	0.617	0.554	0.555	3.015	0.507	1.288	1.961	0.460
Fe Std	0.033	0.023	0.021	0.024	0.038	0.019	0.028	0.016	0.015	0.008	0.011	0.011	0.068	0.037	0.032	0.033	0.031	0.028	0.028	0.150	0.026	0.065	0.098	0.023
Co	0.000	0.000	0.000	0.000	0.000	0.000	0.000	0.000	0.000	0.000	0.000	0.000	0.000	0.000	0.000	0.000	0.000	0.000	0.000	0.000	0.000	0.000	0.000	0.000
Co Std	0.011	0.008	0.007	0.008	0.012	0.006	0.012	0.006	0.005	0.003	0.004	0.004	0.021	0.011	0.010	0.010	0.010	0.009	0.009	0.046	0.008	0.020	0.030	0.008
Ni	0.019	0.008	0.008	0.014	0.004	0.004	0.029	0.019	0.002	0.004	0.005	0.006	0.012	0.014	0.024	0.020	0.015	0.014	0.013	0.017	0.014	0.014	0.022	0.014
Ni Std	0.001	0.001	0.001	0.001	0.001	0.001	0.004	0.002	0.003	0.001	0.001	0.001	0.001	0.001	0.002	0.002	0.001	0.001	0.001	0.002	0.001	0.001	0.002	0.001
Cu	0.171	0.163	0.010	0.004	0.002	0.011	0.025	0.015	0.009	0.001	0.003	0.012	0.045	0.073	0.199	0.277	0.066	0.079	0.061	0.061	0.029	0.103	0.045	0.068
Cu Std	0.009	0.008	0.001	0.001	0.002	0.001	0.003	0.001	0.001	0.002	0.001	0.001	0.003	0.004	0.010	0.014	0.004	0.004	0.003	0.003	0.002	0.005	0.003	0.004
Zn	0.131	0.031	0.069	0.058	0.007	0.024	0.026	0.008	0.003	0.005	0.000	0.020	0.300	0.262	0.261	0.384	0.212	0.279	0.282	0.294	0.239	0.464	0.289	0.209
Zn Std	0.007	0.002	0.004	0.003	0.001	0.002	0.004	0.001	0.003	0.001	0.003	0.002	0.015	0.013	0.013	0.020	0.011	0.014	0.014	0.015	0.012	0.023	0.015	0.011
Ga	0.000	0.004	0.003	0.002	0.000	0.002	0.013	0.002	0.004	0.003	0.002	0.001	0.000	0.004	0.002	0.003	0.003	0.003	0.006	0.005	0.000	0.001	0.000	0.003
Ga Std	0.004	0.004	0.006	0.005	0.004	0.004	0.016	0.005	0.005	0.004	0.005	0.004	0.006	0.005	0.007	0.006	0.005	0.006	0.007	0.006	0.005	0.006	0.006	0.006
As	0.000	0.000	0.002	0.003	0.000	0.002	0.000	0.002	0.000	0.000	0.000	0.000	0.003	0.002	0.004	0.009	0.003	0.001	0.006	0.000	0.003	0.007	0.006	0.002
As Std	0.017	0.007	0.018	0.014	0.005	0.006	0.021	0.007	0.006	0.005	0.006	0.006	0.040	0.041	0.038	0.042	0.026	0.035	0.077	0.047	0.018	0.051	0.030	0.030
Se	0.002	0.002	0.002	0.001	0.001	0.003	0.006	0.003	0.000	0.003	0.002	0.003	0.002	0.003	0.004	0.004	0.002	0.000	0.004	0.004	0.004	0.006	0.001	0.003
Se Std	0.003	0.003	0.004	0.003	0.003	0.001	0.012	0.004	0.003	0.003	0.003	0.003	0.004	0.004	0.005	0.004	0.004	0.004	0.005	0.004	0.004	0.002	0.004	0.004
Br	0.021	0.020	0.011	0.018	0.004	0.005	0.017	0.017	0.008	0.009	0.009	0.006	0.014	0.020	0.047	0.027	0.017	0.034	0.032	0.055	0.018	0.054	0.042	0.027
Br Std	0.002	0.002	0.002	0.002	0.001	0.001	0.004	0.002	0.001	0.001	0.001	0.001	0.002	0.002	0.003	0.002	0.002	0.003	0.003	0.004	0.002	0.003	0.003	0.002
Rb	0.003	0.001	0.001	0.002	0.002	0.001	0.000	0.001	0.001	0.001	0.000	0.002	0.005	0.002	0.003	0.001	0.004	0.004	0.001	0.003	0.003	0.003	0.006	0.002
Rb Std	0.003	0.003	0.003	0.003	0.002	0.002	0.009	0.003	0.003	0.003	0.003	0.002	0.001	0.003	0.004	0.003	0.001	0.001	0.003	0.004	0.003	0.004	0.001	0.003
Sr	0.003	0.005	0.006	0.007	0.008	0.010	0.011	0.015	0.004	0.003	0.004	0.002	0.012	0.005	0.005	0.007	0.010	0.003	0.003	0.018	0.003	0.006	0.012	0.004
Sr Std	0.003	0.001	0.001	0.001	0.001	0.001	0.004	0.002	0.001	0.001	0.001	0.003	0.001	0.001	0.001	0.001	0.001	0.003	0.003	0.002	0.001	0.001	0.001	0.001
Y	0.001	0.000	0.000	0.002	0.000	0.000	0.010	0.002	0.001	0.000	0.001	0.000	0.002	0.002	0.002	0.002	0.002	0.001	0.003	0.012	0.001	0.002	0.001	0.002
Y Std	0.004	0.004	0.005	0.004	0.003	0.003	0.013	0.005	0.004	0.003	0.004	0.003	0.005	0.004	0.005	0.005	0.004	0.005	0.006	0.002	0.004	0.005	0.005	0.005
Zr	0.001	0.001	0.001	0.001	0.002	0.001	0.007	0.004	0.003	0.001	0.003	0.003	0.005	0.003	0.004	0.003	0.002	0.003	0.001	0.007	0.003	0.003	0.005	0.000
Zr Std	0.004	0.004	0.006	0.004	0.004	0.004	0.015	0.005	0.004	0.004	0.005	0.004	0.002	0.004	0.006	0.005	0.005	0.005	0.002	0.005	0.005	0.005	0.002	0.005
Mo	0.000	0.004	0.003	0.003	0.002	0.001	0.015	0.003	0.004	0.006	0.005	0.003	0.011	0.007	0.006	0.008	0.005	0.002	0.004	0.004	0.001	0.007	0.013	0.000
Mo Std	0.008	0.008	0.011	0.009	0.007	0.008	0.030	0.010	0.009	0.008	0.009	0.008	0.003	0.008	0.011	0.009	0.009	0.010	0.009	0.009	0.009	0.009	0.003	0.010
Pd	0.000	0.000	0.000	0.000	0.000	0.006	0.000	0.000	0.000	0.000	0.000	0.002	0.000	0.003	0.000	0.000	0.000	0.000	0.000	0.000	0.000	0.000	0.000	0.001
Pd Std	0.018	0.019	0.024	0.019	0.016	0.018	0.071	0.023	0.020	0.018	0.020	0.018	0.021	0.019	0.025	0.021	0.021	0.022	0.021	0.021	0.020	0.020	0.023	0.021
Ag	0.074	0.021	0.015	0.010	0.000	0.000	0.129	0.159	0.010	0.000	0.004	0.000	0.019	0.000	0.014	0.012	0.019	0.000	0.000	0.000	0.000	0.005	0.030	0.001
Ag Std	0.009	0.025	0.031	0.023	0.021	0.022	0.032	0.015	0.025	0.023	0.025	0.023	0.027	0.023	0.031	0.027	0.027	0.026	0.026	0.027	0.025	0.026	0.010	0.026
Cd	0.006	0.000	0.000	0.006	0.008	0.008	0.013	0.000	0.000	0.012	0.000	0.000	0.005	0.000	0.000	0.000	0.012	0.008	0.000	0.000	0.006	0.000	0.007	0.007
Cd Std	0.022	0.023	0.030	0.023	0.021	0.022	0.087	0.029	0.025	0.023	0.024	0.022	0.026	0.023	0.031	0.026	0.027	0.027	0.026	0.027	0.025	0.025	0.028	0.027
In	0.013	0.000	0.015	0.010	0.006	0.004	0.000	0.016	0.005	0.033	0.000	0.007	0.000	0.000	0.000	0.000	0.000	0.003	0.002	0.000	0.000	0.000	0.025	0.000
In Std	0.026	0.027	0.035	0.027	0.024	0.025	0.101	0.034	0.028	0.009	0.028	0.027	0.029	0.027	0.037	0.030	0.031	0.031	0.030	0.031	0.030	0.029	0.031	0.031
Sn	0.012	0.004	0.000	0.000	0.001	0.000	0.000	0.000	0.000	0.020	0.000	0.000	0.030	0.005	0.000	0.000	0.002	0.041	0.032	0.004	0.000	0.025	0.016	0.004
Sn Std	0.036	0.036	0.045	0.036	0.033	0.033	0.134	0.046	0.037	0.034	0.039	0.035	0.041	0.037	0.049	0.041	0.042	0.043	0.041	0.041	0.040	0.040	0.042	0.041
Sb	0.000	0.000	0.000	0.000	0.000	0.000	0.021	0.001	0.000	0.004	0.000	0.000	0.000	0.013	0.000	0.000	0.008	0.000	0.030	0.001	0.000	0.000	0.008	0.006
Sb Std	0.042	0.042	0.055	0.044	0.038	0.039	0.160	0.053	0.044	0.041	0.046	0.041	0.048	0.044	0.058	0.047	0.049	0.049	0.047	0.050	0.046	0.046	0.050	0.049
Ba	0.026	0.000	0.240	0.000	0.000	0.000	0.105	0.111	0.000	0.028	0.084	0.018	0.000	0.000	0.000	0.145	0.289	0.100	0.027	0.187	0.000	0.073	0.117	0.000
Ba Std	0.153	0.154	0.068	0.160	0.137	0.142	0.568	0.192	0.159	0.150	0.164	0.149	0.171	0.154	0.208	0.172	0.061	0.178	0.170	0.058	0.169	0.166	0.176	0.175
La	0.065	0.000	0.000	0.000	0.079	0.087	0.000	0.048	0.058	0.000	0.041	0.002	0.143	0.000	0.052	0.000	0.089	0.027	0.036	0.084	0.000	0.050	0.220	0.152
La Std	0.226	0.227	0.292	0.236	0.203	0.209	0.847	0.281	0.233	0.219	0.241	0.216	0.251	0.225	0.306	0.251	0.253	0.259	0.251	0.253	0.245	0.246	0.260	0.260
Au	0.006	0.002	0.007	0.005	0.001	0.004	0.021	0.004	0.004	0.000	0.005	0.004	0.000	0.014	0.016	0.018	0.009	0.012	0.011	0.012	0.008	0.017	0.010	0.000
Au Std	0.009	0.007	0.010	0.008	0.006	0.007	0.026	0.009	0.007	0.007	0.007	0.007	0.014	0.004	0.005	0.006	0.011	0.013	0.013	0.013	0.012	0.019	0.014	0.012
Hg	0.002	0.001	0.004	0.002	0.002	0.001	0.006	0.005	0.005	0.004	0.003	0.005	0.006	0.005	0.001	0.003	0.003	0.003	0.006	0.016	0.007	0.006	0.008	0.005
Hg Std	0.006	0.006	0.008	0.007	0.005	0.006	0.023	0.008	0.007	0.006	0.007	0.006	0.007	0.007	0.009	0.007	0.007	0.008	0.007	0.003	0.007	0.007	0.003	0.008
Tl	0.000	0.000	0.000	0.000	0.002	0.000	0.011	0.003	0.002	0.001	0.000	0.002	0.000	0.000	0.000	0.000	0.000	0.000	0.000	0.000	0.000	0.000	0.000	0.000
Tl Std	0.007	0.006	0.009	0.007	0.005	0.006	0.023	0.008	0.006	0.006	0.006	0.006	0.010	0.010	0.008	0.010	0.009	0.009	0.015	0.011	0.010	0.011	0.009	0.009
Pb	0.094	0.021	0.099	0.073	0.013	0.015	0.031	0.007	0.008	0.007	0.013	0.016	0.245	0.251	0.226	0.259	0.152	0.214	0.480	0.288	0.103	0.316	0.182	0.180
Pb Std	0.006	0.003	0.007	0.005	0.003	0.003	0.010	0.010	0.008	0.008	0.003	0.003	0.013	0.014	0.012	0.014	0.009	0.012	0.025	0.015	0.007	0.017	0.010	0.010
U	0.004	0.001	0.000	0.003	0.002	0.003	0.011	0.004	0.000	0.003	0.004	0.000	0.003	0.002	0.006	0.004	0.004	0.002	0.006	0.003	0.003	0.006	0.005	0.006
U Std	0.006	0.006	0.008	0.006	0.005	0.006	0.022	0.007	0.006	0.006	0.006	0.006	0.007	0.006	0.008	0.007	0.007	0.007	0.007	0.007	0.007	0.007	0.007	0.007

TABLE A-III. Trace Metal Concentration in the Ambient Fine Particle in Kolkata During the Year 2001.

	Mar 16, '01	Mar 22, '01	Mar 28, '01	Apr 03, '01	Apr 09, '01	Jun 08, '01	Jun 14, '01	Jun 20, '01	Jun 26, '01	Jul 02, '01	Oct 11, '01	Oct 17, '01	Oct 23, '01	Oct 29, '01	Dec 05, '01	Dec 11, '01	Dec 17, '01	Dec 23, '01	Dec 29, '01
Mg	0.064	0.082	0.148	0.158	0.107	0.026	0.006	0.096	0.142	0.025	0.056	0.040	0.022	0.029	0.041	0.000	0.023	0.045	0.056
Mg Std	0.084	0.026	0.033	0.028	0.027	0.072	0.045	0.024	0.035	0.065	0.095	0.053	0.179	0.074	0.136	0.271	0.392	0.365	0.288
Al	0.700	0.392	0.466	0.654	0.475	0.072	0.012	0.233	0.540	0.179	0.213	0.026	0.268	0.025	0.874	0.615	0.543	0.742	0.653
Al Std	0.042	0.027	0.033	0.039	0.031	0.011	0.028	0.019	0.034	0.017	0.017	0.027	0.021	0.027	0.052	0.040	0.036	0.045	0.042
Si	2.004	1.460	1.398	1.774	1.431	0.246	0.176	0.683	1.608	0.623	0.378	0.243	0.769	0.084	2.328	1.995	1.362	2.191	1.888
Si Std	0.102	0.075	0.074	0.090	0.073	0.016	0.012	0.037	0.082	0.034	0.023	0.016	0.042	0.009	0.120	0.103	0.072	0.113	0.098
P	0.000	0.000	0.000	0.000	0.000	0.000	0.000	0.000	0.000	0.000	0.000	0.000	0.014	0.001	0.000	0.000	0.000	0.000	0.000
P Std	0.023	0.020	0.025	0.019	0.018	0.012	0.011	0.015	0.016	0.015	0.018	0.013	0.022	0.012	0.030	0.032	0.031	0.034	0.032
K	1.365	1.327	0.990	0.856	0.861	0.359	0.207	0.358	0.412	0.551	0.599	0.343	0.933	0.417	4.863	3.341	2.890	3.820	3.834
K Std	0.070	0.068	0.052	0.044	0.044	0.020	0.012	0.020	0.022	0.030	0.032	0.019	0.049	0.023	0.246	0.169	0.145	0.192	0.193
Ca	0.402	0.362	0.500	0.652	0.328	0.105	0.045	0.246	0.363	0.150	0.132	0.060	0.194	0.036	0.933	0.571	0.361	0.804	0.724
Ca Std	0.023	0.021	0.028	0.034	0.019	0.008	0.006	0.015	0.020	0.011	0.010	0.007	0.013	0.006	0.055	0.035	0.025	0.046	0.043
Ti	0.068	0.032	0.044	0.066	0.049	0.004	0.000	0.002	0.027	0.054	0.020	0.000	0.047	0.000	0.106	0.025	0.088	0.106	0.088
Ti Std	0.020	0.072	0.084	0.022	0.064	0.058	0.059	0.062	0.060	0.060	0.061	0.072	0.062	0.064	0.023	0.076	0.024	0.023	0.024
V	0.007	0.000	0.003	0.006	0.002	0.001	0.000	0.000	0.000	0.003	0.003	0.000	0.003	0.002	0.004	0.000	0.012	0.012	0.012
V Std	0.025	0.046	0.035	0.027	0.026	0.024	0.024	0.026	0.025	0.025	0.025	0.045	0.026	0.026	0.028	0.031	0.030	0.028	0.030
Cr	0.002	0.000	0.000	0.002	0.003	0.000	0.001	0.000	0.002	0.002	0.011	0.000	0.004	0.000	0.007	0.007	0.001	0.008	0.010
Cr Std	0.005	0.013	0.007	0.006	0.006	0.005	0.005	0.005	0.005	0.005	0.002	0.013	0.006	0.005	0.002	0.007	0.006	0.002	0.002
Mn	0.034	0.041	0.011	0.015	0.016	0.010	0.012	0.007	0.012	0.011	0.015	0.000	0.036	0.000	0.117	0.045	0.043	0.089	0.070
Mn Std	0.003	0.003	0.002	0.002	0.002	0.002	0.002	0.002	0.002	0.002	0.002	0.006	0.003	0.004	0.007	0.003	0.003	0.005	0.004
Fe	0.667	0.554	0.470	0.625	0.475	0.151	0.067	0.241	0.482	0.253	0.316	0.050	0.366	0.037	1.351	0.757	0.576	1.146	0.944
Fe Std	0.034	0.028	0.024	0.031	0.024	0.008	0.004	0.013	0.024	0.013	0.017	0.003	0.019	0.003	0.068	0.038	0.029	0.058	0.048
Co	0.000	0.000	0.000	0.000	0.000	0.000	0.000	0.000	0.000	0.000	0.000	0.002	0.000	0.000	0.000	0.000	0.000	0.000	0.000
Co Std	0.011	0.009	0.008	0.010	0.008	0.003	0.003	0.005	0.008	0.005	0.006	0.003	0.006	0.003	0.021	0.012	0.010	0.018	0.015
Ni	0.003	0.001	0.001	0.004	0.002	0.001	0.000	0.001	0.001	0.002	0.011	0.000	0.001	0.000	0.004	0.003	0.001	0.005	0.003
Ni Std	0.001	0.003	0.004	0.001	0.003	0.003	0.003	0.003	0.003	0.003	0.001	0.003	0.003	0.003	0.004	0.004	0.003	0.001	0.003
Cu	0.014	0.006	0.012	0.008	0.007	0.011	0.006	0.009	0.008	0.008	0.165	0.052	0.075	0.019	0.103	0.184	0.059	0.109	0.084
Cu Std	0.001	0.001	0.002	0.001	0.001	0.001	0.001	0.001	0.001	0.001	0.009	0.003	0.004	0.002	0.006	0.010	0.003	0.006	0.005
Zn	0.192	0.165	0.042	0.047	0.039	0.013	0.020	0.022	0.032	0.028	0.259	0.040	0.610	0.014	0.998	0.619	0.440	1.115	0.592
Zn Std	0.010	0.009	0.003	0.003	0.002	0.001	0.002	0.002	0.002	0.002	0.013	0.003	0.031	0.002	0.050	0.031	0.022	0.056	0.030
Ga	0.003	0.001	0.000	0.003	0.002	0.003	0.005	0.002	0.005	0.002	0.005	0.001	0.011	0.006	0.004	0.013	0.017	0.022	0.012
Ga Std	0.006	0.006	0.007	0.006	0.005	0.007	0.005	0.005	0.008	0.005	0.009	0.006	0.016	0.008	0.010	0.024	0.034	0.032	0.025
As	0.005	0.002	0.000	0.003	0.003	0.004	0.000	0.002	0.005	0.003	0.020	0.007	0.025	0.017	0.005	0.032	0.063	0.027	0.017
As Std	0.039	0.027	0.010	0.013	0.008	0.069	0.027	0.010	0.084	0.009	0.107	0.034	0.232	0.078	0.123	0.347	0.527	0.488	0.367
Se	0.003	0.004	0.003	0.005	0.003	0.002	0.000	0.004	0.001	0.006	0.003	0.003	0.006	0.002	0.004	0.004	0.003	0.002	0.002
Se Std	0.004	0.004	0.005	0.001	0.004	0.004	0.004	0.004	0.005	0.001	0.005	0.004	0.008	0.005	0.007	0.011	0.016	0.015	0.012
Br	0.029	0.020	0.017	0.015	0.015	0.006	0.003	0.008	0.006	0.010	0.005	0.009	0.010	0.004	0.067	0.053	0.036	0.065	0.071
Br Std	0.002	0.002	0.002	0.002	0.002	0.002	0.004	0.002	0.002	0.002	0.007	0.002	0.012	0.006	0.004	0.006	0.009	0.009	0.007
Rb	0.005	0.003	0.000	0.002	0.003	0.001	0.002	0.001	0.002	0.002	0.004	0.000	0.004	0.001	0.009	0.011	0.008	0.010	0.010
Rb Std	0.001	0.001	0.004	0.003	0.001	0.003	0.003	0.003	0.003	0.003	0.001	0.003	0.001	0.003	0.002	0.002	0.002	0.002	0.002
Sr	0.004	0.002	0.006	0.004	0.004	0.001	0.002	0.003	0.006	0.004	0.001	0.002	0.001	0.001	0.007	0.005	0.000	0.006	0.002
Sr Std	0.001	0.004	0.002	0.001	0.001	0.003	0.003	0.004	0.001	0.001	0.003	0.004	0.004	0.004	0.001	0.002	0.005	0.002	0.004
Y	0.002	0.002	0.003	0.000	0.000	0.003	0.000	0.002	0.005	0.001	0.007	0.000	0.011	0.004	0.006	0.014	0.024	0.020	0.019
Y Std	0.005	0.005	0.006	0.005	0.005	0.006	0.004	0.005	0.006	0.004	0.008	0.005	0.014	0.006	0.009	0.020	0.030	0.027	0.021
Zr	0.004	0.001	0.003	0.000	0.001	0.002	0.003	0.002	0.003	0.002	0.004	0.002	0.003	0.004	0.007	0.003	0.001	0.001	0.003
Zr Std	0.005	0.005	0.007	0.005	0.005	0.005	0.005	0.005	0.005	0.005	0.005	0.005	0.005	0.005	0.002	0.007	0.007	0.006	0.006
Mo	0.000	0.003	0.006	0.000	0.001	0.000	0.004	0.005	0.004	0.001	0.009	0.006	0.002	0.005	0.007	0.012	0.004	0.003	0.004
Mo Std	0.010	0.011	0.014	0.010	0.010	0.009	0.009	0.010	0.010	0.010	0.010	0.011	0.010	0.010	0.011	0.012	0.012	0.011	0.012
Pd	0.000	0.001	0.000	0.000	0.000	0.000	0.000	0.000	0.003	0.000	0.000	0.000	0.000	0.000	0.000	0.000	0.002	0.011	0.000
Pd Std	0.021	0.023	0.029	0.023	0.023	0.022	0.022	0.023	0.022	0.021	0.023	0.023	0.022	0.023	0.024	0.027	0.026	0.024	0.026
Ag	0.000	0.005	0.013	0.000	0.009	0.000	0.000	0.005	0.003	0.008	0.006	0.000	0.006	0.000	0.003	0.016	0.009	0.005	0.012
Ag Std	0.027	0.028	0.038	0.029	0.028	0.027	0.027	0.029	0.027	0.028	0.028	0.029	0.028	0.029	0.030	0.033	0.032	0.030	0.032
Cd	0.019	0.028	0.015	0.001	0.001	0.006	0.000	0.000	0.009	0.004	0.026	0.000	0.031	0.000	0.031	0.015	0.042	0.033	0.032
Cd Std	0.026	0.029	0.036	0.028	0.028	0.027	0.027	0.029	0.028	0.027	0.028	0.030	0.010	0.029	0.031	0.033	0.011	0.011	0.011
In	0.028	0.000	0.014	0.000	0.000	0.005	0.007	0.011	0.003	0.000	0.010	0.001	0.000	0.000	0.000	0.000	0.000	0.000	0.000
In Std	0.031	0.033	0.042	0.033	0.033	0.030	0.030	0.034	0.032	0.031	0.032	0.035	0.033	0.033	0.034	0.038	0.036	0.034	0.036
Sn	0.033	0.006	0.019	0.000	0.000	0.015	0.017	0.000	0.018	0.017	0.000	0.000	0.021	0.008	0.006	0.026	0.073	0.019	0.000
Sn Std	0.043	0.046	0.058	0.045	0.044	0.041	0.042	0.045	0.043	0.042	0.043	0.046	0.045	0.045	0.045	0.053	0.017	0.048	0.050
Sb	0.000	0.000	0.000	0.000	0.000	0.000	0.000	0.000	0.000	0.000	0.000	0.000	0.023	0.000	0.031	0.000	0.063	0.042	0.039
Sb Std	0.049	0.055	0.069	0.053	0.052	0.049	0.050	0.053	0.049	0.049	0.051	0.055	0.054	0.054	0.055	0.062	0.020	0.058	0.061
Ba	0.020	0.000	0.077	0.027	0.000	0.000	0.104	0.070	0.060	0.058	0.024	0.101	0.017	0.022	0.095	0.147	0.065	0.065	0.003
Ba Std	0.180	0.196	0.251	0.194	0.192	0.171	0.175	0.186	0.179	0.180	0.182	0.195	0.185	0.192	0.196	0.222	0.212	0.198	0.212
La	0.069	0.140	0.113	0.032	0.014	0.000	0.000	0.081	0.000	0.025	0.089	0.181	0.000	0.015	0.084	0.026	0.000	0.000	0.050
La Std	0.262	0.289	0.371	0.279	0.282	0.257	0.256	0.279	0.262	0.264	0.268	0.285	0.274	0.282	0.285	0.325	0.309	0.293	0.310
Au	0.008	0.006	0.004	0.000	0.005	0.004	0.007	0.003	0.004	0.007	0.009	0.000	0.020	0.004	0.000	0.018	0.011	0.024	0.023
Au Std	0.011	0.011	0.012	0.009	0.009	0.008	0.008	0.009	0.008	0.008	0.013	0.010	0.023	0.009	0.037	0.026	0.020	0.040	0.024
Hg	0.001	0.003	0.000	0.004	0.002	0.003	0.003	0.003	0.002	0.005	0.007	0.002	0.000	0.004	0.004	0.000	0.000	0.000	0.002
Hg Std	0.007	0.008	0.010	0.008	0.008	0.007	0.007	0.008	0.008	0.007	0.008	0.008	0.010	0.008	0.010	0.012	0.015	0.014	0.012
Tl	0.000	0.000	0.003	0.000	0.001	0.000	0.000	0.000	0.000	0.002	0.000	0.000	0.000	0.000	0.000	0.000	0.000	0.000	0.000
Tl Std	0.010	0.009	0.010	0.008	0.008	0.014	0.008	0.008	0.016	0.007	0.019	0.010	0.039	0.015	0.022	0.058	0.087	0.080	0.061
Pb	0.238	0.155	0.025	0.063	0.024	0.430	0.160	0.042	0.527	0.033	0.675	0.204	1.470	0.488	0.775	2.207	3.355	3.107	2.336
Pb Std	0.013	0.009	0.005	0.005	0.004	0.023	0.009	0.004	0.027	0.004	0.035	0.012	0.075	0.025	0.040	0.112	0.167	0.156	0.117
U	0.002	0.002	0.005	0.005	0.000	0.000	0.001	0.003	0.003	0.004	0.004	0.003	0.002	0.000	0.004	0.005	0.006	0.005	0.006
U Std	0.007	0.008	0.010	0.008	0.007	0.007	0.007	0.007	0.007	0.007	0.007	0.008	0.008	0.007	0.008	0.010	0.010	0.010	0.009

TABLE A-IV. Emissions from the three Asian coals. Units for $\mu g/m^3$.

Species	Indian Coal				Chinese Coal				Bangladeshi Coal			
	PM$_{2.5}$	Std Dev	PM$_{1.8}$	Std Dev	PM$_{2.5}$	Std Dev	PM$_{1.8}$	Std Dev	PM$_{2.5}$	Std Dev	PM$_{1.8}$	Std Dev
Mass	395.48	11.15	270.00	38.28	75.33	4.34	56.23	9.57	532.26	18.82	307.71	18.43
Organic Matter	42.37	5.89	39.33	3.65	19.00	3.79	21.97	2.55	70.73	6.02	50.81	3.41
Elemental Carbon	276.93	17.26	208.52	6.60	29.89	4.35	30.58	2.62	411.97	23.24	252.91	7.41
Sulfate	15.45	1.10	10.89	1.55	2.48	0.78	2.00	1.12	3.49	0.88	3.12	1.26
Nitrate	0.51	0.98	0.66	1.39	1.10	0.70	0.45	1.00	0.13	0.78	0.05	1.12
Ammonium	6.13	0.32	3.41	0.46	1.12	0.23	0.00	0.33	3.82	0.26	0.00	0.37
Chloride	0.15	0.70	0.90	0.99	0.07	0.50	1.24	0.71	0.28	0.56	0.83	0.80
Others	53.94	N/A	6.29	N/A	21.66	N/A	0.00	N/A	41.84	N/A	0.00	N/A

TABLE A-V. Trace species emissions from three Asian coals as analyzed by Neutron Activation. Units for

µg/m³.

	D4-06-MT-05	Err	D4-06-MT-06	Err	D4-06-MT-07	Err	D4-06-MT-08	Err	D4-06-MT-09	Err	D4-06-MT-10	Err	D4-06-MT-AF	Err	D4-09-MT-05	Err	D4-09-MT-06	Err	D4-09-MT-07	Err	D4-09-MT-08	Err	D4-09-MT-09	Err	D4-09-MT-10	Err	D4-09-MT-AF	Err
Na	1.5E-03	2.1E-04	2.7E-04	1.5E-04	7.2E-04	1.7E-04	3.2E-05	1.5E-04	0.0E+00	0.0E+00	0.0E+00	0.0E+00	0.0E+00	0.0E+00	1.8E-03	1.1E-04	1.7E-04	6.0E-05	0.0E+00	0.0E+00	0.0E+00	0.0E+00	0.0E+00	0.0E+00	0.0E+00	0.0E+00	0.0E+00	0.0E+00
Mg	0.0E+00	0.0E+00	0.0E+00	0.0E+00	0.0E+00	0.0E+00	0.0E+00	0.0E+00	0.0E+00	0.0E+00	0.0E+00	0.0E+00	0.0E+00	0.0E+00	1.3E-03	4.1E-04	0.0E+00	0.0E+00	0.0E+00	0.0E+00	0.0E+00	0.0E+00	4.5E-04	2.5E-04	0.0E+00	0.0E+00	0.0E+00	0.0E+00
Al	0.0E+00	0.0E+00	0.0E+00	0.0E+00	0.0E+00	0.0E+00	0.0E+00	0.0E+00	0.0E+00	0.0E+00	0.0E+00	0.0E+00	0.0E+00	0.0E+00	5.8E-02	7.0E-03	0.0E+00	0.0E+00	0.0E+00	0.0E+00	0.0E+00	0.0E+00	0.0E+00	0.0E+00	0.0E+00	0.0E+00	2.4E-02	3.4E-03
Cl	8.5E-04	2.9E-04	6.4E-04	2.5E-04	3.3E-04	2.3E-04	9.7E-04	3.2E-04	1.5E-03	3.3E-04	6.2E-04	1.7E-04	2.6E-04	9.2E-05	5.7E-04	1.3E-04	1.0E-03	1.6E-04	7.6E-04	1.3E-04	3.4E-04	1.4E-04	9.7E-04	1.6E-04	5.5E-04	1.5E-04	2.7E-04	6.8E-05
K	0.0E+00	0.0E+00	0.0E+00	0.0E+00	0.0E+00	0.0E+00	0.0E+00	0.0E+00	0.0E+00	0.0E+00	0.0E+00	0.0E+00	0.0E+00	0.0E+00	0.0E+00	0.0E+00	0.0E+00	0.0E+00	0.0E+00	0.0E+00	0.0E+00	0.0E+00	0.0E+00	0.0E+00	0.0E+00	0.0E+00	0.0E+00	0.0E+00
Sc	7.8E-06	7.1E-07	1.9E-06	3.5E-07	0.0E+00	0.0E+00	0.0E+00	0.0E+00	5.9E-07	2.8E-07	0.0E+00	0.0E+00	0.0E+00	0.0E+00	2.5E-06	4.5E-07	0.0E+00	0.0E+00	0.0E+00	0.0E+00	0.0E+00	0.0E+00	0.0E+00	0.0E+00	0.0E+00	0.0E+00	1.6E-07	8.1E-08
Ti	0.0E+00	0.0E+00	0.0E+00	0.0E+00	0.0E+00	0.0E+00	0.0E+00	0.0E+00	0.0E+00	0.0E+00	0.0E+00	0.0E+00	0.0E+00	0.0E+00	0.0E+00	0.0E+00	0.0E+00	0.0E+00	0.0E+00	0.0E+00	0.0E+00	0.0E+00	0.0E+00	0.0E+00	0.0E+00	0.0E+00	0.0E+00	0.0E+00
V	1.3E-04	2.3E-05	0.0E+00	0.0E+00	5.7E-05	1.6E-05	4.9E-05	1.5E-05	4.1E-05	9.9E-06	0.0E+00	0.0E+00	0.0E+00	0.0E+00	1.2E-04	1.2E-05	1.6E-05	4.7E-06	0.0E+00	0.0E+00	2.9E-05	5.5E-06	5.7E-05	6.9E-06	0.0E+00	0.0E+00	0.0E+00	0.0E+00
Cr	0.0E+00	0.0E+00	0.0E+00	0.0E+00	0.0E+00	0.0E+00	0.0E+00	0.0E+00	0.0E+00	0.0E+00	9.8E-05	5.0E-05	0.0E+00	0.0E+00	0.0E+00	0.0E+00	1.2E-05	3.1E-05	0.0E+00	0.0E+00	0.0E+00	0.0E+00	0.0E+00	0.0E+00	0.0E+00	0.0E+00	0.0E+00	0.0E+00
Mn	0.0E+00	0.0E+00	0.0E+00	0.0E+00	0.0E+00	0.0E+00	0.0E+00	0.0E+00	0.0E+00	0.0E+00	0.0E+00	0.0E+00	0.0E+00	0.0E+00	0.0E+00	0.0E+00	0.0E+00	0.0E+00	0.0E+00	0.0E+00	0.0E+00	0.0E+00	0.0E+00	0.0E+00	0.0E+00	0.0E+00	0.0E+00	0.0E+00
Fe	0.0E+00	0.0E+00	0.0E+00	0.0E+00	0.0E+00	0.0E+00	0.0E+00	0.0E+00	0.0E+00	0.0E+00	0.0E+00	0.0E+00	0.0E+00	0.0E+00	0.0E+00	0.0E+00	0.0E+00	0.0E+00	0.0E+00	0.0E+00	0.0E+00	0.0E+00	0.0E+00	0.0E+00	0.0E+00	0.0E+00	0.0E+00	0.0E+00
Co	2.1E-05	6.8E-06	3.6E-05	8.4E-06	2.0E-06	7.3E-06	3.6E-05	1.3E-05	1.7E-05	7.4E-06	7.0E-05	1.5E-05	0.0E+00	0.0E+00	5.1E-06	8.4E-06	2.9E-05	1.1E-05	2.7E-05	9.5E-06	0.0E+00	0.0E+00	8.4E-07	8.3E-06	9.8E-06	1.4E-05	8.8E-06	2.9E-06
Zn	0.0E+00	0.0E+00	0.0E+00	0.0E+00	0.0E+00	0.0E+00	0.0E+00	0.0E+00	0.0E+00	0.0E+00	0.0E+00	0.0E+00	0.0E+00	0.0E+00	0.0E+00	0.0E+00	0.0E+00	0.0E+00	0.0E+00	0.0E+00	0.0E+00	0.0E+00	0.0E+00	8.5E-05	0.0E+00	0.0E+00	0.0E+00	0.0E+00
As	0.0E+00	0.0E+00	0.0E+00	0.0E+00	0.0E+00	0.0E+00	3.9E-06	1.5E-06	4.6E-06	1.1E-06	0.0E+00	0.0E+00	0.0E+00	0.0E+00	0.0E+00	0.0E+00	0.0E+00	0.0E+00	3.6E-06	3.9E-07	3.8E-06	3.9E-07	4.9E-06	4.2E-07	1.6E-06	3.7E-07	6.1E-06	2.6E-07
Se	0.0E+00	0.0E+00	0.0E+00	0.0E+00	0.0E+00	0.0E+00	0.0E+00	0.0E+00	0.0E+00	0.0E+00	0.0E+00	0.0E+00	0.0E+00	0.0E+00	0.0E+00	0.0E+00	0.0E+00	0.0E+00	0.0E+00	0.0E+00	0.0E+00	0.0E+00	0.0E+00	0.0E+00	0.0E+00	0.0E+00	0.0E+00	0.0E+00
Br	0.0E+00	0.0E+00	0.0E+00	0.0E+00	0.0E+00	0.0E+00	1.9E-05	3.3E-06	0.0E+00	0.0E+00	0.0E+00	0.0E+00	0.0E+00	0.0E+00	0.0E+00	0.0E+00	0.0E+00	0.0E+00	7.5E-06	1.4E-06	8.8E-06	1.5E-06	1.0E-05	1.7E-06	0.0E+00	0.0E+00	5.4E-06	8.7E-07
Sr	0.0E+00	0.0E+00	0.0E+00	0.0E+00	0.0E+00	0.0E+00	0.0E+00	0.0E+00	0.0E+00	0.0E+00	0.0E+00	0.0E+00	0.0E+00	0.0E+00	0.0E+00	0.0E+00	0.0E+00	0.0E+00	0.0E+00	0.0E+00	0.0E+00	0.0E+00	0.0E+00	0.0E+00	0.0E+00	0.0E+00	0.0E+00	0.0E+00
Mo	0.0E+00	0.0E+00	0.0E+00	0.0E+00	0.0E+00	0.0E+00	0.0E+00	0.0E+00	0.0E+00	0.0E+00	0.0E+00	0.0E+00	0.0E+00	0.0E+00	0.0E+00	0.0E+00	0.0E+00	0.0E+00	0.0E+00	0.0E+00	0.0E+00	0.0E+00	0.0E+00	0.0E+00	0.0E+00	0.0E+00	7.4E-07	6.1E-07
Cd	0.0E+00	0.0E+00	0.0E+00	0.0E+00	0.0E+00	0.0E+00	0.0E+00	0.0E+00	0.0E+00	0.0E+00	0.0E+00	0.0E+00	0.0E+00	0.0E+00	0.0E+00	0.0E+00	0.0E+00	0.0E+00	0.0E+00	0.0E+00	0.0E+00	0.0E+00	0.0E+00	0.0E+00	0.0E+00	0.0E+00	0.0E+00	0.0E+00
Sb	1.1E-05	1.9E-06	6.8E-06	8.8E-07	0.0E+00	0.0E+00	0.0E+00	0.0E+00	5.3E-07	7.1E-07	0.0E+00	0.0E+00	2.7E-06	5.6E-07	0.0E+00	0.0E+00	4.1E-06	3.6E-06	1.8E-06	2.8E-07	3.1E-06	3.8E-07	4.3E-06	4.6E-07	1.5E-06	7.5E-07	3.5E-06	2.9E-07
Cs	0.0E+00	0.0E+00	0.0E+00	0.0E+00	0.0E+00	0.0E+00	0.0E+00	0.0E+00	6.2E-08	0.0E+00	0.0E+00	0.0E+00	0.0E+00	0.0E+00	0.0E+00	0.0E+00	1.6E-05	5.0E-06	0.0E+00	0.0E+00	0.0E+00	0.0E+00	0.0E+00	0.0E+00	0.0E+00	0.0E+00	0.0E+00	0.0E+00
Ba	0.0E+00	0.0E+00	0.0E+00	0.0E+00	0.0E+00	0.0E+00	0.0E+00	0.0E+00	0.0E+00	0.0E+00	0.0E+00	0.0E+00	0.0E+00	0.0E+00	0.0E+00	0.0E+00	0.0E+00	0.0E+00	0.0E+00	0.0E+00	0.0E+00	0.0E+00	0.0E+00	0.0E+00	0.0E+00	0.0E+00	0.0E+00	0.0E+00
La	6.6E-06	6.5E-07	1.8E-06	2.6E-07	0.0E+00	0.0E+00	1.6E-06	5.7E-07	0.0E+00	0.0E+00	0.0E+00	0.0E+00	0.0E+00	0.0E+00	8.9E-06	7.2E-07	0.0E+00	0.0E+00	2.2E-07	1.3E-07	0.0E+00	0.0E+00	0.0E+00	0.0E+00	0.0E+00	0.0E+00	0.0E+00	0.0E+00
Ce	0.0E+00	0.0E+00	0.0E+00	0.0E+00	0.0E+00	0.0E+00	0.0E+00	0.0E+00	0.0E+00	0.0E+00	0.0E+00	0.0E+00	0.0E+00	0.0E+00	0.0E+00	0.0E+00	0.0E+00	0.0E+00	0.0E+00	0.0E+00	0.0E+00	0.0E+00	0.0E+00	0.0E+00	0.0E+00	0.0E+00	0.0E+00	0.0E+00
Nd	0.0E+00	0.0E+00	0.0E+00	0.0E+00	0.0E+00	0.0E+00	0.0E+00	0.0E+00	0.0E+00	0.0E+00	0.0E+00	0.0E+00	0.0E+00	0.0E+00	8.1E-05	2.0E-05	0.0E+00	0.0E+00	0.0E+00	0.0E+00	0.0E+00	0.0E+00	6.4E-05	1.9E-05	0.0E+00	0.0E+00	0.0E+00	0.0E+00
Sm	2.0E-06	4.8E-07	7.1E-07	1.1E-07	0.0E+00	0.0E+00	0.0E+00	0.0E+00	0.0E+00	0.0E+00	0.0E+00	0.0E+00	0.0E+00	0.0E+00	5.4E-07	1.7E-07	0.0E+00	0.0E+00	0.0E+00	0.0E+00	0.0E+00	0.0E+00	0.0E+00	0.0E+00	0.0E+00	0.0E+00	0.0E+00	0.0E+00
Eu	0.0E+00	0.0E+00	0.0E+00	0.0E+00	2.1E-05	6.5E-06	0.0E+00	0.0E+00	0.0E+00	0.0E+00	0.0E+00	0.0E+00	0.0E+00	0.0E+00	5.8E-06	2.1E-06	0.0E+00	0.0E+00	0.0E+00	0.0E+00	7.8E-06	3.6E-06	0.0E+00	0.0E+00	0.0E+00	0.0E+00	0.0E+00	0.0E+00
Lu	0.0E+00	0.0E+00	0.0E+00	0.0E+00	0.0E+00	0.0E+00	0.0E+00	0.0E+00	0.0E+00	0.0E+00	0.0E+00	0.0E+00	0.0E+00	0.0E+00	0.0E+00	0.0E+00	0.0E+00	0.0E+00	0.0E+00	0.0E+00	0.0E+00	0.0E+00	0.0E+00	0.0E+00	0.0E+00	0.0E+00	0.0E+00	0.0E+00
Hf	0.0E+00	0.0E+00	0.0E+00	0.0E+00	0.0E+00	0.0E+00	0.0E+00	0.0E+00	0.0E+00	0.0E+00	0.0E+00	0.0E+00	0.0E+00	0.0E+00	0.0E+00	0.0E+00	0.0E+00	0.0E+00	0.0E+00	0.0E+00	0.0E+00	0.0E+00	0.0E+00	0.0E+00	0.0E+00	0.0E+00	0.0E+00	0.0E+00
Ta	0.0E+00	0.0E+00	0.0E+00	0.0E+00	0.0E+00	0.0E+00	0.0E+00	0.0E+00	0.0E+00	0.0E+00	0.0E+00	0.0E+00	0.0E+00	0.0E+00	0.0E+00	0.0E+00	0.0E+00	0.0E+00	0.0E+00	0.0E+00	0.0E+00	0.0E+00	0.0E+00	0.0E+00	0.0E+00	0.0E+00	0.0E+00	0.0E+00
Au	0.0E+00	0.0E+00	0.0E+00	0.0E+00	0.0E+00	0.0E+00	0.0E+00	0.0E+00	0.0E+00	0.0E+00	0.0E+00	0.0E+00	0.0E+00	0.0E+00	0.0E+00	0.0E+00	0.0E+00	0.0E+00	0.0E+00	0.0E+00	0.0E+00	0.0E+00	1.9E-08	5.8E-10	0.0E+00	0.0E+00	4.1E-08	0.0E+00
Hg	4.9E-06	1.1E-06	4.3E-06	6.8E-08	0.0E+00	0.0E+00	4.6E-06	6.5E-07	0.0E+00	0.0E+00	7.5E-06	5.3E-07	3.5E-07	2.2E-07	0.0E+00	0.0E+00	2.9E-06	1.1E-07	3.6E-06	2.5E-07	3.6E-06	3.0E-07	1.0E-06	3.4E-07	1.9E-06	3.4E-07		
Th	0.0E+00	0.0E+00	0.0E+00	0.0E+00	0.0E+00	0.0E+00	0.0E+00	0.0E+00	0.0E+00	0.0E+00	0.0E+00	0.0E+00	0.0E+00	0.0E+00	0.0E+00	0.0E+00	0.0E+00	0.0E+00	0.0E+00	0.0E+00	0.0E+00	0.0E+00	0.0E+00	0.0E+00	0.0E+00	0.0E+00	0.0E+00	0.0E+00
U	0.0E+00	0.0E+00	0.0E+00	0.0E+00	0.0E+00	0.0E+00	0.0E+00	0.0E+00	0.0E+00	0.0E+00	0.0E+00	0.0E+00	0.0E+00	0.0E+00	0.0E+00	0.0E+00	0.0E+00	0.0E+00	0.0E+00	0.0E+00	0.0E+00	0.0E+00	0.0E+00	0.0E+00	0.0E+00	0.0E+00	0.0E+00	0.0E+00

TABLE A-VI. Relative Response Factor (RRF) calculations for the target organic species used in CMB analysis.

n-Tetracosane	57, 71, 85	#2		21.87	21.87	21.87	609751	799126	24.56	381901	24.5	668106								
n-Pentacosane	57, 71, 85	#2 Use n-C24	n-C28 (Octacosane-D58)	21.87	21.87	21.87	609751	799126	24.56	381901	24.5	668106	20.5	5	4.1	196	40	4.90	0.52	0.70	0.61
n-Hexacosane	57, 71, 85	#2 Use n-C24	n-C28 (Octacosane-D58)	21.87	21.87	21.87	609751	799126	24.56	381901	24.5	668106	20.5	5	4.1	196	40	4.90	0.52	0.70	0.61
n-Heptacosane	57, 71, 85	#2 Use n-C28	n-C28 (Octacosane-D58)	24.90	24.90	24.90	453178	825643	24.56	381901	24.5	668106	20.5	5	4.1	196	40	4.90	0.71	0.68	0.69
n-Octacosane	57, 71, 85	#2	n-C28 (Octacosane-D58)	24.90	24.90	24.90	453178	825643	24.56	381901	24.5	668106	20.5	5	4.1	196	40	4.90	0.71	0.68	0.69
n-Nonacosane	57, 71, 85	#2 Use n-C28	n-C28 (Octacosane-D58)	24.90	24.90	24.90	453178	825643	24.56	381901	24.5	668106	20.5	5	4.1	196	40	4.90	0.71	0.68	0.69
n-Triacontane	57, 71, 85	#2	n-C28 (Octacosane-D58)	26.32	26.32	26.32	709869	1302407	24.56	381901	24.5	668106	20.5	5	4.1	196	40	4.90	0.45	0.43	0.44
n-Hentriacontane	57, 71, 85	#2 Use n-C32	n-C28 (Octacosane-D58)	26.32	26.32	26.32	709869	1302407	24.56	381901	24.5	668106	20.5	5	4.1	196	40	4.90	0.45	0.43	0.44
n-Dotriacontane	57, 71, 85	#2	n-C36 (Hexatriacontane-D74)	28.10	28.07	28.08	327559	789000	32.76	304016	32.7	1071942	20.5	5	4.1	406	40	10.15	0.37	0.55	0.46
n-Tritriacontane	57, 71, 85	#2 Use n-C36	n-C36 (Hexatriacontane-D74)	28.10	28.07	28.08	327559	789000	32.76	304016	32.7	1071942	20.5	5	4.1	406	40	10.15	0.37	0.55	0.46
20S&R-5a(H), 14b(H), 17b(H)-Cholestanes	218, 217	#1 ABB 20R-C27-Cholestane	aaa-20R-Cholestane-D4	25.23	25.22	25.22	32631	57172	25.50	20801	25.5	34064	1	5	0.2	15	40	0.38	0.34	0.32	0.33
20R-5a(H), 14a(H), 17a(H)-Cholestane	217, 218	#1 AAA-20S&R-C27-Cholestane	aaa-20R-Cholestane-D4	25.52	25.52	25.52	20320	30757	25.50	20801	25.5	34064	1	5	0.2	15	40	0.38	0.55	0.59	0.57
20S&R-5a(H), 14b(H), 17b(H)-Ergostanes	217, 218	#1 ABB-20R-C28-methylcholestane	aaa-20R-Cholestane-D4	26.03	26.02	26.02	18810	35411	25.50	20801	25.5	34064	1	5	0.2	15	40	0.38	0.59	0.51	0.55
20S&R-5a(H), 14b(H), 17b(H)-Sitostanes	217, 218	#1 ABB-20R-C29-Ethylcholestane	aaa-20R-Cholestane-D4	26.68	26.67	26.68	15575	31438	25.50	20801	25.5	34064	1	5	0.2	15	40	0.38	0.71	0.58	0.65
22, 29, 30-Trisnorneohopane (T m)	191	#1 17A-22,29,30-Trisnorhopane	aaa-20R-Cholestane-D4	26.12	26.11	26.12	14801	22008	25.50	20801	25.5	34064	1	5	0.2	15	40	0.38	0.75	0.83	0.79
17a(H), 21b(H)-29-Norhopane	191	#1 17B21A-30-Nohopane	aaa-20R-Cholestane-D4	28.02	28.00	28.01	17504	28647	25.50	20801	25.5	34064	1	5	0.2	15	40	0.38	0.63	0.63	0.63
17a(H), 21b(H)-Hopane	191	#1 17a(H), 21b(H)-Hopane	aaa-20R-Cholestane-D4	29.64	29.63	29.63	19355	43071	25.50	20801	25.5	34064	1	5	0.2	15	40	0.38	0.57	0.42	0.50
22S-17a(H), 21b(H)-30-Homohopane	191	#1 Use 17a(H), 21b(H)-Hopane	aaa-20R-Cholestane-D4	29.64	29.63	29.63	19355	43071	25.50	20801	25.5	34064	1	5	0.2	15	40	0.38	0.57	0.42	0.50
22R-17a(H), 21b(H)-30-Homohopane	191	#1 Use 17a(H), 21b(H)-Hopane	aaa-20R-Cholestane-D4	29.64	29.63	29.63	19355	43071	25.50	20801	25.5	34064	1	5	0.2	15	40	0.38	0.57	0.42	0.50
22S-17a(H), 21b(H)-30-Bishomohopane	191	#1 Use 17a(H), 21b(H)-Hopane	aaa-20R-Cholestane-D4	29.64	29.63	29.63	19355	43071	25.50	20801	25.5	34064	1	5	0.2	15	40	0.38	0.57	0.42	0.50
22R-17a(H), 21b(H)-30-Bishomohopane	191	#1 Use 17a(H), 21b(H)-Hopane	aaa-20R-Cholestane-D4	29.64	29.63	29.63	19355	43071	25.50	20801	25.5	34064	1	5	0.2	15	40	0.38	0.57	0.42	0.50
n-9-Hexadecenoic acid, MW 256	74, 87	#3	Heptadecanoic Acid-D33	17.63	17.63	17.63	1212211	1659271	18.36	542801	18.4	646211	30	5	6	176	40	4.40	0.61	0.53	0.57
Pimaric acid	121	#6 Use isopimaric acid	Heptadecanoic Acid-D33	21.29	21.29	21.29	161568	181239	18.36	542801	18.4	646211	57.3	5	11.46	176	40	4.40	8.75	9.29	9.02
Isopimaric acid	121	#6 Isopimaric Acid	Heptadecanoic Acid-D33	21.29	21.29	21.29	161568	181239	18.36	542801	18.4	646211	57.3	5	11.46	176	40	4.40	8.75	9.29	9.02
Hexadecanamide	59, 72	Use Octadecanamide	Heptadecanoic Acid-D33	21.82	21.81	21.82	265703	545751	18.36	542801	18.4	646211	8.4	2	4.2	176	40	4.40	1.95	1.13	1.54
Octadecanamide	59, 72	#5	Heptadecanoic Acid-D33	21.82	21.81	21.82	265703	545751	18.36	542801	18.4	646211	8.4	2	4.2	176	40	4.40	1.95	1.13	1.54
Benzo[b]fluoranthene	252	#1	Dibenz[ah]anthracene-D14	25.03	25.03	25.03	194603	364199	28.40	1028027	28.4	1468302	4	5	0.8	192	40	4.80	0.88	0.67	0.78
Benzo[k]fluoranthene	252	#1	Dibenz[ah]anthracene-D14	25.08	25.08	25.08	113519	174542	28.40	1028027	28.4	1468302	2	5	0.4	192	40	4.80	0.75	0.70	0.73
Benzo[e]pyrene	252	#1 Use Benzo[a]pyrene	Dibenz[ah]anthracene-D14	25.69	25.68	25.68	88017	162709	28.40	1028027	28.4	1468302	2	5	0.4	192	40	4.80	0.97	0.75	0.86
Indeno[1,2,3-cd]fluoranthene	276	Use Indeno[1,2,3-cd]pyrene	Dibenz[ah]anthracene-D14	29.11	29.10	29.10	185182	325233	28.40	1028027	28.4	1468302	2	5	0.4	192	40	4.80	0.46	0.38	0.42
Indeno[1,2,3-cd]pyrene/o-Phenylenepyrene	276	#1	Dibenz[ah]anthracene-D14	29.11	29.10	29.10	185182	325233	28.40	1028027	28.4	1468302	2	5	0.4	192	40	4.80	0.46	0.38	0.42
Picene	278	#1 dibenzo[a,h]anthracene	Dibenz[ah]anthracene-D14	28.49	28.48	28.48	208609	319431	28.40	1028027	28.4	1468302	4	5	0.8	192	40	4.80	0.82	0.77	0.79
Coronene	300	#1	Dibenz[ah]anthracene-D14	35.08	35.09	35.08	80203	132188	28.40	1028027	28.4	1468302	2.5	5	0.5	192	40	4.80	1.34	1.16	1.25
Cholesterol	275, 365, 386	#4	Cholesterol-2,2,3,4,4,6-D6	27.78	27.79	27.79	6040416	8381796	27.79	2845857	27.8	3984962	2000	10	200	394	40	9.85	9.57	9.65	9.61
Stigmasterol	412, 271	#4	Cholesterol-2,2,3,4,4,6-D6	29.30	29.31	29.30	3816997	5516836	27.79	2845857	27.8	3984962	1664	10	166.4	394	40	9.85	12.60	12.20	12.40
Levoglucosan	60, 73	#4	Levoglucosan-U-13C6	13.23	13.28	13.25	6863757	9226755	13.18	1307767	13.3	1746603	1540	10	154	1250	40	31.25	0.94	0.93	0.94

TABLE A-VII. Concentrations in μg/m^3 for Delhi, Mumbai, Kolkata, and Chandigarh for the target organic compounds used in CMB.

	03C5DEL	06C8DEL	10C3DEL	12C6DEL	12C2DEL	1217DEL	1223DEL	0110DEL	0104DEL	03C5KOL	06C5KOL	10C5KOL	12C5KOL	03C6MUM	10C7MUM	12C7MUM	06C5CHA	12C6DEL
n-Pentacosane	32.12	4.47	37.55	102.43	27.45	147.65	111.88	99.49	125.70	18.78	10.92	23.69	117.92	5.84	18.70	21.59	21.33	85.36
n-Hexacosane	32.14	6.19	36.17	85.92	21.93	126.69	90.66	82.37	107.94	14.54	19.89	14.11	90.70	7.48	20.48	20.68	13.15	71.60
n-Heptacosane	49.19	9.62	54.32	105.10	28.20	169.18	110.57	97.29	120.27	22.32	15.81	24.71	103.57	12.04	22.71	21.89	22.31	87.59
n-Octacosane	37.23	7.01	43.45	76.67	20.45	123.39	80.41	72.88	86.24	13.68	17.70	19.13	73.75	8.50	24.31	16.43	8.69	63.90
n-Nonacosane	86.17	16.79	77.38	150.32	50.05	232.05	154.10	144.74	170.66	27.37	18.84	45.29	86.32	24.13	31.64	23.58	12.25	125.26
n-Triacontane	16.60	3.63	23.50	33.44	8.67	47.41	48.94	24.34	37.86	12.19	16.69	29.11	31.71	3.73	17.88	7.72	3.61	27.87
n-Hentriacontane	39.36	7.04	43.02	71.70	23.51	97.49	106.69	59.65	71.15	12.56	8.59	10.31	61.99	8.08	32.95	12.92	6.92	59.75
n-Dotricontane	31.92	8.38	53.27	94.62	20.80	163.75	136.22	61.57	90.76	16.09	27.10	24.06	81.76	14.07	9.97	20.02	78.34	78.85
n-Tritriacontane	47.12	10.89	74.32	121.76	33.63	187.19	154.79	98.92	134.29	12.26	14.23	29.36	105.14	11.61	13.94	23.22	5.08	101.47
20S&R-5a(H), 14b(H), 17b(H)-Cholestanes	0.81	0.24	1.08	2.99	0.67	5.17	3.74	2.14	3.20	1.51	0.50	2.43	2.98	0.29	0.49	0.77	1.97	2.49
20R-5a(H), 14a(H), 17a(H)-Cholestane	0.72	0.19	0.66	2.09	0.41	2.97	3.35	1.34	2.36	0.92	0.70	2.31	5.34	0.18	0.28	0.61	0.50	1.74
20S&R-5a(H), 14b(H), 17b(H)-Ergostanes	1.95	0.32	1.04	4.30	0.84	5.75	4.27	5.45	5.18	1.22	0.65	2.10	9.19	0.41	0.98	2.41	1.40	3.58
20S&R-5a(H), 14b(H), 17b(H)-Sitostanes	3.23	0.73	3.80	8.05	1.85	9.56	9.31	8.25	11.27	1.51	1.22	4.30	9.39	1.04	1.80	2.84	3.66	6.71
22, 29, 30-Trisnorneohopane	0.92	0.53	2.19	5.35	1.55	7.19	6.51	4.85	6.67	1.72	0.45	2.29	8.97	0.30	1.43	1.10	3.28	4.46
17a(H), 21b(H)-29-Norhopane	4.75	1.56	9.89	17.37	3.14	27.33	26.08	12.94	17.35	5.43	3.28	5.30	21.97	1.20	2.59	5.06	8.93	14.47
17a(H), 21b(H)-Hopane	3.83	1.65	7.37	15.42	2.58	25.66	21.83	11.22	15.81	6.74	4.01	8.52	19.98	0.99	1.42	3.66	11.05	12.85
22S-17a(H), 21b(H)-30-Homohopane	1.88	1.05	3.89	7.46	1.49	12.06	9.23	6.34	8.19	4.06	1.81	3.27	9.82	0.69	1.64	2.09	3.36	6.22
22R-17a(H), 21b(H)-30-Homohopane	1.26	0.94	3.59	6.25	1.18	9.85	7.12	5.57	7.51	3.66	1.17	3.03	9.77	0.69	1.57	1.84	2.88	5.21
22S-17a(H), 21b(H)-30-Bishomohopane	1.19	0.71	2.61	4.99	0.87	7.69	7.66	3.30	5.44	2.50	0.71	2.40	6.19	0.51	0.97	1.51	2.05	4.16
22R-17a(H), 21b(H)-30-Bishomohopane	1.10	0.52	1.96	5.85	0.71	16.87	5.13	2.67	3.87	1.94	0.60	3.06	6.07	0.40	0.75	1.22	1.61	4.87
n-9-Hexadecenoic acid	7.65	3.17	8.97	24.97	9.34	28.56	42.95	22.60	21.39	14.77	6.28	3.69	30.98	4.22	4.42	5.93	5.40	20.81
Pimaric acid	2.93	1.01	6.53	19.45	8.01	17.94	35.92	17.87	17.52	35.47	11.18	11.62	40.73	4.37	9.27	8.35	16.29	16.21
Isopimaric acid	2.93	1.12	7.36	28.67	7.93	25.12	33.29	16.01	61.00	4.03	2.06	6.43	21.06	3.58	3.23	5.59	5.74	23.89
hexadecanamide	17.40	4.14	18.96	44.58	8.70	87.23	59.31	25.03	42.65	7.62	2.93	6.90	36.59	4.32	2.76	6.97	5.02	37.15
octadecanamide	6.87	1.35	7.55	15.32	3.39	33.99	18.19	7.82	13.22	2.31	1.13	3.98	9.36	1.30	1.18	2.15	1.65	12.77
Benzo[b]fluoranthene	7.11	1.26	9.97	30.62	7.82	41.70	30.56	45.11	27.90	4.48	1.67	6.07	53.59	1.25	3.95	6.71	0.68	25.52
Benzo[k]fluoranthene	6.94	1.13	8.10	28.39	6.45	38.53	28.21	39.23	29.51	4.36	1.31	5.10	40.86	1.25	3.48	5.59	0.53	23.66
Benzo[e]pyrene	6.39	0.82	7.54	25.77	6.02	27.04	21.83	48.25	25.70	4.19	0.88	5.01	39.38	0.45	2.13	2.69	0.40	21.47
Indeno[1,2,3-cd]fluoranthene	3.51	0.92	5.07	16.58	3.18	19.55	14.02	32.90	13.23	2.44	1.08	3.36	23.41	0.81	2.26	3.26	0.43	13.81
Indeno[1,2,3-cd]pyrene	3.90	1.06	6.57	18.49	3.51	20.89	14.92	37.75	15.40	2.85	1.61	3.85	26.13	0.95	2.32	3.58	0.49	15.41
Picene	1.26	0.28	1.54	5.11	0.87	5.39	3.32	12.34	3.64	0.66	0.27	0.82	7.12	0.14	0.48	0.93	0.16	4.26
Coronene	6.51	1.64	11.16	21.60	5.25	32.76	21.13	28.91	19.93	3.58	1.70	3.95	35.95	0.76	2.43	5.13	0.65	18.00
Cholesterol	BDL	BDL	BDL	BDL	BDL	BDL	BDL	BDL	BDL	BDL	90.76	106.84	BDL	BDL	BDL	BDL	0.00	0.00
stigmasterol	77.26	29.20	164.40	295.86	115.99	481.74	240.53	264.19	376.86	49.81	21.79	36.85	301.28	10.33	142.54	34.61	60.05	246.55
Levoglucosan	1026.60	210.46	1773.64	5258.30	1366.21	9600.20	4742.44	4606.94	5975.72	336.45	75.12	474.38	5491.95	74.52	392.43	907.96	140.30	4381.92

TABLE A-VIIIa. Source emissions profiles used for CMB analysis (Part I).

PNO	SID	SIZE	EC	PEC	AL	PAL	SI	PSI	NC25	PNC25	NC26	PNC26	NC27	PNC27	NC28	PNC28	NC29	PNC29	NC30	PNC30	NC31	PNC31	NC32	PNC32
1	OAKWOO	FINE	0.0470	0.0034	0.0003	0.0001	0.0003	0.0001	0.0000	0.0000	0.0001	0.0000	0.0001	0.0000	0.0000	0.0000	0.0001	0.0000	0.0000	0.0000	0.0000	0.0000	0.0000	0.0000
2	EUCALY	FINE	0.0595	0.0046	0.0001	0.0001	0.0002	0.0000	0.0000	0.0000	0.0001	0.0000	0.0001	0.0000	0.0000	0.0000	0.0000	0.0000	0.0000	0.0000	0.0000	0.0000	0.0000	0.0000
3	C*HWOO	FINE	0.0532	0.0040	0.0002	0.0001	0.0003	0.0001	0.0000	0.0000	0.0001	0.0000	0.0001	0.0000	0.0000	0.0000	0.0000	0.0000	0.0000	0.0000	0.0000	0.0000	0.0000	0.0000
4	PINEWO	FINE	0.0250	0.0018	0.0001	0.0001	0.0001	0.0000	0.0001	0.0000	0.0001	0.0000	0.0001	0.0000	0.0000	0.0000	0.0000	0.0000	0.0000	0.0000	0.0000	0.0000	0.0000	0.0000
5	DIESEL	FINE	1.3322	0.1139	0.0026	0.0046	0.0207	0.0013	0.0005	0.0001	0.0006	0.0001	0.0005	0.0001	0.0004	0.0001	0.0001	0.0000	0.0000	0.0000	0.0000	0.0000	0.0000	0.0000
6	NONCAT	FINE	0.0167	0.0048	0.0000	0.0004	0.0014	0.0001	0.0010	0.0002	0.0015	0.0003	0.0008	0.0002	0.0002	0.0000	0.0002	0.0000	0.0000	0.0000	0.0000	0.0000	0.0000	0.0000
7	CATCAR	FINE	0.2357	0.0481	0.0060	0.0053	0.0057	0.0025	0.0006	0.0001	0.0003	0.0001	0.0008	0.0002	0.0002	0.0000	0.0002	0.0000	0.0000	0.0000	0.0000	0.0000	0.0000	0.0000
8	C*CARS	FINE	0.0170	0.0048	0.0000	0.0004	0.0014	0.0001	0.0010	0.0002	0.0015	0.0003	0.0008	0.0002	0.0002	0.0000	0.0002	0.0000	0.0000	0.0000	0.0000	0.0000	0.0000	0.0000
9	VEGETA	FINE	0.0290	0.0122	0.0793	0.0129	0.2577	0.0556	0.0007	0.0001	0.0003	0.0001	0.0025	0.0005	0.0007	0.0001	0.0184	0.0037	0.0013	0.0003	0.0293	0.0059	0.0023	0.0005
10	MEATCH	FINE	0.0000	0.0088	0.0007	0.0003	0.0014	0.0003	0.0000	0.0000	0.0000	0.0000	0.0000	0.0000	0.0001	0.0000	0.0001	0.0000	0.0000	0.0000	0.0000	0.0000	0.0000	0.0000
11	RDFRES	FINE	0.0000	0.0253	0.2131	0.0131	0.6212	0.0111	0.0004	0.0001	0.0005	0.0001	0.0005	0.0001	0.0004	0.0001	0.0010	0.0002	0.0003	0.0001	0.0003	0.0001	0.0001	0.0000
12	RDBAKE	FINE	0.0671	0.1409	0.2799	0.0154	0.8356	0.0134	0.0003	0.0001	0.0003	0.0001	0.0004	0.0001	0.0002	0.0000	0.0007	0.0001	0.0002	0.0000	0.0002	0.0000	0.0001	0.0000
13	RDKWRE	FINE	0.1163	0.1395	0.3326	0.0147	0.9171	0.0140	0.0003	0.0001	0.0003	0.0001	0.0004	0.0001	0.0003	0.0001	0.0008	0.0002	0.0002	0.0000	0.0002	0.0000	0.0001	0.0000
14	C*RDDU	FINE	0.0611	0.1154	0.2752	0.0145	0.7913	0.0129	0.0003	0.0001	0.0004	0.0001	0.0004	0.0001	0.0003	0.0001	0.0008	0.0002	0.0002	0.0000	0.0003	0.0001	0.0001	0.0000
15	CIGSMO	FINE	0.0098	0.0022	0.0000	0.0007	0.0000	0.0004	0.0004	0.0001	0.0000	0.0000	0.0026	0.0005	0.0002	0.0000	0.0029	0.0006	0.0009	0.0002	0.0119	0.0024	0.0014	0.0003
16	FUELOI	FINE	6.0208	0.4299	0.0875	0.0060	0.1854	0.0122	0.0005	0.0001	0.0003	0.0001	0.0002	0.0000	0.0001	0.0000	0.0001	0.0000	0.0001	0.0000	0.0000	0.0000	0.0000	0.0000
17	COAL	FINE	1.0346	0.0533	0.0032	0.0009	0.0233	0.0049	0.0017	0.0003	0.0010	0.0002	0.0009	0.0002	0.0005	0.0001	0.0010	0.0002	0.0003	0.0001	0.0005	0.0001	0.0001	0.0000
18	NATGAS	FINE	0.0789	0.2052	0.0026	0.0065	0.0033	0.0086	0.0014	0.0003	0.0006	0.0001	0.0008	0.0002	0.0003	0.0001	0.0013	0.0003	0.0002	0.0000	0.0004	0.0001	0.0000	0.0000
19	COCOLV	FINE	0.2308	0.0223	0.0000	0.0000	0.0000	0.0000	0.0000	0.0000	0.0005	0.0001	0.0013	0.0002	0.0008	0.0001	0.0014	0.0002	0.0015	0.0002	0.0008	0.0001	0.0009	0.0001
20	RICEST	FINE	0.0195	0.0039	0.0000	0.0000	0.0000	0.0000	0.0004	0.0001	0.0004	0.0001	0.0009	0.0001	0.0007	0.0001	0.0018	0.0003	0.0009	0.0001	0.0015	0.0002	0.0004	0.0001
21	COWDNG	FINE	0.0126	0.0015	0.0000	0.0000	0.0000	0.0000	0.0023	0.0003	0.0027	0.0004	0.0044	0.0007	0.0036	0.0006	0.0067	0.0011	0.0046	0.0007	0.0052	0.0008	0.0035	0.0005
22	BRIQUT	FINE	0.0203	0.0033	0.0000	0.0000	0.0000	0.0000	0.0021	0.0003	0.0013	0.0002	0.0054	0.0009	0.0026	0.0004	0.0128	0.0021	0.0036	0.0006	0.0099	0.0015	0.0024	0.0003
23	JACKBR	FINE	0.0367	0.0033	0.0000	0.0000	0.0000	0.0000	0.0003	0.0000	0.0003	0.0000	0.0007	0.0001	0.0003	0.0001	0.0006	0.0001	0.0003	0.0000	0.0000	0.0000	0.0000	0.0000
24	C*INBIO	FINE	0.0768	0.0115	0.0000	0.0000	0.0000	0.0000	0.0007	0.0001	0.0006	0.0001	0.0021	0.0004	0.0011	0.0002	0.0042	0.0011	0.0016	0.0003	0.0030	0.0008	0.0009	0.0002

TABLE A-VIIIb. Source emissions profiles used for CMB analysis (Part II).

PNO	SID	SIZE	NC33	PNC33	ABBCHL	PABBCHL	AAACHL	PAAACHL	ERGO	PERGO	SITO	PSITO	TRINO	PTRINO	29NOR	P29NOR	HOPA	PHOPA	9HEXA	P9HEXA	ISOPIM	PISOPIM
1	OAKWOO	FINE	0.0000	0.0000	0.0000	0.0000	0.0000	0.0000	0.0000	0.0000	0.0000	0.0000	0.0000	0.0000	0.0000	0.0000	0.0000	0.0000	0.0000	0.0000	0.0012	0.0002
2	EUCALY	FINE	0.0000	0.0000	0.0000	0.0000	0.0000	0.0000	0.0000	0.0000	0.0000	0.0000	0.0000	0.0000	0.0000	0.0000	0.0000	0.0000	0.0000	0.0000	0.0000	0.0000
3	C*HWOO	FINE	0.0000	0.0000	0.0000	0.0000	0.0000	0.0000	0.0000	0.0000	0.0000	0.0000	0.0000	0.0000	0.0000	0.0000	0.0000	0.0000	0.0000	0.0000	0.0006	0.0002
4	PINEWO	FINE	0.0000	0.0000	0.0000	0.0000	0.0000	0.0000	0.0000	0.0000	0.0000	0.0000	0.0000	0.0000	0.0000	0.0000	0.0000	0.0000	0.0000	0.0000	0.0081	0.0016
5	DIESEL	FINE	0.0000	0.0000	0.0000	0.0000	0.0000	0.0000	0.0001	0.0000	0.0000	0.0000	0.0000	0.0000	0.0002	0.0000	0.0002	0.0000	0.0000	0.0000	0.0000	0.0000
6	NONCAT	FINE	0.0000	0.0000	0.0003	0.0001	0.0002	0.0000	0.0003	0.0001	0.0003	0.0001	0.0003	0.0001	0.0006	0.0001	0.0006	0.0001	0.0000	0.0000	0.0000	0.0000
7	CATCAR	FINE	0.0000	0.0000	0.0000	0.0000	0.0000	0.0000	0.0000	0.0000	0.0000	0.0000	0.0000	0.0000	0.0000	0.0000	0.0000	0.0000	0.0000	0.0000	0.0000	0.0000
8	C*CARS	FINE	0.0000	0.0000	0.0003	0.0001	0.0002	0.0000	0.0003	0.0001	0.0003	0.0001	0.0003	0.0001	0.0006	0.0001	0.0006	0.0001	0.0000	0.0000	0.0000	0.0000
9	VEGETA	FINE	0.0143	0.0029	0.0000	0.0000	0.0000	0.0000	0.0000	0.0000	0.0000	0.0000	0.0000	0.0000	0.0000	0.0000	0.0000	0.0000	0.0000	0.0000	0.0000	0.0000
10	MEATCH	FINE	0.0000	0.0000	0.0000	0.0000	0.0000	0.0000	0.0000	0.0000	0.0000	0.0000	0.0000	0.0000	0.0000	0.0000	0.0000	0.0000	0.0019	0.0004	0.0000	0.0000
11	RDFRES	FINE	0.0001	0.0000	0.0000	0.0000	0.0000	0.0000	0.0000	0.0000	0.0000	0.0000	0.0000	0.0000	0.0000	0.0000	0.0000	0.0000	0.0057	0.0011	0.0000	0.0000
12	RDBAKE	FINE	0.0001	0.0000	0.0000	0.0000	0.0000	0.0000	0.0000	0.0000	0.0000	0.0000	0.0000	0.0000	0.0000	0.0000	0.0000	0.0000	0.0038	0.0008	0.0000	0.0000
13	RDKWRE	FINE	0.0001	0.0000	0.0000	0.0000	0.0000	0.0000	0.0000	0.0000	0.0000	0.0000	0.0000	0.0000	0.0000	0.0000	0.0000	0.0000	0.0043	0.0009	0.0000	0.0000
14	C*RDDU	FINE	0.0001	0.0000	0.0000	0.0000	0.0000	0.0000	0.0000	0.0000	0.0000	0.0000	0.0000	0.0000	0.0000	0.0000	0.0000	0.0000	0.0046	0.0009	0.0000	0.0000
15	CIGSMO	FINE	0.0040	0.0008	0.0000	0.0000	0.0000	0.0000	0.0000	0.0000	0.0000	0.0000	0.0000	0.0000	0.0000	0.0000	0.0000	0.0000	0.0000	0.0000	0.0000	0.0000
16	FUELOI	FINE	0.0000	0.0000	0.0000	0.0000	0.0000	0.0000	0.0001	0.0000	0.0001	0.0000	0.0000	0.0000	0.0001	0.0000	0.0001	0.0000	0.0000	0.0000	0.0000	0.0000
17	COAL	FINE	0.0001	0.0000	0.0000	0.0000	0.0000	0.0000	0.0000	0.0000	0.0000	0.0000	0.0001	0.0000	0.0001	0.0000	0.0002	0.0000	0.0000	0.0000	0.0000	0.0000
18	NATGAS	FINE	0.0000	0.0000	0.0000	0.0000	0.0000	0.0000	0.0000	0.0000	0.0000	0.0000	0.0000	0.0000	0.0000	0.0000	0.0000	0.0000	0.0000	0.0000	0.0000	0.0000
19	COCOLV	FINE	0.0000	0.0000	0.0000	0.0000	0.0000	0.0000	0.0000	0.0000	0.0000	0.0000	0.0000	0.0000	0.0000	0.0000	0.0000	0.0000	0.0000	0.0000	0.0000	0.0000
20	RICEST	FINE	0.0000	0.0000	0.0000	0.0000	0.0000	0.0000	0.0000	0.0000	0.0000	0.0000	0.0000	0.0000	0.0000	0.0000	0.0000	0.0000	0.0000	0.0000	0.0000	0.0000
21	COWDNG	FINE	0.0062	0.0011	0.0000	0.0000	0.0000	0.0000	0.0000	0.0000	0.0000	0.0000	0.0000	0.0000	0.0000	0.0000	0.0000	0.0000	0.0000	0.0000	0.0006	0.0001
22	BRIQUT	FINE	0.0075	0.0013	0.0000	0.0000	0.0000	0.0000	0.0000	0.0000	0.0000	0.0000	0.0000	0.0000	0.0000	0.0000	0.0000	0.0000	0.0000	0.0000	0.0011	0.0002
23	JACKBR	FINE	0.0000	0.0000	0.0000	0.0000	0.0000	0.0000	0.0000	0.0000	0.0000	0.0000	0.0000	0.0000	0.0000	0.0000	0.0000	0.0000	0.0000	0.0000	0.0000	0.0000
24	C*INBIO	FINE	0.0019	0.0007	0.0000	0.0000	0.0000	0.0000	0.0000	0.0000	0.0000	0.0000	0.0000	0.0000	0.0000	0.0000	0.0000	0.0000	0.0000	0.0000	0.0003	0.0001

TABLE A-VIIIc. Source emissions profiles used for CMB analysis (Part III).

PNO	SID	SIZE	HXDCMD	PHXDCMD	OCDCMD	POCDCMD	BbF	PBbF	BkF	PBkF	BeP	PBeP	ICDF	PICDF	ICDP	PICDP	PICENE	PPICENE	CORO	PCORO	STIGRL	PSTIGRL	LEVO	PLEVO
1	OAKWOO	FINE	0.0000	0.0000	0.0000	0.0000	0.0001	0.0000	0.0001	0.0000	0.0001	0.0000	0.0000	0.0000	0.0000	0.0000	0.0000	0.0000	0.0000	0.0000	0.0000	0.0000	0.2321	0.0464
2	EUCALY	FINE	0.0000	0.0000	0.0000	0.0000	0.0001	0.0000	0.0001	0.0000	0.0001	0.0000	0.0000	0.0000	0.0000	0.0000	0.0000	0.0000	0.0000	0.0000	0.0000	0.0000	0.5222	0.1044
3	C*HWOO	FINE	0.0000	0.0000	0.0000	0.0000	0.0001	0.0000	0.0001	0.0000	0.0001	0.0000	0.0000	0.0000	0.0000	0.0000	0.0000	0.0000	0.0000	0.0000	0.0000	0.0000	0.3772	0.0808
4	PINEWO	FINE	0.0000	0.0000	0.0000	0.0000	0.0001	0.0000	0.0001	0.0000	0.0001	0.0000	0.0000	0.0000	0.0001	0.0000	0.0000	0.0000	0.0000	0.0000	0.0000	0.0000	0.2585	0.0517
5	DIESEL	FINE	0.0000	0.0000	0.0000	0.0000	0.0000	0.0000	0.0000	0.0000	0.0000	0.0000	0.0000	0.0000	0.0000	0.0000	0.0000	0.0000	0.0000	0.0000	0.0000	0.0000	0.0000	0.0000
6	NONCAT	FINE	0.0000	0.0000	0.0000	0.0000	0.0001	0.0000	0.0001	0.0000	0.0001	0.0000	0.0001	0.0000	0.0002	0.0000	0.0000	0.0000	0.0000	0.0000	0.0000	0.0000	0.0000	0.0000
7	CATCAR	FINE	0.0000	0.0000	0.0000	0.0000	0.0000	0.0000	0.0000	0.0000	0.0000	0.0000	0.0000	0.0000	0.0001	0.0000	0.0000	0.0000	0.0000	0.0000	0.0000	0.0000	0.0000	0.0000
8	C*CARS	FINE	0.0000	0.0000	0.0000	0.0000	0.0001	0.0000	0.0001	0.0000	0.0001	0.0000	0.0001	0.0000	0.0002	0.0000	0.0000	0.0000	0.0000	0.0000	0.0000	0.0000	0.0000	0.0000
9	VEGETA	FINE	0.0000	0.0000	0.0000	0.0000	0.0000	0.0000	0.0000	0.0000	0.0000	0.0000	0.0000	0.0000	0.0000	0.0000	0.0000	0.0000	0.0000	0.0000	0.0000	0.0000	0.0000	0.0000
10	MEATCH	FINE	0.0000	0.0000	0.0000	0.0000	0.0000	0.0000	0.0000	0.0000	0.0000	0.0000	0.0000	0.0000	0.0000	0.0000	0.0000	0.0000	0.0000	0.0000	0.0000	0.0000	0.0000	0.0000
11	RDFRES	FINE	0.0000	0.0000	0.0000	0.0000	0.0000	0.0000	0.0000	0.0000	0.0000	0.0000	0.0000	0.0000	0.0000	0.0000	0.0000	0.0000	0.0000	0.0000	0.0000	0.0000	0.0000	0.0000
12	RDBAKE	FINE	0.0000	0.0000	0.0000	0.0000	0.0000	0.0000	0.0000	0.0000	0.0000	0.0000	0.0000	0.0000	0.0000	0.0000	0.0000	0.0000	0.0000	0.0000	0.0000	0.0000	0.0000	0.0000
13	RDKWRE	FINE	0.0000	0.0000	0.0000	0.0000	0.0000	0.0000	0.0000	0.0000	0.0000	0.0000	0.0000	0.0000	0.0000	0.0000	0.0000	0.0000	0.0000	0.0000	0.0000	0.0000	0.0000	0.0000
14	C*RDDU	FINE	0.0000	0.0000	0.0000	0.0000	0.0000	0.0000	0.0000	0.0000	0.0000	0.0000	0.0000	0.0000	0.0000	0.0000	0.0000	0.0000	0.0000	0.0000	0.0000	0.0000	0.0000	0.0000
15	CIGSMO	FINE	0.0000	0.0000	0.0000	0.0000	0.0000	0.0000	0.0000	0.0000	0.0000	0.0000	0.0000	0.0000	0.0000	0.0000	0.0000	0.0000	0.0000	0.0000	0.0000	0.0000	0.0096	0.0019
16	FUELOI	FINE	0.0000	0.0000	0.0000	0.0000	0.0002	0.0000	0.0002	0.0000	0.0001	0.0000	0.0000	0.0000	0.0000	0.0000	0.0000	0.0000	0.0000	0.0000	0.0000	0.0000	0.0000	0.0000
17	COAL	FINE	0.0000	0.0000	0.0000	0.0000	0.0020	0.0004	0.0019	0.0004	0.0012	0.0002	0.0007	0.0001	0.0023	0.0005	0.0003	0.0001	0.0000	0.0000	0.0000	0.0000	0.0000	0.0000
18	NATGAS	FINE	0.0000	0.0000	0.0000	0.0000	0.0073	0.0015	0.0101	0.0020	0.0030	0.0006	0.0000	0.0000	0.0000	0.0000	0.0000	0.0000	0.0000	0.0000	0.0000	0.0000	0.0000	0.0000
19	COCOLV	FINE	0.0000	0.0000	0.0000	0.0000	0.0006	0.0001	0.0007	0.0001	0.0005	0.0001	0.0003	0.0000	0.0008	0.0001	0.0000	0.0000	0.0047	0.0016	0.0000	0.0000	0.0565	0.0107
20	RICEST	FINE	0.0000	0.0000	0.0000	0.0000	0.0001	0.0000	0.0001	0.0000	0.0000	0.0000	0.0000	0.0000	0.0000	0.0000	0.0000	0.0000	0.0000	0.0000	0.0141	0.0046	0.0325	0.0062
21	COWDNG	FINE	0.0016	0.0003	0.0015	0.0002	0.0003	0.0000	0.0002	0.0000	0.0002	0.0000	0.0001	0.0000	0.0003	0.0000	0.0000	0.0000	0.0007	0.0002	0.0179	0.0058	0.0400	0.0076
22	BRIQUT	FINE	0.0005	0.0001	0.0000	0.0000	0.0006	0.0001	0.0007	0.0001	0.0005	0.0001	0.0003	0.0000	0.0009	0.0001	0.0000	0.0000	0.0044	0.0015	0.0173	0.0056	0.1787	0.0340
23	JACKBR	FINE	0.0001	0.0000	0.0000	0.0000	0.0003	0.0000	0.0003	0.0001	0.0002	0.0000	0.0001	0.0000	0.0002	0.0000	0.0000	0.0000	0.0010	0.0003	0.0052	0.0017	0.0826	0.0157
24	C*INBIO	FINE	0.0002	0.0000	0.0000	0.0000	0.0004	0.0001	0.0004	0.0001	0.0003	0.0001	0.0002	0.0000	0.0005	0.0001	0.0000	0.0000	0.0025	0.0011	0.0091	0.0037	0.0876	0.0197

References

Eldering, Annmarie; Ogren, J. A., Chowdhury, Zohir; Hughes, Lara S.; Cass, Glen R.. (2002) "Aerosol optical properties during INDOEX based on measured aerosol particle size and composition", *Journal of Geophysical Research-Atmospheres*, 107.

Hildemann LM, Markowski GR, Cass GR. 1991a. Chemical-Composition of Emissions from Urban Sources of Fine Organic Aerosol. *Environmental Science & Technology*. 25: 744-759.

Hildemann LM, Markowski GR, Jones MC, Cass GR. 1991b. Submicrometer aerosol mass distributions of emissions from boilers, fireplaces, automobiles, diesel trucks, and meat cooking operations. *Aerosol Science and Technology*. 14: 138-152.